The Dissertation Committee for Brian Thomas Welsh Certifies that this is the approved version of the following dissertation:

Activation and Allosteric Modulation of the α1 Glycine Receptor

Committee:

S. John Mihic, Supervisor

Richard W. Aldrich

Alejandro M. Dopico

R. Adron Harris

Harold H. Zakon

Activation and Allosteric Modulation of the α1 Glycine Receptor

by

Brian Thomas Welsh, B.S.

Dissertation

Presented to the Faculty of the Graduate School of

The University of Texas at Austin

in Partial Fulfillment

of the Requirements

for the Degree of

Doctor of Philosophy

The University of Texas at Austin

May 2010

Dedication

This dissertation is dedicated to my mother and father who have always provided love and support for all of my choices in life, and to my future wife Pamela for her encouragement and love along the way.

Acknowledgements

I could not have made it through graduate school without the help of so many around me and so I would like to express my thanks here for all that they've done. First and foremost I would like to thank my advisor, S. John Mihic, for taking me in to the lab and teaching me so much of what I know about both pharmacology and neuroscience. For always having an open door to discuss anything (and I do mean anything), for always remaining positive, for calming me down when I thought the world was ending, and for sending me more email joke forwards than any other human ever, I am grateful. You have taught me how to think like a scientist and how to overcome the challenges of the field. I personally could not have asked for a better mentor throughout graduate school.

I'd also like to thank the other members of my committee that have provided valuable advice and support for my project. Adron Harris, Director of the Waggoner Center for Alcohol and Addiction Research, was right down the hall and ready to offer advice at a moments notice. His weekly meetings of the Center provided one of the best forums to present my data, in addition to the chance to learn about all of the other interesting research going on around me. I'd like to thank Rick Aldrich for always being excited to discuss the minutia of single channel data analysis; without Rick I'm not sure that I would've understood exactly what I was doing. Harold Zakon's lab was my first rotation in graduate school and it was my semester spent in his lab, along with his early

lectures on electrophysiology that inspired me to become an ion-channel electrophysiologist. And finally thanks to Alex Dopico who was helpful from 550 miles away and for flying in multiple times to sit on my committee.

I also received a lot of financial support that made this research possible. This included an NIAAA grant to S. John Mihic (R01-AA11525) and to myself (17802-01A1). Two institutional training grants also supported this work, one to Rueben Gonzales (5 T32 AA007471) and the other to the University of Texas Neuroscience Graduate Program (T 32DA 018926). The Bruce/Jones Predoctoral Fellowship and the University of Texas Bruton Continuing Fellowship provided additional supplements.

There are a few ex-members of my lab that I'd like to thank for helping me out when I didn't know a thing about how to do electrophysiology. Rachel Phelan taught me what I know of two-electrode voltage clamp technique. Michael Roberts taught me single-channel recording which was both a blessing and a curse; his were big shoes to fill. I'd like to thank Michelle Dupré for challenging me and making me think about things differently. And finally a big thanks to Beth Goldstein, for all of the time spent working out single channel data analysis protocols. It was quite a long road and I don't think that I would've remained sane if I were on it alone.

Then there are all those people that I will leave behind in the lab that are much deserving of my gratitude too. Megan Tipps was a wonderful lab mate, lunch partner, and editor of this dissertation. She is certainly in rare company having read this thing. Thanks to Jelena Todorovic who was always up for discussing all sorts of crazy ideas about how the glycine receptor works and who often provided so many delicious baked goods. They will be missed. I'd like to thank Hunter Allen for being a "super-undergrad" and doing some really great research to help me out. Also, to Dean Kirson for his help with the finishing touches to some of the data contained herein and for the

company of his dog Coffee, who spent almost as many hours in my room as I did while writing this. A few other very generous people provided helpful input including Weiyan Li and Anthony Auerbach and his lab members.

Of course my path through graduate school was aided by so many non-scientists that helped take care of everything else that I needed. Chris Mazzucco, the graduate school coordinator when I first arrived at the university, was instrumental in my adjustment to Austin and graduate school life, and without her I very well may have upped and turned around. Debbie James and Anita Mote provided unbelievable administrative assistance and were the people to go to for answers on how to get things done. Finally, there is Marsha Berkman to whom I owe special thanks for making my time spent in (and out of) the lab so much more interesting. Her belief in me was invaluable and our conversations about life changed the way that I see the world.

To Pamela, thank you for being there smiling at the end of every day, for listening, for loving, and for putting up with the ranting of a poor, scientist graduate student. Again, many thanks to my parents Mark and Susan Welsh to whom this dissertation is dedicated; you both are amazing role models and it was comforting to know that you were always just a phone call away whenever I needed anything. Thanks to my two lovely sisters, Alexandra and Erin, who always seemed eager to listen to my trials throughout school. And also to my closest friends, both here in Austin and abroad, who kept me laughing and made my time spent in school pass much faster. I am so very lucky to have you all in my life.

Activation and Allosteric Modulation of the α1 Glycine Receptor

Publication No._____

Brian Thomas Welsh, Ph.D.

The University of Texas at Austin, 2010

Supervisor: S. John Mihic

The glycine receptor (GlyR) is a ligand-gated ion channel and member of the nicotinic acetylcholine receptor superfamily. Glycine and the partial agonist taurine are both believed to be the endogenous ligands of the receptor. Partial agonists have lower efficacies than full agonists, eliciting submaximal responses even at saturating concentrations. Recent evidence suggests that efficacy at these receptors is determined by conformational changes that occur early in the process of receptor activation. We previously identified a mutation of the aspartate-97 residue to arginine (D97R), which produces a spontaneously active mutant with behavior that mimics the effects of saturating glycine concentrations on wildtype (WT) GlyR. This D97 residue is hypothesized to form an electrostatic interaction with arginine-119 on an adjacent subunit to stabilize a closed channel closed state. We found that the disruption of this bond converts taurine into a full agonist and greatly increases the efficacies of other β-amino acid partial agonists. Our findings suggest that the determination of efficacy in the GlyR involves the disruption of an inter-subunit electrostatic interaction soon after binding.

We next investigated whether the taurine efficacy could be enhanced by ethanol, a well-studied positive allosteric modulator of receptor function. Whole-cell recordings of WT GlyRs demonstrated that alcohol could potentiate the effect of low concentrations of taurine, but did not increase the efficacy of a saturating concentration. Therefore we sought to understand the mechanism by which alcohol enhances the GlyR, because ethanol's actions at inhibitory receptors in the brain are thought to produce many of the physiological effects associated with its use. We examined the effects of 3 μM glycine ± 50 or 200 mM ethanol on outside-out patches expressing WT α1 GlyR, to determine the effects of alcohol at the single-channel level. Alcohol enhanced GlyR function in a very specific manner. It had minimal effects on open and closed dwell times. Instead, ethanol potentiated GlyR function almost exclusively by increasing burst durations and increasing the number of channel openings per burst, without affecting the percentage of open time within bursts. Kinetic modeling suggests that ethanol increases burst durations by decreasing the rate of glycine unbinding.

Table of Contents

List of Tables

List of Figures

List of Abbreviations

$5\text{-}HT_3$	5-hydroxy tryptamine
a	area, amplitude, likelihood
ACh	acetylcholine
AChBP	acetylcholine binding protein
AMPA	α-amino-3-hydroxyl-5-methyl-4-isoxazole-propionate
ANOVA	analysis of variance
ATP	adenosine triphosphate
β-ABA	β-aminobutyric acid
β-AIBA	β-aminoisobutyric acid
BEC	blood ethanol concentration
BLA	basolateral amygdala
Br^-	bromide ion
Cl^-	chloride ion
CMV	Cytomegalovirus
CNS	central nervous system
EC	effective concentration
ELIC	*Escherichia coli* ligand-gated ion channel
EtOH	ethanol, alcohol
F^-	fluoride ion
g	conductance
GABA	γ-aminobutyric acid
$GABA_AR$	$GABA_A$ receptor

GLIC	*Gleobacter violaceus* ligand-gated ion channel
GlyR	glycine receptor
GLYT	glycine transporter
GTP	guanosine triphosphate
HEK	human embryonic kidney
I	current
I^-	iodide ion
IPSC	inhibitory postsynaptic current
LBD	ligand binding domain
LGIC	ligand-gated ion channel
MAC	minimum alveolar concentration
MBS	modified Barth's saline
MIL	maximum interval likelihood
MTS	methane thiosulfonate
nAcc	nucleus accumbens
nAChR	nicotinic acetylcholine receptor
NMDA	N-methyl-D-aspartate
PKA	protein kinase A
PKC	protein kinase C
PMTS	propyl methanethiosulfonate
P_{open}	open probability
REFER	rate-equilibrium free-energy relationship
SCAM	substituted cysteine accessibility method
SEM	standard error of the mean
τ	time constant

τ_{crit}	critical time
TM	transmembrane
VTA	ventral tegmental area
WT	wild-type
Zn^{2+}	zinc

AMINO ACID RESIDUE ABBREVIATIONS AND NAMING CONVENTIONS

Amino acid residues are often abbreviated using single letters, as in the list below. Point mutations to a protein's structure are referred to using the following nomenclature: (new residue)(residue position)(old residue). Therefore, if the aspartate at position 97 of the glycine receptor were replaced with an arginine, the mutant would be known as D97R GlyR.

Single-letter amino acid abbreviations

A	Alanine	M	Methionine
C	Cysteine	N	Asparagine
D	Aspartate	P	Proline
E	Glutamate	Q	Glutamine
F	Phenylalanine	R	Arginine
G	Glycine	S	Serine
H	Histidine	T	Threonine
I	Isoleucine	V	Valine
K	Lysine	W	Tryptophan
L	Leucine	Y	Tyrosine

1.0 | INTRODUCTION

1.1 - Cys-loop family of ion channels: Basic Structure and Function

The nervous system is an intricate network of neurons through which precise communication is essential. Information within this network is transferred from electrical signals to chemical signals at specific junctions between neurons called synapses. Electrical signals traveling along a presynaptic cell result in the release of neurotransmitters into the synapse. These chemical messengers (ligands) quickly diffuse across the synaptic cleft and bind to specific receptors on the target postsynaptic cell to relay messages. Ligand-gated ion channels (LGICs) constitute one particular class of receptors. Each member of this unique set of membrane-embedded proteins contains an integral pore that allows ions to flow into and/or out of the postsynaptic neuron following ligand binding. This ion flux influences the resting state of the postsynaptic cell and ultimately determines the output of a system of neurons such as the brain.

The LGICs are classified according to their structures into three superfamilies: ATP-gated channels, ionotropic glutamate receptors, and cys-loop receptors. The cys-loop receptor family is the largest of these superfamilies and its name is derived from the characteristic loop formed by a disulfide bond between cysteine residues in the extracellular domain of the receptor. Cys-loop receptors are composed of five subunits (pentameric) that surround a central ion-conducting pore (**Fig. 1.1**). Its members include cationic receptors such as serotonin (5-HT_3) and nicotinic acetylcholine receptors (nAChR), and the anionic receptors $GABA_A$ and $GABA_C$ receptors, and the glycine receptor (GlyR). Most of the structural information obtained for this family of receptors

has been derived from detailed studies of the *Torpedo* nAChR, the crystal structure of the snail ACh-binding protein (AChBP), and most recently, the crystal structures of the Gleobacter (GLIC) and *Erwinia* (ELIC) prokaryotic ligand-gated ion channels (Colquhoun and Sivilotti, 2004; Bocquet et al., 2009; Hilf and Dutzler, 2008). The nAChR is frequently considered the prototype for the cys-loop receptor family and will be described throughout this chapter as such.

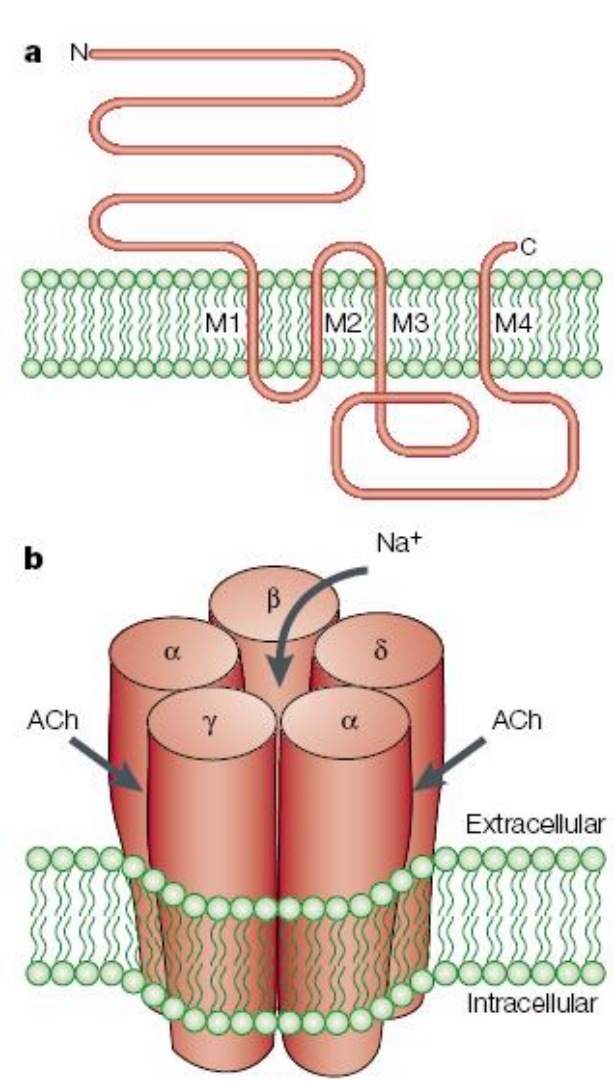

Figure 1.1 - Schematic of a nicotinic acetylcholine receptor

(A) Basic cartoon of a nicotinic acetylcholine receptor subunit showing the extracellular N-terminal ligand binding domain as well as the four transmembrane domains (M1-M4). *(B)* Arrangement of five nAChR subunits to form a single receptor and the location of inter-subunit binding sites for acetylcholine. *Adapted from Karlin A. (2002). Emerging structure of the nicotinic acetylcholine receptors. Nat Rev Neurosci* ***3:*** *103.*

Cys-loop receptors can be assembled with varying stoichiometries and *in vivo* they are often composed of different types of subunits depending on receptor type. Different subunits have unique, often similar, structures that alter the overall activation and deactivation rates of ion channels as well as their rates of desensitization and their responses to allosteric modulators. Receptor subunit composition may even differ depending on the tissue and stage of animal development, resulting in cellular responses that can be tailored specifically for certain functions. For example, the nAChR consists of five classes of subunits: α, β, γ, ε, and δ. While the adult muscle-type nAChR is composed of $(\alpha_1)_2\beta_1\gamma\delta$ subunits, neuronal AChRs contain α_2-α_{10} and β_2-β_4 subunits (Mishina et al., 1986; Karlin, 2002). Similarly, for the GlyR four α subunits (α_1-α_4) and one β subunit have been identified. Early in development, homomeric α_2 GlyRs are expressed (Rajendra et al., 1997) but a switch occurs during development resulting in $\alpha_1\beta$ heteromers becoming the primary GlyR type in the adult spinal cord (Malosio et al., 1991). Variable subunit composition of these ion channels also allows tweaking of other receptor characteristics such as sensitivity to ligand and channel conductance.

The structures of the subunits in this superfamily have some key features in common which can be broken down into three distinct domains. There is an extracellular portion that faces the synaptic cleft, four hydrophobic transmembrane domains (TM1-TM4), and an intracellular loop (Gotti et al., 2009). A brief overview of each of these receptor regions and their functions should begin with the extracellular portion of the protein where the signal to activate the receptor is initiated.

The ligand-binding portion of the cys-loop receptors is in the extracellular region of the protein where agonists bind to the receptor to initiate channel opening. Given the diversity of subunit stoichiometry possibilities and the intricate folding of this region, the

exact binding location for agonists originally was not clear. In the case of the nAChR, affinity-labeling experiments using α-bungarotoxin, an antagonist of the nAChR found in snake venom, demonstrated strong labeling of the α subunits (Oswald and Changeux, 1982). But it wasn't until high-resolution structures of the AChBP were determined that truly detailed information about the ligand-binding site became available. Brejc et al. (2001) published a 4.6 Å crystal structure of the AChBP that showed the ligand-binding site was situated at the subunit interface and composed of a series of loops on the principal side and a series of β-strands on the adjacent side, with many of the specific ligand binding residues being highly conserved throughout the superfamily. These data from the AChBP also showed the location of the conserved cys-loop protruding from the bottom of the subunit, positioned such that it could interact with the transmembrane domains during channel activation (Sine, 2002). So while the AChBP lacked the complete structure of the ion channel, it provided excellent information regarding the location of agonist binding and how that information might be transmitted throughout the protein.

The next major structural components of the LGIC are the transmembrane domains. These are composed of four membrane-spanning α-helical segments that anchor the protein in the lipid-bilayer with short connecting loops between them. The extracellular domain is directly connected to TM1, but the TM2 helix is perhaps the best studied because it contains the pore-lining residues which ions must pass upon channel activation. Crystal structures of AChRs from *Torpedo marmorota* have been used to examine the M2 pore region in detail. The pore is approximately 40 Å long with the M2 helices from each of the five subunits tilting slightly towards the central axis until the middle of the lipid bilayer whereupon they splay back out (Miyazawa et al., 2003). This architecture has some functional significance. The extracellular region of the TM2

domains is spread apart slightly, allowing ions to enter the pore either laterally or through the outer vestibule (Miyazawa et al., 2003). The constricted region near the center of TM2 is composed primarily of hydrophobic residues that may function as a selectivity gate to hydrated ions (Unwin, 1993; Unwin 2003). The other transmembrane domains are arranged surrounding TM2. Looking down at the pore with TM2 at the center, the transmembrane helices TM1 and TM3 are situated on either side and are largely separated from TM2 by a water filled space. Analysis of the related ELIC structure suggests that while the TM1 and TM3 helices serve to shield and stabilize the pore, the TM4 helix has little interaction with the other transmembrane domains (Hilf and Dutzler, 2008).

Lastly, the large intracellular portion of these LGIC subunits connects TM3 to TM4. This region varies considerably among members of the superfamily in both its amino acid composition and its structure, and as a result its role varies as well. In the *Torpedo* nAChR the intracellular domains are thought to form a hanging structure that affect ion permeation near the pore (Lynch, 2004). Similarly, in the case of the 5-HT_{3A} receptor, it has been shown that specific charged residues from the intracellular loop may be involved in the ion permeation pathway (Kelley et al., 2003). For the GlyR however, the cytoplasmic loop serves to cluster $\alpha 1\beta$ receptors at synapses via the loop's interaction with the molecule gephyrin. This intracellular protein functions as a structural scaffold in inhibitory neurons and the β-subunit of the GlyR contains a binding site for gephyrin (Meyer et al., 1995). Gephyrin interactions with $GABA_A$ receptors are also important in localizing them to the post-synaptic structure (Lüscher and Keller, 2004).

Besides its role in ion permeation and receptor clustering, the intracellular loop is also involved in modulatory functions. For example, the loop contains a consensus sequence for protein kinase C phosphorylation that most likely serves to enhance GlyR

function (Legendre, 2001). Further consideration of receptor structure and function, specific to the glycine receptor, can be found in the next section.

1.2 - The Glycine Receptor (GlyR)

The glycine receptor is crucial for mediating inhibitory neurotransmission throughout the central nervous system. Glycine was first proposed as a neurotransmitter in the spinal cord in 1967 due to its distribution throughout the region (Davidoff et al., 1967). Functional studies later that year confirmed glycine's hyperpolarizing action on post-synaptic spinal motoneurons (Werman et al., 1967). Glycine release at the synapse occurs much like that of other neurotransmitters. Glycine, derived from either catalysis of serine by serine-hydroxymethyltransferase or by reuptake from the cleft, is packaged into synaptic vesicles and released when the vesicles fuse with the plasma membrane (Daly and Aprison, 1974; Legendre, 2001). Once in the synaptic cleft, glycine can bind to postsynaptic GlyRs before being taken up by the high affinity glycine transporters GLYT1 (glial) and GLYT2 (neuronal). Glycine receptor activation is usually thought to be inhibitory because the typical resting potential for a neuron, -70mV, is near the chloride reversal potential. In primary sensory neurons, intracellular chloride is high and although the activation of GlyRs at rest causes little hyperpolarization, glycinergic input reduces the effect of excitatory inputs on a cell; a phenomenon known as shunting (Price et al., 2009). In this regard, the GlyR functions in the balance of neuronal activation and inhibition.

A primary example of GlyR inhibitory function can be found in the spinal cord. Here, GlyRs play an important role in regulating pain-signaling pathways making GlyR modulators important targets with therapeutic potential (Laube et al., 2002). Noxious

stimuli sensors (nociceptors) in the peripherary send signals that travel to the spinal cord dorsal horn and then up towards higher brain regions. This relay of information is critical in protecting an organism from harm in its environment. However, if this circuit becomes sensitized due to decreased glycine release or decreased GlyR sensitivity, persistent neuropathic pain may occur. For example, the release of prostaglandins results in a reduced responsiveness of α3-containing GlyRs, a mechanism that has been implicated in pain sensitization (Ahmadi et al., 2001). This makes selective agonists or positive allosteric modulators of α3 GlyRs good targets for the development of new analgesics (Zeilhofer, 2005). Glycine receptors in the spinal cord also function in the anesthetic response as described in Sections 1.7.2 and 1.7.3.

The GlyR is composed of two distinct subunits, α and β which were purified from the adult rat spinal cord using strychnine, a potent inhibitor of GlyR function (Pfeiffer et al., 1982). The first GlyR subunit to be cloned was the α subunit and it was noted that its sequence was similar to nicotinic acetylcholine receptor proteins (Grenningloh et al., 1987). There are a total of four highly-homologous α-subunit primary structures (80-90% sequence identity) and one β-subunit that shares about 47% sequence identity with the α1 subunit (Lynch, 2004). Like the nAChR, the GlyR is composed of five subunits with the α subunit capable of forming fully functional receptors on its own (Legendre, 2001). The β subunit cannot form functional homomeric receptors yet it is distributed widely throughout the adult central nervous system (Malosio et al., 1991). The β subunit is important for the clustering of the GlyR at synapses due to its interaction with the protein gephyrin (see Section 1.1) and it is assumed that most GlyRs in the adult are αβ heteromers. Subunit stoichiometry of the αβ GlyR was initially thought to be three α-subunits and two β-subunits, but a more recent study using tandem constructs suggested

that the true assembly is two α and three β (Langosch et al., 1988; Grudzinska et al., 2005).

The precise distribution of GlyRs in the central nervous system has not been determined. The use of [^{3}H]-strychnine has shown GlyR expression in the spinal cord, pons, thalamus, and hypothalamus (Zarbin et al., 1981), but the distribution of GlyRs in higher brain regions is less clear. Using a monoclonal GlyR α-subunit antibody, GlyRs have also been shown to exist in the cerebellum, olfactory bulb, and hippocampus (van den Pol and Gorcs, 1988). *In situ* hybridization experiments in the rat highlight the differential expression of GlyR subunits throughout the CNS. For example, α1 transcripts can be found in the lower central nervous system regions such as the spinal cord and brain stem, α2 transcripts in the hippocampus and cerebral cortex, and α3 in the olfactory bulb and cerebellum (Betz, 1991). Studies investigating the role of the GlyR in alcohol addiction have examined GlyR expression in the forebrain regions as well, in particular the nucleus accumbens which is believed to be important in mediating the reinforcing effects of drugs of abuse. Here, the GlyR subunits α1, α2, α3 and β are all expressed in the adult rat, with α2 being the most prevalent (Jonsson et al., 2009). Finally, GlyRs are present throughout the retina in amacrine, rod bipolar, and ganglion cells and are believed to function in the circuit that is involved in the switch from day to night vision (Lynch, 2004).

The basic structure of the GlyR is described in Section 1.1 but there are important features that define this receptor that are necessary to mention for a complete understanding. The ligand binding pocket is formed from three loops (domains A, B, C) from the + side of the interface and three β strands (domains D, E, F) on the – face of an adjacent subunit (Lynch, 2004). Of these, domain B of the α subunit is thought to contain the "principal" glycine-binding site in part because it functions as such in the

nAChR. In the GlyR, mutations in domain B such as F159Y andY161F dramatically altered the sensitivity of the receptor to a variety of molecules including glycine, β-alanine, taurine, and strychnine, supporting this domain's role in ligand binding (Schmieden et al., 1993). Through the use of docking simulations glycine is thought to orient itself with its α-carboxyl group toward the + side and its α-amino group toward the – side; bridging the interface of adjacent subunits and interacting primarily with the charged residues E157 and R65 (Grudzinska et al., 2005). Loop C may be involved in a second glycine binding site as amino acids here, particularly Y202, have been implicated in glycine affinity (Rajendra et al., 1995). Determining binding residues solely through mutational studies is difficult though since it is possible that there are long-range (allosteric) effects of the mutations on the actual binding pocket or on receptor gating.

The GlyR is strongly selective for anions with a permeability sequence in cultured neurons of $I^- > Br^- > Cl^- > F^-$ (Bormann et al., 1987). Residues present in the TM2 domain, just above and below the narrowest portion of the channel pore, are positioned to act as the main selectivity filter, according to data from the crystal structures (Miyazawa et al., 2003). This is consistent with the earlier results from a SCAM (substituted cysteine accessibility method) study that probed the access of sulfhydryl-specific reagents that were added from either side of the membrane. Using this technique it was determined that the four residues from –2' to +2' (based on a common numbering system of TM2 residues in which position 1' is the putative cytoplasmic side and 19' is the outermost residue) represented the narrowest part of the channel and hence the gate (Wilson and Karlin, 1998). Taking into consideration both permeation ability and anion size, experiments using various preparations estimated that the effective pore diameter of the GlyR to be 5.2 to 6 Å (Borman et al., 1987; Rundsröm et al., 1994; Fatima-shad and Barry, 1993). A more recent estimate combining the modeling results from the

Miyazawa study with results from a Brownian dynamics simulation, suggests the pore is slightly larger, between 6 Å and 8.3 Å (O'Mara et al., 2003). There is strong evidence from mutational studies that the residues in this region determine channel permeability. Mutations of the nAChR such as E1'A and V13'T, substitutions based on the amino acids present in the α1 GlyR, were successful at switching the receptor from a cation-selective channel into anion-selective channel (Galzi et al., 1992). These homologous mutations were also made in the 5-HT_3R with similar results (Gunthorpe and Lummis, 2001). The TM2 pore-lining residues are therefore crucial in determining ion permeation in this superfamily of receptors.

Simulations of ion permeation through the $GABA_A$ receptor show that two chloride ions are stabilized in the central portion of the pore, with other chloride ions found above in the outer vestibule (O'Mara et al., 2005). As more chloride ions enter from the outside their presence results in a domino effect driving the ions through the channel. Presumably a similar permeation mechanism is present in the GlyR. The single channel conductance of the GlyR varies depending on expression system and subunit composition. For example, homomeric human α1 GlyRs have been reported to have up to five conductance states ranging from the most frequently occurring 86-88 picosiemens (pS) state to the least common 18 pS state (Borman et al., 1993; Rajendra et al., 1995). The addition of the β-subunit to form α1β heteromers eliminates the higher conductance states and results in a primary conductance of 44 pS (Borman et al., 1993). Exactly how the channel opens to one conductance state or another is not yet understood. A study investigating the properties of GlyRs in cultured mouse spinal neurons determined that channel conductance is not dependent on the concentration of agonist (Twyman and MacDonald, 1991). Regardless, these anionic channels are extremely important for inhibitory neurotransmission.

Since the GlyR serves to maintain an inhibitory tone throughout the nervous system, diseases that affect GlyR functioning disrupt this balance and result in an increased level of excitability in the nervous system. One particular example of this is human hereditary hyperekplexia (startle disease), which reduces the magnitude of glycine-gated currents either by reducing GlyR conductance and affinity, or decreasing GlyR expression. The most common form of hyperekplexia results from a dominant mutation in the GlyR α1 subunit on chromosome location 5q (Ryan et al., 1992). This 5q mutation specifically affects the R271 residue producing either R271L or R271Q point mutations. Both of these mutations have been studied more closely in heterologously-expressed GlyRs. These mutations had two significant effects on the receptor: a drastic decrease in glycine sensitivity and a decrease in the receptor main conductance state receptor (Langosch et al., 1994). In general, other mutations of the α1 GlyR that lead to this disease do so by affecting these two aspects of channel function (Lynch, 2004). Interestingly, two other mutations that produce this startle phenotype are found in an area of the GlyR structure that has been implicated in alcohol and anesthetic binding (see section 1.7.2 below). For example, a single channel study of the α1 A52S mutation in the extracellular portion of the receptor found that the mutation altered the kinetics of glycine binding (Plested et al., 2007) (see section 1.4 below). The other mutation, α1 S267N, was discovered in a patient presenting symptoms of hyperekplexia. This residue is located in the second transmembrane segment and mutations here result in a reduction in glycine sensitivity, as well as changes in the receptors modulation by alcohol (Becker et al., 2008). However, a link between the disease and its effects on alcohol tolerance are not clear, and in the case of the hyperekplexic patient with the S267N mutation there were no subjective differences in ethanol sensitivity reported.

1.3 - Activation and gating of the GlyR and related ion channels

In order to maintain accurate information transfer at the synaptic level, ligand-gated ion channels must remain closed until an appropriate signal activates the channel. Therefore receptors, such as the nAChR receptor, have an extremely low spontaneous opening rate of 2 x $10^{-3}s^{-1}$ in the absence of ligand (Jackson, 1986) The GlyR spontaneous activity is also either extremely rare or non-existent (Lynch, 2004). So the ligand serves as the signal to open the channel by greatly increasing the channel's open probability. Ligand-gated ion channels in the nAChR superfamily contain multiple agonist binding sites and an increase in the number of agonist molecules bound is expected to increase the open probability. This has been demonstrated for the nAChR and for the $GABA_AR$ (Colquhoun and Sakmann, 1985; Jones and Westbrook, 1995). In the case of the nAChR, the increase in the efficacy of gating is so large that the equilibrium gating constant (governing transitions from closed to open states) is estimated to increase approximately ten-million-fold with two agonist molecules bound (Sine and Engel, 2006). Recently, extensive analysis of the GlyR has demonstrated this to be true for this receptor as well. Two single channel studies, one of the $\alpha 1$ homomeric GlyR (Beato et al., 2004) and one of the $\alpha 1\beta$ GlyR (Burzomato et al., 2004), found that the efficacy of gating for these receptors increases with each additional glycine molecule bound. This was determined by fitting the data to a scheme with a maximum of three ligand molecules bound and such an increase in agonist efficacy is indicative of cooperativity in binding (see sections 1.4 and 1.5 below for detailed descriptions of these studies and mechanisms).

It is interesting to consider the structural basis for this apparent cooperativity and the increase in agonist affinity that precedes channel gating. Wyman and Allen (1951),

describing the binding of oxygen to hemoglobin, proposed that binding could lead to an increase in affinity resulting from a conformation change (Colquhoun, 2006). This was later described in great detail in the Monod-Wyman-Changeux (MWC) model. The MWC model supposes that all of the binding sites are initially equal but that sequential binding of agonist molecules to subunits results in structural changes, leading to a new conformation with higher affinity for the ligand, thus changing the equilibrium of the system (Monod et al., 1965). Crystal structures of the AChBP with nicotine bound suggest that the increase in agonist affinity in nAChRs occurs when the C-loop structure collapses to cover the agonist-binding site (Celie et al., 2004). Molecular model simulations and fluorescence studies of the AChBP also support C-loop collapse as the structural mechanism of increased affinity (Gao et al., 2005). Situated in the nAChR binding pocket, the agonist is stabilized by a number of atomic interactions with aromatic residues including π-cation forces, most notably with W143, before the capping of the pocket by loop C occurs (Zhong et al., 1998; Sine and Engel, 2006). This "capping" essentially traps the ligand in the pocket, preventing it from unbinding and resulting in increased agonist affinity.

Once the agonist binds, the channel must transmit this signal to the pore roughly 50 Å away almost instantaneously (Miyazawa et al., 1999). Anthony Auerbach's lab has rigorously studied the activation of the nAChR and related channels using rate-equilibrium free-energy relationships (REFERs) and Φ-values. REFER analysis was first developed to describe the transition states for a reaction based on the equilibria of the end points, using the free energy change of the reaction itself (Grundwald, 1985). In the case of a LGIC, the endpoints were the open and closed states of the channel. It has been noted that mutations near the binding site mainly affect the rate constants for channel opening while mutations near the pore primarily affect the channel closing rates

(Colquhoun and Sivilotti, 2004). The slopes of these relationships (Φ-values) can be used to "indicate the extent to which a local site in the protein has progressed in the gating reaction at the transition state", with similar Φ-values representing domains of the protein which move together as a rigid body (**Figure 1.2**) (Auerbach, 2005; Purohit et al., 2007). The movements of the domains from ligand binding to channel opening has been described as a Brownian conformational wave, asynchronous and "coarse-grained", which moves roughly along the long axis of the protein as the channel transitions from closed to open (Chakrapani et al., 2003; Mitra et al., 2004; Auerbach, 2005).

As the conformational wave progresses away from the agonist-binding site, the extracellular domain must interface with the transmembrane domains in order to affect the channel gate. This interaction occurs where the β-sheets (secondary structures) from the binding domain interface with both TM1 and the α-helical structures of the TM2-TM3 loop (yellow and green areas in **Figure 1.2**) (Sine and Engel, 2006). In the glycine and $GABA_A$ receptors a conserved aspartate residue (D148) in the cys-loop of the α subunit is believed to be crucial for coupling agonist binding to channel gating. Mutations at this position in the GlyR result in a decrease in agonist potency and Hill slope (Schofield et al., 2003). Kash et al. (2003) also suggested that residues at this interface interact through specific electrostatic interactions that move closer to one another during gating movements of the $GABA_A$ receptor, stating that this movement may be involved in coupling ligand binding to channel opening.

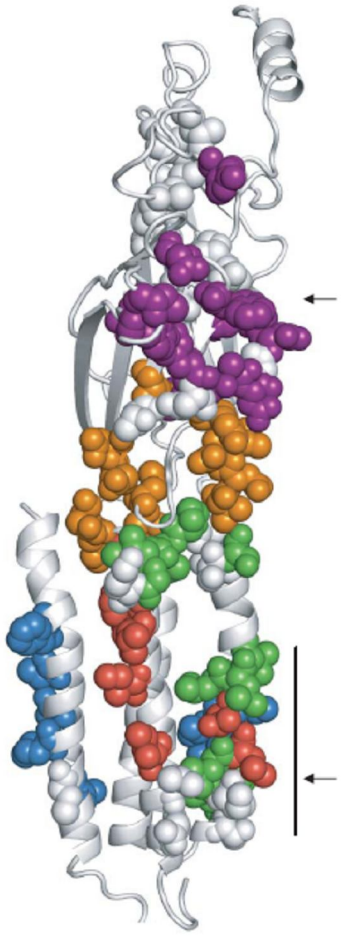

Figure 1.2 – Map of Φ-values in the nAChR

A single nAChR α-subunit showing the clustered Φ domains. The upper arrow represents the ligand-binding domain while the lower arrow represents the channel gate. The domains move as such, earliest to latest: purple, orange, green, blue, red. *Adapted from Purohit et al., 2007. A Stepwise mechanism for acetylcholine receptor channel gating. Nature* ***446:*** *932.*

Stronger evidence demonstrating the importance of this interface for channel activation comes from a chimera channel study. The AChBP was attached to the pore domain from a 5-HT_3 receptor in an attempt to create a channel that opened in response to acetylcholine. Functional chimaeric channels were only created when amino acids from three loops (β1-2, β8-9, and the cys-loop) of the AChBP subunit were changed to their 5-HT_3 homologues (Bouzat et al., 2004). Once altered, the extracellular domain could then communicate its binding signal to the channel gate.

Two specific residues near the interface of extracellular domain and the TM2-TM3 linker may serve as part of a common pathway for receptor activation. Arginine 209, which is at the distal end of β-strand 10, and glutamate 45, at the base of the β1-β2 linker, are invariant in this family (Lee and Sine, 2005). The interaction between these two residues has been closely investigated in AChR α-subunits using mutant cycle analysis. By analyzing the single channel activity of mutant receptors in which each of these residues was mutated independently (E45R and R209Q) and then together (E45R / R209Q) it was determined that the residues had a free-energy coupling of approximately –3.1 $kcalmol^{-1}$ (Lee and Sine, 2005). This is very similar to the energy coupling of a salt bridge in a hydrophobic region. Furthermore, a double charge swap mutant (E45R/R209E) nearly restored normal channel gating, highlighting the possible electrostatic interaction between these residues. Lee and Sine also demonstrated that P272 is coupled to E45 (and nearby V46), perhaps through hydrophobic interactions, which serves to connect the extracellular domain residues to the TM2-TM3 linker region (Lee and Sine, 2005). These residues at this interface are therefore physically proximal to, and ideally positioned, to transfer the signal from the ligand-binding domain to the TM2 region.

The P272 residue is of significance for its role in channel activation, not only because of its position at the top of the TM2-TM3 linker region, but also because proline is unique in that it can change its conformation (isomerize) between *cis*- and *trans*-forms. A series of experiments showed that substitutions of unnatural amino acids at the P272 position altered receptor activation, e.g. residues that favored the *cis*- conformation favored receptor activation (Lummis et al., 2005). The Φ-value for this residue also suggests that the motion in this part of the protein (TM2-TM3) precedes the opening of the gate (Jha et al., 2007). The signal transduction pathway from agonist binding to opening the channel gate would then proceed as such: the capping of loop C (after agonist binding) disrupts the Arg 209 / Glu 45 interaction sending a signal through to P272 at the apex of the M2-M3 linker region. Proline 272 may then isomerize from *trans*- to *cis*-, bending the TM2-TM3 loop and creating a disruption in TM2 that opens the channel gate (Sine and Engel 2006).

As the conformational wave moves down towards TM2, it approaches the hydrophobic residues forming the channel gate that provide an energetic barrier to permeating ions (Beckstein et al., 2001). Electron images from acetylcholine-activated nAChRs in the open-channel state, show that when the channel opens, the TM2 α-helices from the subunits rotate such that the restricted kinked-region that occupies the middle of the pore moves over to the side (Unwin, 1995). The twisting of the TM2 region, caused by the descending binding signal, is therefore enough to weaken the hydrophobic interactions, destabilize the girdle, and open up the pore (Miyazawa et al., 2003; Sine and Engel 2006). The other three helices (TM1, 3, and 4) are then assumed to support the open conformation through new interactions.

The magnitude of the conformational changes involved in opening the channel gate has recently been suggested to be relatively small compared to what was previously

thought. Using a novel technique, known as single-channel proton-transfer, the degree of movement of residues in the pore was investigated. This method works by introducing basic residues (lysine, histidine, arginine) into the α-helix structure of the TM2 pore that when protonated, prevent cations from passing and therefore results in a change in the single channel current kinetics (Cymes et al., 2005). Cymes et al. determined that the rotation of TM2 was minimal. A follow-up study using the same technique, but investigating the movements of TM1 and TM3, also supported the conclusion that there is a "limited rearrangement of the pore domain" (Cymes and Grosman, 2008). This minor adjustment in the TM2 orientation is consistent with simulations of nAChR gating that suggest a 1.5 Å widening of the narrowest portion of the pore upon a 15° clock-wise rotation of each of the TM2 helices is sufficient to open the channel (Corry, 2006).

1.4 - Introduction to single channel measurements and theory

Single channel recording is one of the most powerful tools available to channel physiologists for studying the behavior of ion channels over time. The patch-clamp technique allowed Neher and Sakmann (1976) to be the first to show current flowing through a single native nAChR; a method for which they won the Nobel Prize in Physiology and Medicine in 1991. Briefly, the technique involves placing a glass pipette with a tip roughly 1 μm in diameter firmly against the cell membrane and applying a slight amount of suction to form a tight seal with the lipid bilayer. An electrode in the pipette then allows the current from activated ion channels to be measured. Variations on this technique involve breaking into the cell membrane and/or pulling off small patches of the lipid bilayer. Since the data acquired from the study of single channel currents is complex due to the channels random behavior, it requires advanced theories and analyses

in order to understand and interpret the results; therefore a simple introduction is provided here to better understand the process.

It is helpful to know exactly what information is available from a single channel current trace when viewing the data. **Figure 1.3** shows a simple example recording with the basic features of the data labeled. Here, openings appear as downward deflections away from the baseline (closed). The magnitudes of the openings (amplitude) is a measure of the current (I) flowing through the channel which can be used to determine the unitary channel conductance (g) based on the voltage (V) using the following equation from Ohm's Law:

$$g = I/V \qquad \textit{Equation 1.1}$$

Each event, opening or closing, has a measured lifetime and combined with the information regarding the sequence of these events, contains a significant amount of information about the channel's kinetic behavior (see below). One notable aspect of the channel activity is that the openings are often grouped into bursts of activity rather than occurring singly; a phenomenon which was predicted by Colquhoun and Hawkes, who attributed the burst behavior to single activations of the receptor. That is to say, a burst begins when the channel opens after agonist binds and ends after the channel closes and the ligand disassociates (Colquhoun and Hawkes, 1977; Pallotta, 1991). This burst structure is relevant for understanding synaptic currents because the properties of the burst dictate the rate of decay and the amplitude of the response at the synapse (Colquhoun, 2006). This intricate structure of the burst, in particular the brief closing events, was not apparent until the invention of the high resistance (giga-ohm) seal which allowed high resolution recordings as a result of reduced background noise (Hamill et al., 1981).

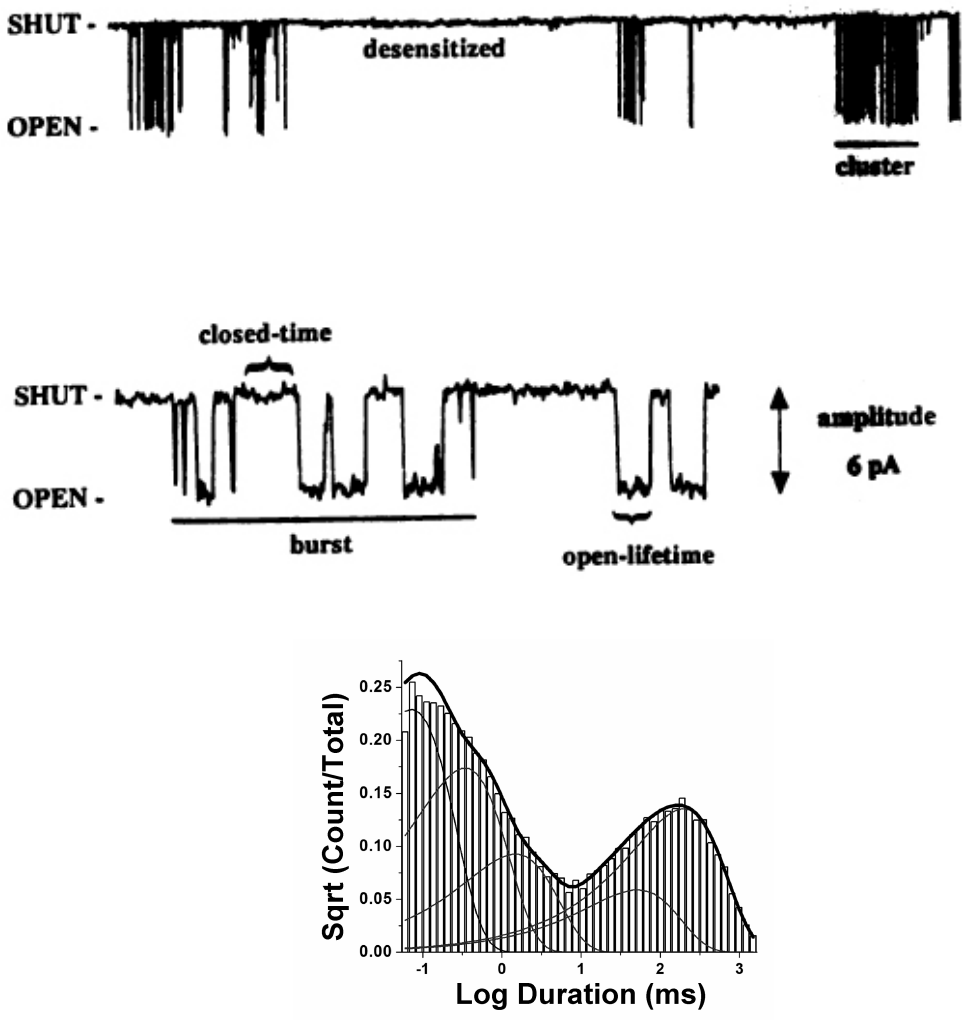

Figure 1.3 – Example of a single channel current tracing and fit

Top: Above, Single channel openings organized into bursts of activity. Below, a time-expanded view of the burst composition demonstrating a series of brief openings and closures. *Adapted from Palotta 1991. Single ion channel's view of classical receptor theory. The FASEB Journal.*

Bottom: Histogram of closed time durations showing the overall fit (thick line) and individual exponential components (thin lines).

Besides the rather straightforward measurements such as current amplitude described above, information regarding the channel gating mechanism and kinetics is contained within the series of opening and closing durations. The durations of these events typically span many orders of magnitude (from μs - sec) and are highly variable. Histograms are constructed from thousands of events and plotted on a logarithmic time scale to aid in display (**Fig. 1.3**). The distribution of these events can often be fit with multiple exponential components that are of notable significance. For example, each kinetic open state of a channel may have its own distinct closing probability that results in an exponential distribution of open times for that individual state, with multiple exponential components perhaps representing additional open states (Pallotta, 1991). The same holds true for closed durations and closed states, the distributions of which are also used to estimate the rate constants for binding and gating in addition to separating the recording into bursts. The vertical axis of the histogram is presented as the square-root of events/bin which allows for easy recognition of exponential peaks (each corresponds directly to its time constant) while the height of each peak corresponds to the number of events in that component (Sigworth and Sine, 1987).

Originally the histograms for open, closed, and burst durations were fit separately using mixtures of exponential probability density functions. The resulting empirical fits, time constants (τ) and areas (a), had the disadvantage of lacking kinetic and mechanistic significance with no good way to correct for short missed events in the record (Colquhoun, 2006). Short closings cause problems because a missed event will result in the appearance of a much longer opening (apparent opening) than what actually occurred. But adjacent open and closed times are usually correlated for receptors in the nAChR family, so by analyzing the joint distributions of both sets of events additional information about how the states are connected becomes available (Hatton et al., 2003;

Beato et al., 2004). Kinetic mechanisms can then be fit and evaluated with the apparent joint and conditional distributions using a process known as maximum interval likelihood (MIL). Although there are quantitative methods to determine which mechanism is most likely given the data, such as log-likelihood comparisons, it is crucial to consider other factors such as structural plausibility and the ability of the proposed mechanism to predict channel behavior (Colquhoun, 2006).

A complete mechanism for the receptor is then composed of a series of logically-connected states with transition rates (the free parameters from the fitting) between them (**Fig. 1.4**). Rates moving horizontally to the right represent agonist binding steps while rates moving downwards represent transitions of the receptor towards an open state. The states marked with stars are open states.

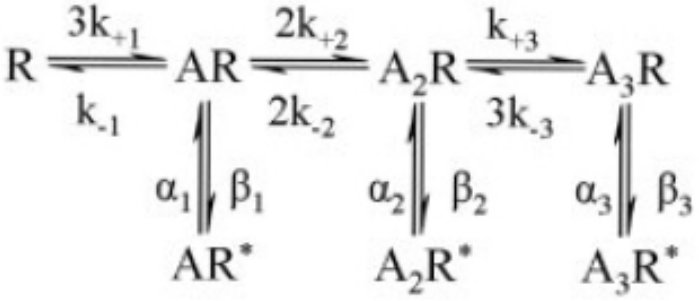

Figure 1.4 - Example of a kinetic mechanism of GlyR activation

k_{+1} and k_{-1} represent binding and unbinding rate constants respectively. α represents shutting rate constants and β represents opening rate constants. States labeled with a star are "open states" and have a measurable conductance. This example has 12 free parameters, four closed states and three open states.

1.5 - Single Channel Properties and Kinetics of Glycine Receptor Function

As the technology and techniques for single channel data acquisition and analyses have improved, new information has been added to our understanding of GlyR function. This section will focus on data from homomeric α1 and heteromeric α1β GlyRs, which are most relevant to this discussion.

Single channel conductance was the first property measured in experiments from GlyR patches as it is the easiest to extract from recordings. For GlyRs expressed in cultured mouse spinal neurons, at least three conductance states have been measured: 45, 31, and 21 pS (Hamill et al., 1983). This agrees very closely with later studies of human α1β GlyRs expressed in HEK293 cells where it was also determined that the highest conducting state occurred most frequently, roughly 88% of the time (Bormann et al., 1993). The latter study also examined homomeric α1 receptors but observed five different conductance states: 86, 64, 46, 30, and 18 pS.

Initial studies examining GlyR kinetics all suggested that the native α1β GlyR had at least three open states (Rajendra et al., 1997). Twyman and MacDonald were one of the first to examine the effect of varying glycine concentration (0.5 – 2 μM) on open times and conductance states. By analyzing the two main conductance levels (42 and 27 pS) separately they determined that mean open time increased with increasing agonist concentration and that openings to either conductance state could be fit with three exponential components (Twyman and MacDonald, 1991). The higher mean open time was a result of an increase in the frequency of the longest duration openings. Closed time durations were also fit with multiple exponentials, the shortest of which did not vary with concentration (Twyman and MacDonald, 1991). Burst structure was analyzed and the

burst length distributions were fit well with four exponentials. Mean burst length for both conductance states increased with agonist concentration as a result of an increase in the frequency of longest burst component rather than an increase in the time constants (τ). The data from these experiments were discussed in terms of a kinetic model with four closed states and three open states (similar to **Fig. 1.4** but with the open states also connected) but the uncertainty of the kinetic relationships of the multiple conductance states was not resolved (Twyman and MacDonald, 1991). This study provided the early framework for understanding GlyR single channel behavior.

More recently, David Colquhoun's lab has performed detailed experiments on recombinant GlyRs expressed in oocytes and HEK293 cells. The first thorough examination of α1 homomeric GlyRs was aimed at resolving the kinetics of the activation mechanism. Like the Twyman and MacDonald study in that data were collected over a narrow glycine concentration range, the researchers arrived at similar conclusions. Across three concentrations (0.3 μM, 1 μM, 10 μM) open durations were fit with a mixture of four exponentials. While the τ's for these open dwell time fits did not vary with glycine concentration, an increase in mean open time as agonist concentration increased was again attributed to an increase in the frequency of long openings (Beato et al., 2002). Mean burst durations also increased at higher agonist concentrations as longer bursts became more frequent, and at 10 μM an extra (fifth) longest component was necessary to describe the burst length distribution (Beato et al., 2002). The data were fit across all the glycine concentrations simultaneously using a mechanism with six closed states and five open states. This model made the assumption that a homomeric α1 receptor would have five glycine binding sites, one at each subunit interface. In this mechanism, each open state represented a different number of agonist molecules bound and the proposed model was able to accurately predict the longer-lived openings

observed at higher liganded states (Beato et al., 2002). The study was hampered in proposing a complete reaction scheme however, by the limited glycine concentration range used.

A follow-up study by the same investigators used a much greater agonist concentration range (10 μM – 1000 μM glycine). While many of the basic conclusions from the previous work held true, some new information was gleaned from testing the higher glycine concentrations, allowing for refinement of the mechanism. For instance, at higher agonist concentrations openings could be grouped into distinct clusters of activity, rather than bursts, separated by periods of desensitization, with significant increases in the probability of being open (P_{open}) during clusters (Beato et al., 2004). The cluster P_{open} ranged from 0.21 at 50 μM glycine to 0.96 at 1000 μM (saturating glycine). Beato et al. (2004) also used the increased size of the data set to compare multiple mechanisms. Some mechanisms modeled different numbers of glycine binding sites (3 vs. 5) or distinct di-liganded states, i.e. a mechanism in which the second glycine binding adjacent to the original bound glycine is considered to be a separate state from one in which the second glycine binding is one site away on the homopentamer. Models were evaluated based on their abilities to match the dwell-time distributions and P_{open} response curves. The previous model with five binding sites proposed by Beato et al. (2002) could only explain the new data adequately with the assumption that there was no increase in efficacy resulting from the binding of a fourth or fifth glycine molecules, a phenomenon that occurs at higher glycine concentrations. Therefore a model containing only three open states (**Fig. 1.4**) was the simplest mechanism that could successfully describe all the data however it predicted some interaction between binding sites while the channel was in the shut state (Beato et al., 2004).

Research on the α1β GlyR attempted to address the apparent interaction between the binding sites, previously detected in other studies, that results in both positive cooperativity of binding and negative cooperativity of unbinding. Using similar protocols as Beato et al. (2004), responses to glycine concentrations ranging from 10 μM to 1000 μM were measured in cell-attached patches containing α1β GlyRs rather than outside-out patches as before (Burzomato et al., 2004). The study attempted to develop a reaction mechanism that modeled a conformational change that accounts for changes in glycine affinity upon binding/unbinding. Many kinetic schemes were tested that included additional closed states. These were represented as either pre-open conformations or desensitized states and included a scheme successfully used to describe $GABA_A$ receptor macroscopic behavior (Jones and Westbrook, 1995). One mechanism (dubbed the "flip mechanism") placed an additional closed state between each resting state and open state. This flip mechanism was determined to be the best at describing the data, despite having fewer free parameters than other models tested (Burzomato et al., 2004). In fact, the previously-published data from the Beato et al. (2004) paper was refit with this new mechanism and the results were in good agreement with the older data. The old scheme (**Fig. 1.4**) implied an interaction between binding sites that were quite far apart without an explanation for how this could occur. This new scheme had the advantage of explaining the increase in agonist affinity as a result of the receptor switching to the flipped state (Burzomato et al., 2004). This flip mechanism (**Fig. 1.5**) is now the best kinetic scheme available to describe single channel behavior in this superfamily of ligand gated ion channels and has since been used to adequately fit both native GlyR channel activity from slices of juvenile rat spinal cords as well as the activation of muscle nicotinic acetylcholine receptors (Beato and Sivilotti, 2007, Lape et al., 2008).

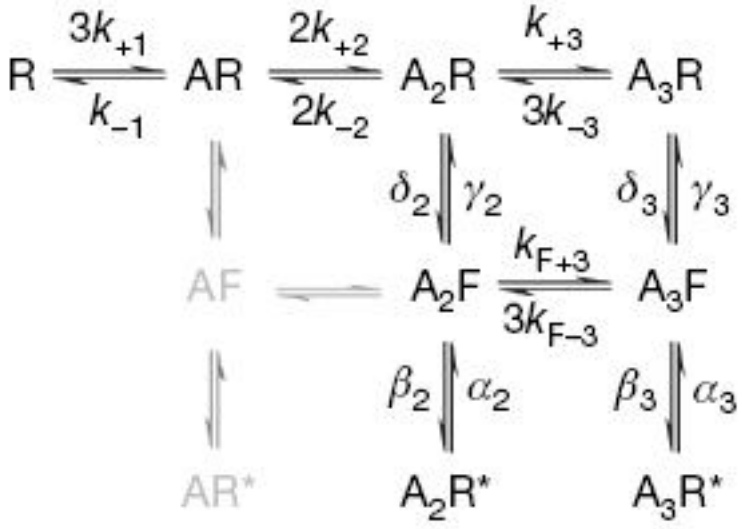

Figure 1.5 – The flip mechanism describing GlyR kinetic behavior

Similar to the mechanism in **Fig. 1.4** but with the addition of intermediate closed states (AF), representing a "flipped" state of the GlyR. The grayed out area represents states that are not likely visited while high concentrations of ligand are present. *Adapted from Lape et al., 2008. On the nature of partial agonism in the nicotinic receptor superfamily. Nature **454:** 722-728.*

The single channel properties of mutant GlyRs that cause hyperekplexia have also been investigated. The α1 K276E mutation in the TM2-TM3 linker region has been identified as one among a number of causes leading to startle disease. It specifically results in the weakening of the lower limbs, in addition to other spasmodic symptoms (Elmslie et al., 1996). The single channel properties of α1(K276E)β receptors expressed in *Xenopus* oocytes were analyzed and compared to wild-type α1β GlyRs. Mutant receptors had a 29-fold decreased sensitivity to glycine, but the main deleterious effect of the mutation was to significantly reduce the mean open time of the channels, implying a defect in channel gating (Lewis et al., 1998). Another α-subunit mutation, A52S that results in a spasmodic phenotype in mice, decreases the glycine sensitivity of homomeric α1 and homomeric α2 GlyRs (Mascia et al., 1996a). This residue is present at the end of loop 2, near the interface with the agonist signal transduction region, and neighboring other residues that result in hyperekplexia (Brejc et al., 2001). Channel properties of GlyRs, both homomeric α1 and heteromeric α1β, that contained the A52S mutation have been assessed in the context of the flip mechanism. The mutation resulted in the loss of apparent cooperativity of glycine binding to receptors due to a reduction in the ability of the mutant receptor to enter the higher-affinity flipped state (Plested et al., 2007). Interestingly the mutation did not greatly decrease the final gating (opening) step of the receptor. These single channel studies of naturally occurring pathological mutants underscore the importance of proper GlyR functioning in the central nervous system.

1.6 - Partial Agonism

Glycine is not the only ligand that can activate the glycine receptor. Many other small amino acids such as taurine and β-alanine can also serve as agonists and are present

in the brain (Shibanoki et al., 1993). However, these amino acids differ from glycine in their abilities to elicit functional responses, a property known as efficacy, and for this reason they are referred to as partial agonists. The efficacy of partial agonists varies considerably and is dependent not only upon the stoichiometry of the GlyR but also the expression system (Lynch, 2004). For example, in *Xenopus* oocytes expressing homomeric α1 GlyRs, taurine has approximately 50% efficacy compared to glycine while taurine efficacy is < 10% in homomeric α2 GlyRs (Schmieden et al., 1992). This is in contrast to HEK293 cells expressing GlyRs in which taurine efficacy on homomeric α1 has been reported to be much higher at ~ 90%, although with the expression of the β subunit taurine efficacy is again near 50% in α1β GlyRs (Moorehouse et al., 1999; Lewis et al., 2003; Lape et al., 2008). The consensus is that taurine is a partial agonist, but these differences in efficacy may have important brain region or cell-type specific effects since GlyR subunit composition varies throughout the brain (Lewis et al., 1991; Farroni and McCool, 2004).

Taurine, in part due to its physiological relevance, has been the focus of many studies. Taurine is found throughout the entire brain and is the second most abundant amino acid present after glutamate (Albrecht and Schousboe, 2005). Despite a lack of evidence for the synaptic release of taurine, it is proposed to play a role as a neurotransmitter throughout the central nervous system. In the rat hippocampus for example, extracellular taurine concentrations are about the same as those of glycine, about 2-3 μM (Shibanoki et al., 1993). Another study found that an amino acid uptake inhibitor for taurine increased the strychnine-sensitive current in CA3 pyramidal cells in hippocampal slice preparations (Mori et al., 2002). This suggests that taurine may regulate tonic GlyR activity and inhibitory tone in the hippocampus.

Taurine has also been detected in the nucleus accumbens (nAcc) where it has been suggested to be the primary endogenous ligand for the GlyR (Ericson et al., 2006). For example, following acute ethanol administration the extracellular taurine concentration increases significantly (Dahchour et al., 1996). This suggests a role for taurine as a neuroprotective agent against excitotoxic effects in the nAcc. A later study demonstrated a 50% increase in dopamine levels within 60 minutes of taurine perfusion, which is similar to the increase in dopamine observed following ethanol administration (Ericson et al., 2006). This study may be especially important for linking taurine activation of the GlyR to alcohol addiction. The possibility of an interaction between taurine and ethanol in the nAcc is relevant because taurine is often found in alcoholic energy drinks such as Sparks (MillerCoors) and Tilt (Anheuser-Busch). One study demonstrated an increase in the brain concentration of taurine, in addition to a decrease in striatal dopaminergic neurotransmission, following intraperitoneal injection of large quantities of taurine in rats, but whether this is achieved under normal circumstances in humans is not known (Salimäki et al., 2003). Interestingly, taurine has since been removed as an ingredient from these energy drinks after the Center for Science in the Public Interest sued MillerCoors in light of criticism from attorney generals across the country who claimed that the mixture of taurine and alcohol was a dangerous combination (Wall Street Journal, Dec 2008).

Taurine binds to the α1 glycine receptor in the same binding pocket as glycine, although not necessarily to exactly the same residues. Co-application of the two agonists results in a reduced response compared to that produced by glycine alone, suggesting that the two ligands do not behave synergistically (Schmieden et al., 1989; Schmieden and Betz, 1995). This phenomenon was also observed using β-alanine and it was attributed to a lack of cooperativity (low Hill slope) as measured from the partial agonist

concentration response curves. It was then proposed that there are two agonist-binding subsites within the LBD in the α1 GlyR: a low affinity subsite that contains residues I111 and A212 that are crucial in determining the taurine response, and a high affinity subsite containing Y161 that determines glycine and strychnine binding (Schmieden et al., 1992; Vandenberg et al., 1992). The overlap of these two sites in the α1 GlyR may account for the inhibitory effect that taurine and β-alanine exhibit on glycinergic currents. The nearby N102 residue has been suggested to be a binding site for taurine based on evidence from the N102C mutation which results in a much greater change in taurine sensitivity compared to that of glycine (Vafa et al., 1999; Han et al., 2001).

Many partial agonists of the α1 GlyR, including taurine and β-alanine, are β-amino acids. One property that is common to these molecules is the ability to stereo-isomerize between two forms: *cis*- (functional groups on the same side of the molecule) and *trans*- (functional groups on the opposite side of the molecule). Schmieden and Betz (1995) proposed that the reduced efficacy of the β-amino acid agonists such as taurine, β-aminobutyric acid (β-ABA), and β-aminoisobutyric acid (β-AIBA) could be attributed to this ability of the molecule to isomerize. Using nipecotic acid, a GlyR antagonist that is fixed in a *trans*- configuration, they demonstrated that mixtures of nipecotic acid with glycine could replicate concentration response curves of partial agonists; i.e. the partial agonist response of β-amino acids was due to the *trans*- isomers present in solution acting as antagonists while the *cis*- isomers acted as agonists. Thus it could be that the *trans*-isomers are binding to a specific site of the GlyR ligand-binding domain that sterically inhibits *cis*- isomers from binding (Schmieden and Betz, 1995). The partial agonism observed with β-amino acids could therefore be a result of what the researchers called "self-inhibition".

A follow-up study attempted to identify the domain of the GlyR binding pocket that is responsible for the proposed *trans*- antagonism. The focus was on the I111 residue and its surrounding region, which was previously implicated as being important for the taurine response (Schmieden et al., 1992). Schmieden et al. made mutations to aromatic and polar residues in this area (K104A, F108A, and T112A) and expressed the mutants in oocytes. Each of these mutations greatly increased the efficacy of taurine and β-ABA while reducing the EC_{50} values, although β-AIBA efficacy remained unaffected (Schmieden et al., 1999). Co-application of glycine and taurine on the K104 mutant resulted in synergy, indicating that both compounds were acting as full agonists. They concluded that these mutations reduce the binding of the *trans*- form of partial agonists while increasing the efficacy of agonistic interactions. They then refined their GlyR agonist binding model to suggest that the 104-112 domain is crucial for determining the efficacy of antagonists (Schmieden et al., 1999). A later study confirmed the importance of T112 for taurine specific gating effects but found that the residues K104, F108, and I111 do not seem to mediate β-amino acid-specific responses for GlyRs expressed in mammalian cell lines (Han et al., 2001). These data together suggest that the roles of the residues in this domain differ greatly depending on the expression system and this may account for some of the differences in the reported efficacies.

Partial agonism has long been conceived in terms of kinetic models. Given a simple reaction mechanism, the efficacy of a compound was defined as β/α, or in other words, the rate at which the channel transitioned from an agonist bound closed state (AR) to the agonist bound open state (AR*) over the rate at which it transitioned back. This is also known as the equilibrium gating constant (See **Fig. 1.4**). Given this model, partial agonists could be thought of as having an open-shut equilibrium that favored the closed state more than full agonists (del Castillo and Katz, 1957). This was the case in a study

by Lewis et al. (2003) comparing the single channel kinetics of homomeric α1 GlyRs using equipotent concentrations of glycine, β-alanine, and taurine. Differences in agonist action were attributed to the channel opening rate (β), with glycine > taurine ~ β-alanine, while the channel closing rates (α) were assumed to be an intrinsic property of the channel and were relatively similar. The result is an estimate of the relative efficacy ratios (as defined above) for these agonists of 16, 8.4, and 3.4 for glycine, β-alanine, and taurine respectively (Lewis et al., 2003). Recently however, this simplistic model for partial agonism in the nAChR superfamily was challenged following a single channel investigation of partial agonists acting on the GlyR or the nAChR. From this study two conclusions emerged. First, it was evident that the within cluster P_{open} for saturating taurine was decreased to 54% compared to 96% with glycine, supporting the theory that full agonists favor the open state more than do partial agonists (Lape et al., 2008). Second, by fitting single channel data obtained from α1β GlyRs in the presence of taurine using the flipped mechanism (described above, section 1.5) and comparing the results to the data obtained from glycine, a new understanding of partial agonism emerged. The significant differences between the two agonists were not in the final opening (β) and closing (α) rates but rather in the rates that governed transitions to (δ) and from (γ) the flipped state (see **Fig. 1.4**). In fact, the α and β rate constants were similar for glycine and taurine while there was a 180-fold difference in the flipping equilibrium constant (Lape et al., 2008). Hence, glycine binds with much greater affinity for the flipped state compared to the resting state than does taurine. A more recent study has confirmed a similar kinetic scheme invoking pre-open, "primed", closed states to describe nAChR activation and determining that the final closed-to-open transition is agonist-independent (Mukhtasimova et al., 2009). These conclusions raise new questions about our understanding of the structural changes that occur following the binding of an

agonist, partial or full, and suggest that the efficacies of partial agonists are determined early in the activation process.

In light of the activation pathway described above in Section 1.3 and the new flipped-mechanism, it is interesting to consider which structural changes may be specific to taurine versus glycine, following agonist binding. An early attempt to make this comparison probed the α1 GlyR TM2-TM3 linker region of GlyRs expressed in HEK293 cells using cysteine mutagenesis, and measured the rate of cysteine-specific methanethiosulfonate-labeling. No difference was found in the normalized reaction rate of cysteine mutants (positions 272-275) following activation by either taurine or glycine indicating that the binding information from these agonists was integrated before reaching this domain (Han et al., 2004). More recently a couple of studies using a technique employing fluorescent changes to identify structural rearrangements have effectively illuminated partial agonist-specific conformational changes. In the M2 pore region, the fluorescence response due to activation by taurine and β-alanine was not as strongly coupled to the current response, as it was for glycine, indicating GlyR agonists activate the pore through different changes in the protein's conformation (Pless et al., 2007). Interestingly, in the extracellular portion of the protein the agonist efficacy correlated negatively with the magnitude of its conformational change (fluorescence), as large movements in loops D and E are not optimal for efficacious gating, while changes in the pre-M1 domain and loops C and F were agonist-independent (Pless and Lynch, 2009b). It was suggested by the authors that the region around A52 may be the site of the closed-flip conformation change because changes in fluorescence here correlated directly with the measured rank order of agonist efficacy; i.e. strychnine (none) < taurine < β-alanine < glycine (Pless and Lynch, 2009a,b).

It is important to briefly consider that the mechanism for partial agonism in the nAChR superfamily may not be the same as it is for other ion channel types for which crystal structures have been determined with different agonists bound. For instance, in the AMPA receptor (GluR2) after ligand binds, the degree of closure of the LBD correlates directly with the efficacy of the agonist; full domain closure results in complete activation and partial closure results in less activation (Armstrong and Gouaux, 2000). The degree of closure also affects the probability of the channel opening to a subconducting state as partial agonists increased the probability of the channel opening to a lower conductance state (Jin et al., 2003). This appears not to be the case in the related NMDA receptor in which partial agonists and full agonists at the glycine-binding site induce the same degree of cleft closure (Inanobe et al., 2005). Kinetic modeling of the NMDA receptor activation suggests that the subunits are tightly coupled. Partial agonists for either the glutamate-binding site or the glycine-binding site resulted in similar channel gating, having broad effects on the kinetic scheme; decreasing the rates leading towards channel opening and increasing the rates leading away from the open state (Kussius and Popescu, 2009). This is in contrast to the flipped-mechanism for the glycine and nAChR for which the root of partial agonism can be isolated to changes in the rate of entering the final pre-open step.

1.7 - Allosteric Modulation of GlyR function

An allosteric modulator is a molecule or ion that binds to a site on a protein that is distinct from the active site and regulates protein function. In the case of ligand-gated ion channels, the active site is the agonist-binding pocket and there are numerous drugs that modulate channel activity by binding to remote sites. According to the model developed

by Monod, Wyman, and Changeux (MWC), allosteric proteins have different structural conformations each with different affinities for ligands (Monod et al., 1965). Karlin applied this concept to LGICs in 1967, as an effective way to explain the functioning of nAChRs. He introduced the notion that a second ligand could bind and affect channel activity as an allosteric modulator (Hogg et al., 2005). Today there are many known allosteric modulators of LGICs and their effects on channel function also vary. Modulators may be either positive and enhance the function of the protein, or act negatively to decrease channel activity. In principle this change in protein function is the result of a change in the energy barriers separating the various open and closed states (Hogg et al., 2005). For the glycine receptor, many of the allosteric modulators are positive, although zinc (Zn^{2+}) acts in a biphasic manner, either enhancing GlyR currents at concentrations in the nanomolar to low micromolar range or inhibiting them at concentrations > 10 μM (Laube et. al, 1995). Some of these GlyR modulators will be considered individually in terms of their roles and functions.

1.7.1 - ZINC

Of the GlyR modulators that have physiological relevance such as zinc, calcium, neurosteroids and G-proteins, Zn^{2+} is perhaps the most thoroughly investigated (Lynch, 2004). Synaptic release of Zn^{2+} has been demonstrated in areas of the brain that overlap with GlyR expression. A good example is the hippocampal mossy fibers, where the concentration in the synapse may exceed 100 μM (Assaf and Chung, 1984; Vogt et al., 2000). Synaptic vesicles containing Zn^{2+} have also been found in the spinal cord where zinc has been shown to co-localize with glycine at synapses (Schrøder et al., 2000; Birinyi et al., 2001). Consequently, as a modulator of GlyR function in the spinal cord, zinc may function in pain processing and sensory pathways. Intrathecal injections of zinc

chloride reduce chemical nociception in mice (Larson and Kitto, 1997). In the hindbrain of zebrafish, Zn^{2+} has been shown to extend the decay of postsynaptic IPSCs, possibly by retarding glycine unbinding and allowing GlyRs to become fully saturated (Suwa et al., 2000). The presence of Zn^{2+} in the CNS and its release in high concentrations supports the theory that this cation is acting as an endogenous neuromodulator.

The α1 GlyR has two distinct zinc binding sites, a high-affinity site that allows for potentiation of glycinergic responses and a low-affinity site that is inhibitory. Common among Zn^{2+} coordinating sites are histidine residues and these constitute the low affinity site in the GlyR (Auld, 2001). Alanine substitution of two histidines, H107A and H109A, in the extracellular domain of the α1 subunit is sufficient to abolish Zn^{2+} inhibition (Harvey et al., 1999). The inhibitory complex formed by these histidines and the zinc ion is believed to occur between α1 subunit interfaces and was supported by studies in which the co-expression of GlyR subunits containing either the H107A or the H109A mutations result in a receptor with inhibitory zinc responses that are similar to those of the wildtype receptor (Nevin et al., 2003). Zinc therefore inhibits GlyR function by stabilizing intersubunit interactions that must be broken in order for the receptor to activate. Mutations that perturb nearby closed state-stabilizing hydrophobic interactions would then be expected to bias the receptor towards activation and antagonize the inhibitory effects of zinc even if these residues were not directly involved in Zn^{2+} binding. This was very recently confirmed by Miller et al. who found that these disruptions, in particular F99A, created zinc-activated GlyRs that also open spontaneously in the absence of glycine (Miller et al., 2008).

The potentiating zinc binding site was more difficult to locate. Initial searches scanned the GlyR sequence for other amino acids known to participate in zinc binding such as glutamate, aspartate, and cysteine (Auld, 2001). Initially, the group of residues

74-82 was identified as an important determinant of Zn^{2+} potentiation because α1/β chimeras that lacked this nine amino acid region did not show zinc potentiation of glycinergic currents (Laube et al., 1995). Three aspartate residues are present near or within this area (D80, D81, and D84) and were considered good candidates for zinc binding, but following individual mutations to each, only D80G abolished zinc potentiation (Laube et al., 2000). It now seemed likely that the D80 residue was a zinc-binding site; however, it demonstrated surprising, ligand-specific effects when mutated. For instance, the D80A mutation selectively abolished zinc potentiation of glycine-gated currents without affecting the zinc modulation of currents elicited by taurine (Lynch et al., 1998). This ambiguity cast doubt on D80 being the sole potentiating Zn^{2+} binding site. A later study identified three residues: E192, D194 and H215, that when mutated, either abolished or significantly attenuated zinc potentiation of both glycine- and taurine-gated currents (Miller et al., 2005). Structural homology modeling with the AChBP by Miller et al. predicted that these residues are located near enough to each other to constitute a zinc binding site.

Presumably when this high affinity site is occupied by zinc, GlyR function is increased. Laube et al. (2000) performed a detailed single channel analysis of zinc modulation and found that 5 μM zinc enhanced the homomeric α1 GlyR in a number of ways. Zinc increased the probability of the receptor being open and caused a slight increase in mean open time but zinc did not affect GlyR conductance. Zinc's main enhancement of GlyR function was due to a roughly four-fold increase in mean burst duration. Kinetic modeling suggested that this was a result of a decrease in the unbinding of glycine (k_{-1}). This same mechanism for zinc potentiation has also been proposed for the nAChR (Hsiao et al., 2008). Of note, however, is that zinc may potentiate taurine-activated GlyRs through a different mechanism than its effect on glycine because Zn^{2+}

increases taurine efficacy (maximal currents). It seems that in addition to zinc decreasing taurine dissociation, as zinc does for glycine, Zn^{2+} also appeared to increase β and thereby promote gating (Laube et al., 2000). The investigators concluded that this might be evidence of a separate gating pathway for taurine.

1.7.2 – VOLATILE ANESTHETICS AND THE ALCOHOL AND ANESTHETIC BINDING POCKET

Various drugs that depress the central nervous system target the glycine receptor and enhance its function, including volatile anesthetics and alcohol (see section below for detailed information on Alcohol). Volatile anesthetics are a class of small, mostly hydrophobic organic compounds that produce a state of general anesthesia when inhaled. These drugs were first used in the 19th century for surgical procedures and are now considered a cornerstone of modern medical practice. Anesthesia is a physiological state that is characterized by analgesia, hypnosis, amnesia, and immobility (Rudolph and Antkowiak, 2004). Each of these components is a crucial aspect of surgical anesthesia and each most likely results from the drug's actions in a different part of the CNS. For example, immobility is thought to arise from anesthetics acting on the spinal cord, hypnosis from actions at subcortical structures and the amnestic effects may arise from anesthetics affecting hippocampal function (Sonner et al., 2003; Rudolph and Antiowiak, 2004; Dutton et al., 2001). Volatile anesthetics that are in clinical use today include isoflurane, sevoflurane, desflurane and enflurane.

The use of anesthetics in clinical situations is very closely monitored for many important reasons. Under-dosing could lead to situations in which the patient experiences pain or even moves about, while over-dosing could result in patient death due to respiratory depression. In order to easily compare the dosing concentrations for each of

these drugs, a standard measure of anesthetic potency was developed called MAC, or Minimum Alveolar Concentration (Eger et al., 1965). One MAC is the alveolar concentration of an inhaled anesthetic at which 50% of patients are unable to respond to a painful stimulus. Anesthesiologists typically use 1.0 to 2.0 MAC for volatile anesthetics during surgical procedures.

A nonspecific mechanism of action was originally proposed to explain how these drugs act. Upon noting a strong positive correlation between the potencies and lipid solubilities of a series of anesthetics, the Meyer and Overton independently hypothesisized that anesthetic efficacy was derived from its ability to disrupt the lipid bilayer of cell membranes (Franks and Lieb, 1997). However, issues such as the "cut-off effect" in which longer chain alcohols, for example, no longer produce receptor hypnosis, in addition to a very small measured effect of anesthetics on membrane fluidity, equivalent to an increase of ~1º Celsius, began to cast doubt on this hypothesis (Pringle et al., 1981; Franks and Lieb, 1982). Rather than a generalized mechanism for anesthesia depending on lipid disordering, a protein site of action was sought to explain the actions of these compounds. This protein theory suggests that anesthetics produce their effects by binding to specific molecular sites on proteins; similar to how many other drugs work. Early support came from a study by Franks and Lieb (1984) using pure firefly luciferase protein. They demonstrated that the activity of the luciferase could be inhibited by clinically-relevant concentrations of anesthetics even though this protein was not embedded in a lipid bilayer. Excellent evidence of an alcohol binding specifically to a protein target also came later from the LUSH crystal structure. LUSH is an odorant binding protein from *Drosophila melanogaster* that has been suggested to mediate the chemoavoidance of ethanol in fruit flies (Kim et al., 1998). The crystal structure of LUSH, determined in the presence of various alcohols, showed an alcohol molecule

stabilized by a network of hydrogen bonds that were provided by a threonine-serine-threonine motif (Kruse et al., 2003). This happens to be quite similar to motifs found in other proteins whose functions are modulated by alcohols such as the nAChR, $GABA_AR$ and the GlyR. These findings were major advances in the understanding of how alcohols and anesthetics can interact with proteins.

Both the $GABA_AR$ and the GlyR demonstrate acute sensitivity to volatile anesthetics and are significantly potentiated by many of these drugs at concentrations less than 1.0 mM (Franks and Lieb, 1994; Mascia et al., 2000). As mentioned above, many subunits from the nAChR superfamily contain a structural component similar to the alcohol binding area of LUSH. In the α1 GlyR for instance, these residues seem to be clustered in a water-filled pocket bounded by residues in at least TM2 and TM3. Specific mutations at residues S267 (TM2) and A288 (TM3) abolished the enhancing effects of ethanol and enflurane (Mihic et al., 1997). Similarly, mutations made at homologous residues in the equivalent positions of the $GABA_A$ receptor α1 and α2 subunits also resulted in a loss of anesthetic effects. Given these results it was proposed that residues between TM2 and TM3 form a specific water-filled pocket that could constitute the binding site for anesthetics and alcohols (Mihic et al., 1997). Other investigations into the role of S267 were performed using SCAM. A cysteine mutation at S267 allowed for the covalent addition of a bulky thiol-containing reagent, propyl methanelthiosulfonate, to the S267C α1 mutant. This addition of PMTS produced irreversible enhancement of the GlyR, similar to that produced by anesthetics, and abolished the potentiating effects of anesthetics after PMTS binding (Mascia et al., 2000). These studies provided strong evidence that binding of a small molecule in this pocket is sufficient to produce anesthetic-like enhancement of the GlyR and the $GABA_AR$.

The location and nature of this pocket continued to be the subject of further research. The nAChR crystal structure also contained a similar region harboring a water-filled cavity. Not surprisingly, the structure suggested that the L257 residue, analogous to S267 α1 GlyR, would face into this pocket (Miyazawa et al., 2003). Other studies using the SCAM on the α1 GlyR probed the boundaries of this cavity. The results indicated that specific residues from all four TM domains were indeed accessible to MTS modification, some only in the open state of the channel, suggesting that the alcohol-binding pocket may expand during channel activation (Lobo et al., 2004; Lobo et al., 2006). Homology modeling of the GlyR agreed with previous data and presented the TM domains surrounding a central cavity with residues known to be involved in anesthetic potency such as I229, S267 and A288 all facing inwards (Bertaccini et al., 2005). Finally, a very recent molecular dynamics simulation of alcohol binding to the GlyR determined that ethanol could reside stably in the pocket formed by these residues (Cheng et al., 2008). This overwhelming body of evidence suggests that the GlyR contains the necessary functional and structural components to be a relevant target of alcohol and anesthetics.

1.7.3 – ALCOHOL

Of all the other modulators of GlyR function none may be more prevalent and have a greater impact on society than does ethyl alcohol. Commonly known simply as "alcohol", this drug is widely used throughout the world and has been so for thousands of years (McGovern et al., 2004). Alcohol is considered to be a CNS depressant, especially at high doses and produces behavioral disinhibition at lower doses. Other major effects on CNS function include balance and motor disruption, delayed reaction time, and impairment of judgment. At extremely high doses alcohol acts as a general anesthetic,

leading to unconsciousness, respiratory depression, and eventually death. Consumed at low to moderate levels though alcohol has potential benefits including a decreased risk for coronary heart disease and stroke (Fuchs et al., 1995; Thun et al., 1997). But alcohol is frequently consumed for its euphoric effects despite the fact that it is also known to induce rapid mood swings and depression.

Aided by its psychotropic effects, excessive alcohol consumption can lead to abuse and addiction that together take a massive toll on society. For example, the estimated total annual cost of alcohol problems in 1995 was $175.9 billion, exceeding the cost of all other drugs of abuse, including tobacco (Rice, 1999). Adjusted for inflation today this is roughly $246 billion or roughly one quarter of what the US government spends on education. The recent results from the 2008 National Survey on Drug Use and Health provide sobering data on the breadth of alcohol use and related problems in the United States. The survey found that alcohol is widely consumed across age groups > 18 years old and that 46% of adults age 21-25 engage in harmful habits such as binge drinking. Among pregnant women an estimated 5% reported current alcohol abuse, defined as either binge or heavy drinking. This harmful behavior can lead to a developmental disorder known as fetal alcohol syndrome that is characterized by numerous physical and neurological abnormalities in children (Bertrand et al., 2005). Finally, an estimated 30.5 million people (12.5% of the population) reported driving under the influence of alcohol within the past year. Despite the massive costs to society and the staggering rates of use and abuse of this legal drug the molecular underpinnings of alcoholism and alcohol's broad pharmacological effects in the brain are not well understood.

It has been established that ethanol's targets are diverse throughout the brain and include many ligand-gated ion channels such as $GABA_A$, $5\text{-}HT_3$ and nAChR. A growing

amount of evidence suggests that ethanol may mediate at least some of its effects *in vivo* via its enhancement of glycine receptor function (Mihic, 1999; Lovinger, 1999; Narahashi et al., 1999). For example, ethanol results in a loss of righting-reflex, causing animals to have difficulty standing upright. Following recovery from this ethanol-induced loss of righting-reflex, intracerebroventricular injections of glycine result in animals losing their righting-reflex again (Williams et al., 1995). Experiments using knock-in mice containing a point mutation at S267 in the GlyR α1 subunit, found evidence supporting the hypothesis that GlyRs are important targets for the motor incoordinating and anesthetic properties of ethanol (Findlay et al., 2002). Perhaps the most interesting and relevant to alcoholism though, is the evidence that glycine receptors in the nucleus accumbens play a role in the voluntary drinking of ethanol. Microdialysis of glycine into the nucleus accumbens increased extracellular accumbal dopamine levels and was accompanied by a decrease in alcohol consumption by alcohol-preferring Wistar rats (Molander et al., 2005). In contrast, the GlyR competitive antagonist strychnine had the opposite effects. Strychnine applied using microdialysis also prevented increases of accumbal dopamine levels after either local or systemic alcohol administration (Molander and Söderpalm, 2005). In line with these findings, the glycine reuptake inhibitor Org 25935, decreased EtOH intake as well as EtOH preference (Molander et al., 2007). These behavioral studies strongly implicate GlyRs in some of the physiological effects associated with alcohol consumption.

Alcohol seems to be less efficacious as an anesthetic than the volatiles such as enflurane or chloroform, both *in vivo* and *in vitro*. For instance, while enflurane produces an almost 300% potentiation of GlyR function at concentrations of just 1.0 mM, ethanol requires much higher concentrations for much more modest potentiation (Beckstead et al., 2000). This action of ethanol on the α1 GlyR has been well studied at the

macroscopic, whole-cell level. Ethanol potentiates glycine-mediated currents in a concentration-dependant manner with concentrations from 5mM to 200mM producing 10% to 120% potentiation respectively (Mascia et al., 1996b). Other studies have examined ethanol's effects on native CNS neurons. Ethanol (10-40mM) potentiates glycine-evoked currents in isolated rat ventral tegmental area neurons, a brain region widely believed to play an important role in the rewarding effects of alcohol (Ye et al., 2001). At the molecular level, investigations into ethanol's actions have been sparse. A recent study by Eggers and Berger has examined ethanol applied to native $\alpha 1\beta$ GlyRs from rat hypoglossal motoneurons. They found that 100mM ethanol increases the channel P_{open} without affecting conductance (Eggers et al., 2004). This resulted in an increased decay time of the glycinergic currents. Using a kinetic model with four closed states and two open states to simulate GlyR whole cell currents, Eggers et al. determined that ethanol probably acts either to decrease the dissociation (k_{off}) or to increase the association (k_{on}) of glycine.

Extensive research has detailed how mutations to the $\alpha 1$ S267 amino acid residue affect glycine receptor function at the whole cell level. After analyzing all 19 mutations at this residue a few interesting observations stand out. First, the percent enhancment of the GlyR by 200 mM ethanol is inversely correlated with the molecular volume of the residue at the S267 position (Ye et. al, 1998). In fact, bulkier residues at 267 such as phenylalanine (F) and tyrosine (Y) show inhibition of receptor function by ethanol. Secondly, Mihic et al. (1997) earlier showed that the S267I mutation appears to abolish ethanol sensitivity in the GlyR. The analogous mutation in $GABA_A$ receptors (S270I) also produced receptors that were insensitive to ethanol (Mihic et al., 1997). It later became evident that, despite not having any apparent effects on its own, ethanol could still antagonize the enhancement produced by volatile anesthetics on the S267I GlyR

(Beckstead et al., 2001). This research suggested a common binding site for ethanol and anesthetics.

Although most structural studies of alcohol binding initially focused on the putative alcohol binding pocket in between TM2 and TM3, it has also been suggested that there is an inhibitory binding site present in the extracellular loop two of the receptor. Differences in glycine and ethanol sensitivity were noted between GlyRs containing α1 and α2 subunits and these differences were localized to a single amino acid difference between the two subunits in the extracellular domain. When the A52 residue in the α1 subunit was mutated to a serine, a conservative substitution for the threonine present in α2, the α1 A52S GlyR mutant behaved much like α2 GlyR in terms of a decreased ethanol sensitivity (Mascia et al., 1996a). Follow-up investigations found that the A52 residue in the α1 subunit was at least partially responsible for the negative modulation of the homomeric α1 GlyR by ethanol, and also proposed that A52 was a part of the same water-filled pocket that the S267 residue occupies (Crawford et. al, 2007). It may be that the "binding pocket" extends to a larger region in the GlyR protein than previously thought and that multiple ethanol molecules can fit in the pocket to produce opposite effects on receptor function.

There is evidence that other structural components outside the alcohol-binding pocket may play some role in ethanol modulation of the GlyR. For instance, mutation of the protein kinase C (PKC) consensus site on the α1 GlyR results in a reduction of ethanol potentiation, particularly to low ethanol concentrations, and suggests that PKC phosphorylation is important in determining ethanol potentiation (Mascia et al., 1998). This same study determined that protein kinase A (PKA) was not involved in ethanol's effect on the GlyR. Also a growing body of research led in part by Luis Aguayo suggests that intracellular modifications produced by G-protein activation are involved. Aguayo et

al. (1996) noted that the addition of intracellular GTP-γ-S (an irreversible G-protein activator) potentiated the effect of ethanol on glycine-evoked currents in cultured mouse spinal neurons. A similar study performed using neurons from the ventral tegmental area (VTA) of rats also reached the conclusion that alcohol acts, at least in part, through the same pathway as G-protein activators. However G-protein activation in these neurons attenuated the ability of ethanol to potentiate GlyR currents (Zhu and Ye, 2005). Two motifs containing basic amino acids are present on the intracellular loop of the GlyR and these are suggested to be the binding and modulation sites for the Gβγ dimer (Yevenes et al., 2006). Recent experiments using Gβγ-binding proteins to reduce the availability of free Gβγ significantly decreased the ability of low concentrations (1-100mM) of ethanol to potentiate the receptor (Yevenes et al., 2008). These experiments suggest a role for Gβγ in low-dose ethanol potentiation and underscore the possibility that ethanol's modulation of the GlyR may be more complicated than one mechanism alone can explain.

1.8 – Dissertation Aims

The objectives of the research presented in this dissertation were to investigate the mechanism of partial agonism for GlyR activation, determine if partial agonist efficacy can be enhanced by ethanol, and to characterize the kinetics of ethanol modulation of the GlyR.

Aim 1. To study the effect of a gating mutation in the α1 GlyR receptor and determine its implications for the activation of the receptor by partial agonists. The hypothesis to be tested is that a mutation at a residue (D97) that is crucial for maintaining the receptor in the closed-channel state will result in a significant increase in the efficacy of partial agonists.

Aim 2. To determine if ethanol can enhance the efficacy of the partial agonist taurine. The hypothesis to be tested is that ethanol will enhance taurine-activated GlyRs in a manner similar to that of glycine-activated GlyRs; e.g. ethanol will enhance submaximal taurine concentrations but have no effect on maximally-effective taurine concentrations.

Aim 3. To investigate the kinetic mechanisms of homomeric α1 GlyR enhancement by ethanol. The hypothesis to be tested was that ethanol would enhance GlyR function by increasing burst durations.

1.9 – Chapter Overview

The remainder of the dissertation will now be divided into four chapters. Chapter 2 explains the methods applied, materials used, and data analysis procedures in detail. The techniques employed were a combination of whole-cell two-electrode electrophysiology and single channel patch clamp recording, both which were performed using oocytes expressing either mutant or WT α1 GlyRs.

Chapter 3 describes the results of the experiments that tested the hypothesis in Aim 1. Previous research had implicated the D97 residue as participating in a key electrostatic interaction with R119 that stabilizes the closed state of the receptor. This D97R mutation results in a GlyR with a very high probability of opening in the absence of agonist. Previous studies by others demonstrated that taurine has a maximum P_{open} roughly half that of a maximally-effective concentration of glycine on the WT GlyR. We expressed D97R mutants in oocytes and found that the mutation increased the efficacy of taurine and other partial agonists suggesting that the D97 electrostatic interaction is a key element in determining the efficacy of an agonist upon GlyR activation.

Chapter 4 describes the results of the studies that tested the hypothesis in Aim 2. It has been demonstrated that taurine is a partial agonist of the WT GlyR and that this is hypothesized to be due to reduced ability of the taurine-activated channel to reach a flipped state. It is also well established that ethanol enhances glycine-gated GlyR currents. We first wanted to determine if ethanol enhanced taurine activated GlyR function and if so, whether ethanol could increase the efficacy of a maximally-effective concentration of taurine, perhaps by easing the transition to the flipped state. We found that while ethanol could enhance the effects of lower taurine concentrations, it had no

effect at saturating taurine concentrations. This suggests that ethanol does not have a significant effect in increasing transitions to the flipped state.

Chapter 5 describes the results of an investigation that tested the hypothesis in Aim 3. The results from Aim 2 suggested that ethanol does not enhance the GlyR by promoting closed-to-flipped transitions. Therefore, to determine the precise mechanism of ethanol enhancement of the glycine receptor, we examined the effects of 50 mM and 200 mM ethanol on outside-out patches containing WT GlyR. The results were then fit with a kinetic model and used to simulate the effect of ethanol on GlyR function. It was determined that ethanol potentiates GlyR currents primarily by increasing the burst duration without having any other major effect on other parameters of channel function. The kinetic mechanism demonstrated that this enhancement was the result of a decrease in the glycine unbinding rate. This specific effect of ethanol, to increase burst duration without affecting P_{open}, explains why ethanol had no effect on taurine efficacy.

Chapter 6 is an overall discussion of the results of experiments that were detailed in the preceding chapters. General conclusions regarding partial agonism and ethanol enhancement of GlyR function are proposed along with possible directions for future research.

2.0 | MATERIALS AND METHODS

This chapter contains detailed descriptions of the experimental procedures and materials used for the investigations in the following chapters. For the compositions of buffers and solutions mentioned throughout, please refer to Section 2.7 for a comprehensive list. A summary of the methods used, in addition to information regarding specific procedures or deviations that may apply to the experiments, can be found in the methods section of the appropriate chapter.

2.1 – Molecular Biology

The human α1 GlyR subunit cDNA was previously subcloned into a modified pBK-CMV vector that lacked the coding for the *lac* promoter and the *lacZ* start codon (Mihic et al., 1997). The Cytomegalovirus (CMV) promoter allows the α1 subunit to be expressed in heterologous expression systems and contains a gene conferring resistance to the antibiotic kanamycin. GlyR- cDNAs were produced using XL1-Blue *E. coli* (Strategene) that were transformed using the GlyR plasmid. The colonies were then grown on agar plates containing 50 μg/ml of kanamycin in order to select for successfully transformed cells. Colonies were chosen from these plates and grown up in LB broth overnight in a shaker incubator. The GlyR cDNA was then isolated using a HiSpeed Plasmid Maxi Kit and protocol (Qiagen, Valencia, CA). Yield and quality of the isolated plasmids were determined using a NanoDrop spectrophotometer (Thermo Scientific, Wilmington, DE). Preparations with an A_{260}/A_{280} ratio near 1.8 were considered suitable for use.

Point mutations to the α1 GlyR subunit cDNA were made using a QuickCgnage Mutagenesis kit from Stratagene. Custom oligonucleotide primers were designed containing the desired point mutation(s) and ordered from Integrated DNA Technologies. These primers were combined with the template α1 GlyR cDNA and DNA polymerase and run through a thermocycling protocol. After several cycles the reaction product was digested using the *DpnI* restriction enzyme to remove the original methylated template DNA, yielding only the point-mutated DNA. These new plasmids could then be used to transfect XL1- Blue *E. coli* as described above. Verification that the desired point mutation(s) was incorporated into the cDNA was accomplished by sending samples of the constructs for sequencing using a dideoxy fluophore method. Once confirmed, constructs containing the appropriate point mutation(s) were available for use with our expression system.

2.2 – *Xenopus* oocyte harvesting, isolation, and cDNA injection

Xenopus laevis frogs were purchased from Xenopus Express (Homosassa, FL) and housed at 19°C on a 12-hour light/dark cycle. Oocytes were surgically removed from an anesthetized animal through a small incision in the lower abdomen. The incision was closed using a suture and the frog was allowed to recover for future harvesting (up to three times).

The thick membrane protecting the oocytes must be mechanically removed before DNA injection. Stage V and VI oocytes were manually isolated and placed in a hypertonic isolation media. This solution allows for the separation of the oocyte's outer membranes so that the thecal and epithelial layers can be removed using forceps. A 10-min exposure to 0.5 mg/ml Sigma type 1A collagenase buffer was used to remove the

follicular layer of oocytes. The oocytes were then washed and placed in an isotonic solution called modified Barth's saline (MBS).

The cDNA to be used for oocyte injection was diluted to 50 ng/μl using sterile deionized water (diH_20). An injector tip was fashioned from a piece of capillary glass that was pulled using a Sutter Instruments P-30 Flaming/Brown puller. The injector was backfilled with mineral oil and attached to a Drummond Nanoject II injector, which was used to front load a 30 nl sample of cDNA. The cDNA was then injected into the animal poles of oocytes by the "blind" method of Colman (1984). Injected oocytes were then placed into 96-well plates containing incubation media that had been sterilized by passage through a 0.22-μm filter. The plates were stored in the dark at 19°C. Oocytes expressed GlyR within 24 h, and all electrophysiological measurements were made within 1-7 days of cDNA injection.

2.3 – Two-electrode voltage-clamp of *Xenopus* oocytes

Currents were recorded with a Warner Instruments OC-725C Oocyte two-electrode voltage clamp from *Xenopus* oocytes that were heterologously expressing WT or mutant α1 GlyR. The electrodes were pulled from capillary glass (FHC) using a Sutter Instrument P-30 puller to tip resistances of 1-5 MΩ and then filled with 3 M KCl. The MBS or MBS + drug solutions were perfused into the chamber at a rate of 2 ml/min using a peristaltic pump (Cole Parmer Instrument Co, Vernon Hills, IL). A waste line removed build up of the excess fluids from the chamber. Oocytes were placed in a small well within this chamber and impaled in the animal pole with each electrode. One of the electrodes measures the voltage of the cell while the other injects current in order to maintain a set potential. The cells are clamped at –70 mV and activation of the GlyRs

opens the channels and allows chloride ions to flow outward. The voltage electrode detects this flux as a depolarizing force, which causes the current electrode to inject negative current in order to keep the cell clamped at the desired voltage. This feedback loop occurs continuously while the output from the amplifier is recorded by a paper chart recorder (Cole Parmer) and used later for data analysis. For all experiments a maximal concentration of glycine was applied twice for at least five seconds, before starting any experimental protocol.

2.4 – Patch clamp electrophysiology

Patch clamp electrophysiology was used to record currents from outside-out oocyte patches expressing either mutant or WT GlyRs. Before outside-out patches were pulled, the vitelline membrane had to be removed to obtain a proper seal. Thus the oocyte was placed in a high-osmolarity stripping solution for 3-5 minutes before manual removal of the vitelline membrane using forceps. Once removed, the oocyte was transferred to the recording chamber filled with MBS, using a Pasteur pipette being careful to ensure that the oocyte is not exposed to the air. The oocyte was turned in the bath, so that the animal pole faced upwards towards the recording electrode, and allowed to adjust to the MBS solution for at least five minutes. Thick-walled borosilicate glass (WPI, Sarasota, FL) was pulled using a P-97 Flaming/Brown micropipette puller (Sutter Instruments) to form patch pipettes. These pipettes were coated with Sylgard 184 (Dow Corning, Midland, MI) just above the tips and fire-polished with a microforge (Narishige) to obtain a smooth tip with resistances of 8 to 15 MΩ. Sylgard is a silicone polymer that helps to reduce the formation of capacitance transients on the recording electrode. The pipettes were then tip-filled with pipette internal solution. Tip-filling was performed by

attaching a syringe with a piece of tubing, to the back end of the electrode and applying suction using the plunger, while the electrode tip is held in a bead of internal solution that rests on a piece of Parafilm (Pechiney Plastic Packaging Company, Chicago, IL). The tubing was removed and the pipette was then backfilled with inline-filtered internal solution using quartz flexible tubing (WPI).

Outside-out patches were held at -80 mV, and recordings were made according to standard methods (Hamill et al., 1981). First, a slight positive pressure was applied to the electrode before it was lowered into the bath in order to prevent particles from clogging the tip. The electrode tip was moved into close proximity to the edge of the oocyte such that the positive pressure began to make a small dimple in the membrane. The tip was then slowly pressed up against the oocyte until a small increase, generally 0.5-1 MΩ, in the tip resistance was observed. The positive pressure was released and the oocyte membrane was allowed to seal around the glass tip. In order to obtain a giga-seal, it was often necessary to apply a small amount of suction. A slight negative holding potential of -20 mV was applied using the Axopatch 200B amplifier (Molecular Devices, Sunnyvale, CA) to help make the seal. Once the resistance of the cell-attached seal exceeded 1 GΩ the "Zap" button was pressed to break into the cell. This resulted in a drop in the measured resistance and the electrode was then slowly pulled away from the oocyte until the patch re-seals and the resistance again exceeds 1 GΩ. The outer membrane of the cell is now facing into the bath while the intracellular side of the membrane faces the interior of the patch pipette. The amplifier is set to outside-out patch mode, the gain is increased to 50-100x and the holding current is set to –80 mV.

Agonist and drug solution were prepared in MBS before being perfused over outside-out patches using an SF-77B Perfusion Fast Step apparatus (Warner Instruments, Hamden, CT). The bath chamber was continuously filled using a 50 ml syringe

containing MBS, using gravity flow. A vacuum line attached to an L-shaped metal piece of tubing in a separate portion of the recording chamber provided an outlet and maintained a steady bath level. Solutions were loaded in to 20 ml glass syringes that were held above the recording chamber and connected to one of three manifolds with polyethylene tubing. The output of the manifold was connected to a piece of three-barrel square glass and its tip was submerged in the bath. Bubbles were expelled from each line that was in use to ensure that the gravity flow delivery worked properly. The electrode and outside-out patch was moved and placed directly under the middle chamber of the three-barrel glass perfusing MBS. Rapid re-positioning of the perfusion barrel could be achieved to switch the patch from MBS perfusion to MBS + drug perfusion when necessary. Steady state patches remained in the solution for the duration of the recording.

The analog output of the Axopatch 200B was filtered at 10 kHz though the internal 4-pole lowpass Bessel filter and then again at 10 kHz through an external 8-pole lowpass Bessel filter, resulting in a final 7 kHz filter. This signal was then digitized at 50 kHz with a Digidata 1322A (Molecular Devices) and recorded on a PC hard drive running using Clampex 9.0 software (Molecular Devices). Membrane voltage, sampling rate, and the perfusion motor were all controlled using the Clampex software interface.

2.5 – Analysis of macroscopic currents

Macroscopic currents of the peak amplitude resulting from GlyR activity were measured from the chart recorder paper and recorded in an Excel spreadsheet (Microsoft, Redmond, WA). These values were grouped according to condition and the mean and standard error of the mean were determined. Statistical analyses were performed using Sigmaplot software (Systat Software, San Jose, CA). Paired t-tests or one-way ANOVAs

with Tukey's posthoc comparisons were considered significant if $p < 0.05$. Concentration-response data were fit using the following four-parameter Hill equation in Sigmaplot 11.

$$y = \min + (\max - \min)/(1+(x/EC_{50})^{-Hillslope}) \qquad \textit{Equation 2.1}$$

2.6 – Analysis of single channel data

Single-channel data were analyzed using the single-channel analysis programs in QuB (Qin et al., 2000a; Qin et al., 200b). The data were recorded through Clampex before being converted to a QuB format for clean up and analysis. Preprocessing of the data involved removal of noise spikes and other errant signals, baseline correction, and the deletion of bursts containing multiple openings (when present). The current amplitude and standard deviation used to represent the open and closed states was determined by selecting bursts of activity by eye, plotting the amplitudes, and fitting two Gaussian functions. The mean amplitude corresponding to open state was used to determine the chord conductance using Ohm's Law (Equation 1.1). The tracings were then idealized using the segmental-k-means algorithm (Qin et al., 2000a,b). Data were initially idealized with a simple two-state C↔O model.

This initial idealization was then fit with multiple exponentials added sequentially to a star model (closed state as the center) using the maximum interval likelihood (MIL) method after imposing a dead time resolution of 60 μS. MIL fits the open and closed dwell time histograms with the following probability density function:

$$f(t) = \Sigma\, a_i \tau_i^{-1} e^{-t/\tau i} \qquad \textit{Equation 2.2}$$

Once the appropriate numbers of open and closed components (determined by log likelihood, a measure of the quality of the fit) were present, the data were re-idealized

and used for dwell-time analyses. Dwell-time distributions were constructed and fit with a mixture of exponential components again using the MIL function, after the data had been binned using a log-time abscissa and a square-root count/total ordinate. The mean open time was calculated as the weighted mean of the time constants according to the following function:

$$\text{Mean} = \Sigma\, a_i\tau \qquad \textit{Equation 2.3}$$

The data were divided into bursts that were defined as being separated by closed time durations equal to or greater than a critical time (τ_{crit}) between groups of openings. Therefore τ_{crit} was calculated using the closed dwell time histograms. For each patch a τ_{crit} was determined such that an equal number of short and long closed time intervals were misclassified as falling inside and outside bursts (Magleby and Pallotta, 1983) according to the equation:

$$a_1 e^{-\tau crit/\tau_1} = a_2(1 - e^{-\tau crit/\tau_2}) \qquad \textit{Equation 2.4}$$

In this equation a_1 and τ_1 refer to the parameters of the faster closed state component on one side of the τ_{crit} while a_2 and τ_2 refer to the parameters of the slower closed state component on the other side. The τ_{crit} often fell in a distinct valley between closed time components, identifying closed times less than τ_{crit} as within bursts and closed times greater than τ_{crit} as outside of bursts. The data could then be chopped into individual bursts based on this τ_{crit} for further analysis.

The analysis of the bursts was very similar to the open dwell time analysis. A file containing the burst lengths was created after the data were chopped. The histogram of the burst durations were then fit using a mixture of exponential probability density functions (Equation 2.2) using MIL and a star model. This model contained only one closed state and open states (representing burst states) were added to it. The weighted

mean of the individual burst component time constants was used to calculate the mean burst duration (Equation 2.3).

The weighted average of the probability of the channel being in the open state (P_{open}) during a burst was determined as a ratio of the total open time and the total burst duration for each patch. This method of determining intraburst P_{open} was used by Burzomato et al. and provides a more accurate estimate of P_{open} than the other approach, which uses the mean of the individual burst ratios, because this weighted method allows longer burst durations to contribute more to the final P_{open} value (Burzomato et al., 2004). The mean number of openings per burst was calculated as the number of opening events divided by the number of bursts. Both the mean number of openings per burst and the burst lengths were calculated individually per patch and then averaged for each condition.

Statistical analyses were performed using SigmaStat (Molecular Devices), using one- and two-way ANOVAs as well as Student's t-test, as indicated.

2.7 – Chemicals and preparation of drug solutions

All reagents used were purchased from Sigma Aldrich (St. Louis, MO) and the solutions were made up in filtered diH_20. Drug solutions, including glycine, were made up in Modified Barth's Solution (MBS):

MBS - 88 mM NaCl, 1 mM KCl, 2.4 mM NaHCO3, 10 mM HEPES, 0.82 mM $MgSO_4 \cdot 7H_2O$, 0.33 mM $Ca(NO_3)_2$, and 0.91 mM $CaCl_2$, pH 7.5

All buffers were pH adjusted with HCl, NaOH, or CsCl as appropriate. The recipes for the other buffers and solutions are as follows:

Isolation media - 108 mM NaCl, 1 mM EDTA, 2 mM KCl, and 10 mM HEPES

Collagenase media - 83 mM NaCl, 2 mM $MgCl_2$, and 5 mM HEPES, 0.5 mg/ml Sigma Type 1A collagenase

Incubation media - MBS + 2 mM sodium pyruvate, 0.5 mM theophylline, 10 U/ml penicillin, 10 mg/l streptomycin, and 50 mg/l gentamicin

Stripping solution - 200 mM sodium methyl sulfate, 20 mM KCl, 10 mM HEPES, and 1 mM $MgCl_2$

Pipette Internal Solution - 88 mM CsCl, 10 mM HEPES, 0.82 mM $MgSO_4 \cdot 7H2O$, 10 mM EGTA, and 0.91 mM $CaCl_2$, pH 7.4

Ethanol solutions were made by pipetting the appropriate volume of 200 proof ethanol into MBS, covering with Parafilm, and then mixing well.

3.0 | CONVERSION OF PARTIAL AGONISTS INTO FULL AGONISTS AT THE GLYCINE RECEPTOR BY DISRUPTION OF AN INTER-SUBUNIT ELECTROSTATIC BOND: IMPLICATIONS FOR CHANNEL GATING

3.1 – Introduction

The inhibitory glycine receptor (GlyR) is expressed throughout the brain and spinal cord and is a member of the Cys-loop ligand-gated ion channel superfamily. Most GlyR in adults are composed of α1β heteromers, but α1 subunits can also readily form functional homomeric receptors in many expression systems, including Xenopus oocytes (Kuhse et. al., 1995). Glycine has long been thought to be the primary endogenous ligand for the synaptic GlyR, but evidence also exists of a role for taurine tonically activating extrasynaptic GlyR (Mori et al., 2002). The concentration of taurine in the cerebrospinal fluid of mammals is typically 10-100 μM, and in rats taurine concentrations are particularly high in the cerebral cortex, olfactory bulb and cerebellum (Huxtable, 1992); GlyR expression has been noted in all these brain regions (Lynch, 2004). For example, taurine may be acting as an endogenous ligand at GlyR to increase dopamine release in the nucleus accumbens, a brain region implicated in reward (Ericson et al., 2006).

The efficacy of taurine is reported to vary substantially depending on the expression system and GlyR subunit composition tested. Taurine most often acts as a partial agonist with an efficacy between 5 – 60% relative to glycine, on homomeric α1 and α2, and heteromeric α1β and α2β GlyR expressed in BLA neurons (McCool and Botting, 2000), HEK 293 cells (Lape et al., 2008) or *Xenopus* oocytes (Schmieden et al.,

1999). Only in the case of homomeric α1 GlyR expressed in HEK 293 cells has taurine been reported to exhibit full efficacy compared to glycine (Han et al., 2001). A recent study of α1β GlyRs proposes a kinetic model for taurine partial efficacy (Lape et al., 2008). Compared to glycine, taurine has a lower affinity for a pre-open (flipped) state of the GlyR; i.e., transition rates between closed and flipped states vary considerably between agonists and partial agonists. However, once this flipped state is adopted transition rates between flipped and open states are similar for both glycine and taurine. This model of partial agonism suggests that the final opening step in the receptor gating process is the same for both partial and full agonists and that once the flipped state is adopted, both types of agonists have the same efficacy in opening the channel.

The GlyR is composed of five subunits, with each consisting of an extracellular ligand binding domain (LBD), four transmembrane segments, and a large intracellular loop between the third and fourth transmembrane segments. Binding of neurotransmitter produces conformational changes that are rapidly transmitted to the membrane-spanning pore, ultimately opening the ion channel. Previously we showed that mutation of the D97 residue to arginine (D97R) in the LBD of the α1 subunit favors spontaneous transitions of channels to the open state (Beckstead et al., 2002). More recently we found that this spontaneous activity was due to the disruption of a crucial inter-subunit electrostatic bond involving D97 near the glycine-binding site and at least R119 of an adjacent subunit (Todorovic et al., submitted). Single channel recordings showed that spontaneous D97R GlyR openings have a P_{open} of 0.91, very similar to that observed when wildtype α1 GlyR are exposed to a saturating concentration of glycine. A high P_{open} of 0.96 is also observed in α1β GlyR exposed to a saturating glycine concentration; however these receptors exhibit a much lower P_{open} of 0.54 in response to at a maximally-effective concentration of taurine (Lape et al., 2008). We thus hypothesized that the efficacy difference between

glycine and taurine might be due to differences in their abilities to break this inter-subunit electrostatic bond in wildtype GlyR and that in D97R receptors with this bond already broken, taurine should behave as a full agonist.

3.2 – Materials and Methods

Isolation, injection and two-electrode voltage clamp of *Xenopus* oocytes were conducted as described in Chapter 2. Specific methods pertaining to the experiments in this chapter are outlined below.

Oocytes were impaled in the animal poles with two high-resistance (0.5-10 MΩ) glass electrodes filled with 3 M KCl. Using a Warner Instruments OC-725C oocyte-clamp (Hamden, CT), oocytes were voltage-clamped at –70 mV while MBS or MBS + 2.5 mM tricine was perfused over them at a rate of 2 ml/min using a Masterflex USA peristaltic pump (Cole Parmer) through 18-gauge polyethylene tubing. All drug solutions were prepared in either MBS or MBS + 2.5 mM tricine as indicated. Drug applications (5-60 sec) were followed by 5-15 minute washout periods as appropriate.

Detailed methods and solutions for patch acquisition and analysis can be found in Welsh et al. 2009. Briefly, outside-out patches were held at –80 mV and recordings were made according to standard methods (Hamill et al., 1981). Taurine was prepared in MBS + 2.5 mM tricine, which served as the external buffer before being perfused over outside-out patches.

Single channel data were acquired using an Axopatch 200B amplifier attached to a computer running pClamp ver. 9 software (Molecular Devices). Data were digitized at 50 kHz, low-pass filtered at 7 kHz, and stored on a PC hard drive to be analyzed using the single channel analysis programs in QuB (Qin et al., 2000a,b); version 1.5.0.0 was

used for preprocessing and Segments were selected by eye that contained clusters of high activity with only one channel present. These portions were then idealized using the segmental-k-means algorithm (SKM) (Qin et al., 2000a,b). Data were idealized with a simple two-state C↔O model and P_{open} was determined using the QuB 'Select' function.

Statistical analyses were performed using paired t-tests or one-way ANOVAs (some repeated measures, as indicated) with Tukey's posthoc comparisons, using SigmaStat ver. 2.03 (Systat Software).

3.3 – Results

3.3.1 – TAURINE BECOMES A FULL AGONIST ON THE D97R α1 GLYR MUTANT

Oocytes were injected with WT or D97R GlyR α1 mutant subunits in order to compare their responses to both glycine and taurine. Perfusion of either 10 mM glycine or 100 mM taurine produced robust inward currents on WT GlyRs, with taurine eliciting 41 ± 4.5 % of the maximal current produced by glycine (**Figs. 3.1A and B**). On the mutant D97R GlyRs, however, maximal taurine and glycine responses were equal (**Figs. 3.1C and D**). In the WT receptor, the EC_{50} of glycine was 316 μM while the taurine EC_{50} was 1.96 mM (**Fig. 3.1B and Table 3.1**). The D97R mutation reduced the affinity of both glycine and taurine, with EC_{50}'s of 760 μM and 10.5 mM respectively (**Fig. 3.1D and Table 3.1**). The D97R mutation also reduced the Hill coefficients of both taurine and glycine from 1.10 – 1.25 in WT GlyR to about 0.8 for each agonist on D97R GlyR (**Table 3.1**). To eliminate the possibility that zinc, an endogenous GlyR modulator, might be contributing to the measured efficacy of these agonists or contaminating any baseline activity of the channels, all solutions contained 2.5 mM tricine to chelate free zinc (Miller et al., 2008). We tested and confirmed that the addition of tricine did not

change the relative efficacies of the two agonists on either WT or D97R GlyRs (**insets to Figs. 3.1B and D**).

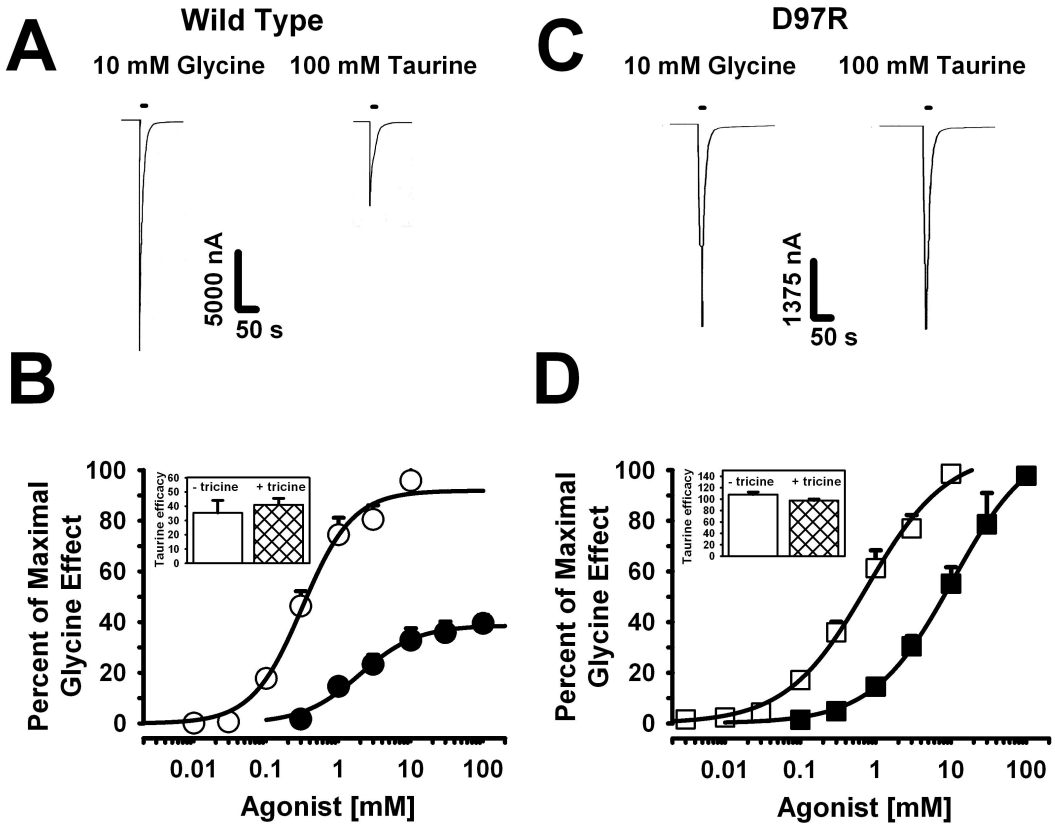

Figure 3.1 The D97R mutation converts taurine from a partial agonist to a full agonist in the α1 GlyR

(A) Representative tracings of whole-cell currents elicited by maximally-effective glycine and taurine concentrations in oocytes expressing WT α1 GlyR. *(B)* Concentration-response curves for glycine (open symbols) and taurine (dark symbols) tested on WT GlyR. A concentration of 10 mM glycine elicited an average current of 27.6 ± 2.9 μA, considerably higher than the 11.8 ± 1.7 μA average current elicited by 100 mM taurine [$t(9) = 8.6$, $p<0.001$]. *(C)* Representative tracings of whole-cell currents elicited by maximally-effective glycine and taurine concentrations in oocytes expressing D97R α1 GlyR. *(D)* Concentration response curves for glycine (open symbols) and taurine (dark symbols) applied to D97R α1 GlyR. A concentration of 10 mM glycine elicited an average current of 3.68 ± 0.37 μA, which was not significantly different than the 3.56 ± 0.36 μA average current elicited by 100 mM taurine [$t(10) = 1.27$, $p>0.23$]. All current values in graphs are normalized to the maximal currents obtained with glycine ($I/I_{max\ glycine}$). *Insets to Figs. 1B and 1D* compare the efficacy of taurine in the absence (empty bars) and presence (hatched bars) of 2.5 mM tricine.

Ligand	α1 WT (4-6)		D97R (3-7)		D97E (3-6)		K281P (6)		D97R/R119E (3-10)	
	EC_{50} (mM)	Hill Slope	EC_{50} (mM)	Hill Slope	EC_{50} (mM)	Hill Slope	EC_{50} (mM)	Hill Slope	EC_{50} (mM)	Hill Slope
Glycine	0.32	1.25	0.76	0.81	1.13	0.77	0.83	1.29	> 300	n.d.
Taurine	1.96	1.10	10.5	0.82	4.74	1.17	28.5	1.85	> 300	n.d.
β-ABA	5.79	0.79	11.7	1.2	9.4	1.26	n.d.	n.d.	n.d.	n.d.
β-AIBA	4.39	0.96	23.7	0.94	n.d.	n.d.	n.d.	n.d.	n.d.	n.d.
	Imax (% of max glycine)									
Taurine	41.0 ± 4.5 (10)		97.5 ± 2.8 (11)		95.6 ± 4.7 (6)		18.4 ± 3.6 (10)		n.d.	
β-ABA	17.3 ± 9.2 (4)		88.9 ± 5.0 (4)		70.9 ± 6.34 (4)		n.d.		n.d.	
β-AIBA	15.3 ± 3.3 (4)		61.0 ± 1.2 (4)		49.2 ± 4.4 (4)		n.d.		n.d.	

Table 3.1 – Summary of responses for WT GlyR and mutants to glycine and partial agonists

Responses from oocytes injected with cDNA from each of the mutants listed. The data from each mutant for all agonists were fit with equation 2.1 listed in the methods chapter. I_{max} values for taurine, β-ABA, and β-AIBA are given as a percentage of maximal glycine current ± the S.E.M. (n) is the number of oocytes used for the experiments.

n.d. not determined

3.3.2 – SINGLE CHANNEL RECORDINGS OF D97R (IN TRICINE)

Figure 3.2 shows single channel tracings obtained from an outside-out patch pulled from oocytes expressing D97R receptors. In the absence of ligand as well as contaminating Zn^{2+}, the D97R receptor displayed spontaneous openings grouped into clusters of channel activity (**Fig. 3.2A**). These clusters had a P_{open} of 0.92 and exhibited the same behavior as that described in the paper by Todorovic et al. (submitted). In that paper we did not use tricine to remove contaminating zinc. The tracings shown in **Fig. 3.2A** in the presence of 2.5 mM tricine demonstrate that contaminating zinc is not the cause of the spontaneous activity in the D97R mutant, nor is it required to observe high P_{open} clusters of channel activity. When a saturating concentration of taurine was applied to the same patch, the P_{open} of the clusters increased slightly to 0.98 (**Fig. 3.2B**). As expected, the conductance of the openings remained unchanged in the presence of taurine and was roughly 90 pS during agonist application.

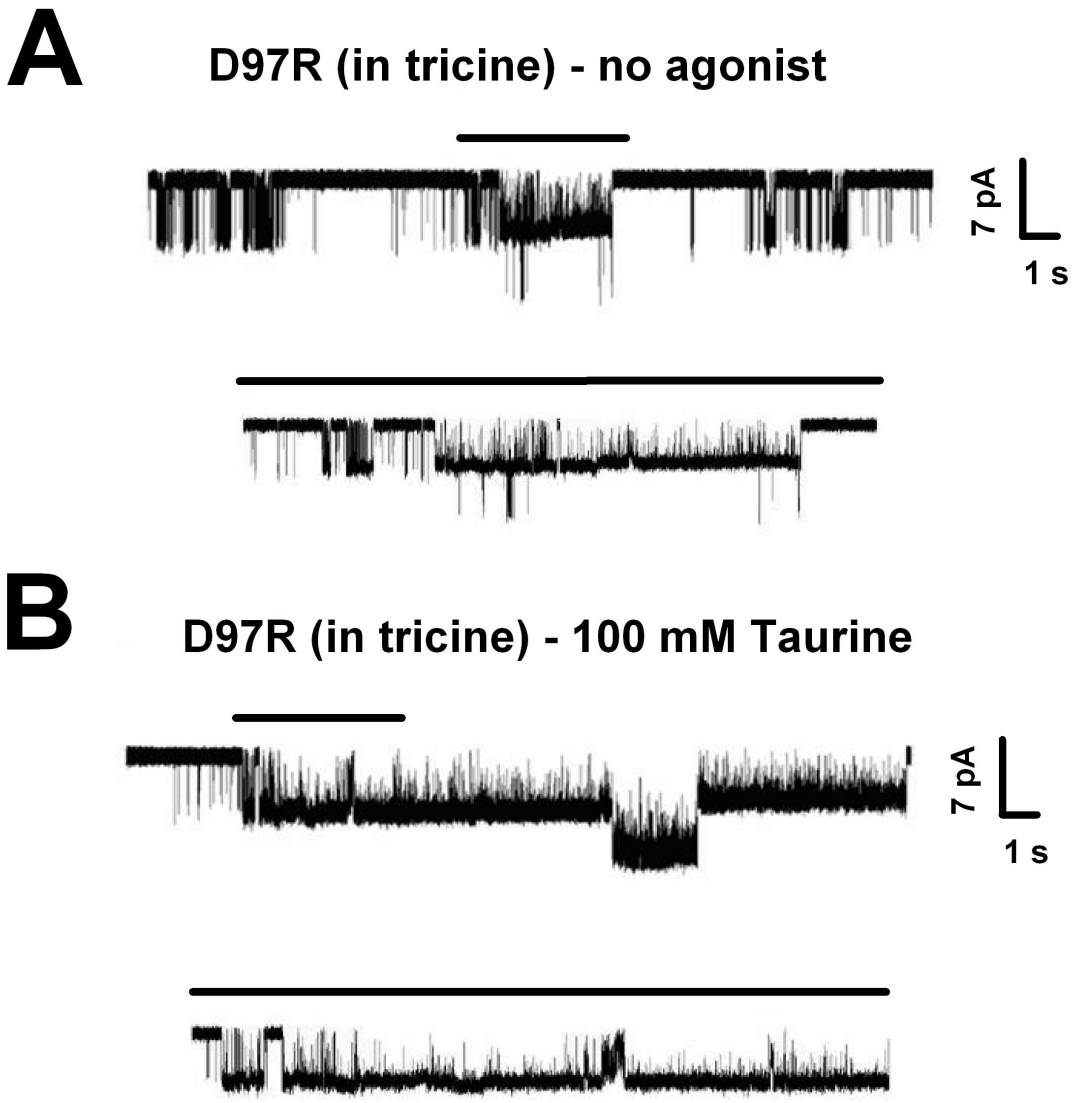

Figure 3.2 – Example traces of D97R single channel activity

(A) Single channel traces were obtained from an outside-out patch pulled from oocytes expressing D97R in the absence of agonist but in the presence of 2.5 mM tricine. The top tracing represents 20 sec of recording while the lower tracing shows an expanded view of the tracing under the horizontal bar shown in the top trace. *(B)* In that same patch 100 mM taurine was applied and recordings generated are displayed as in **Fig. 3.2A.**

3.3.3 – TAURINE AS AN AGONIST ON OTHER SPONTANEOUSLY OPENING MUTANTS

It is possible that the spontaneous activity present in these mutant GlyRs leads to the observed increase in taurine's efficacy and for comparison another spontaneously-active mutant was sought. Previous work in our lab characterizing a mutation at K281 in the TM2-TM3 linker region of the α1 GlyR subunit showed that the insertion of a proline at this site produced receptors that displayed channel opening in the absence of agonist (Dupre et al., 2007). Because the K281P mutation is located in a portion of the receptor structure not contributing to the LBD, it provided an opportunity to investigate whether the efficacy of taurine is determined before reaching this area of the protein or whether a shift in equilibrium towards opening is enough to increase efficacy. In contrast to the D97R mutant, taurine displayed partial agonist activity on receptors containing the K281P mutation. Maximal taurine produced only 18.4 ± 3.6% of the current produced by maximal glycine (**Fig. 3.3A and Table 3.1**). These results suggest that spontaneously activity in general is not sufficient to convert taurine into a full agonist.

To test whether the increase in taurine's efficacy was due specifically to the positive charge introduced at the D97 position, a conservative mutation at this residue was tested. In receptors containing the negative charge-conserving glutamate mutation at D97 (D97E), taurine still behaved as a full agonist, displaying 95.6 ± 4.7% of the current produced by maximal glycine (**Fig. 3.3B**). Additionally, D97E α1 GlyR displayed spontaneous activity and a reduction in both glycine and taurine affinities, similar to the D97R mutant (**Table 3.1**).

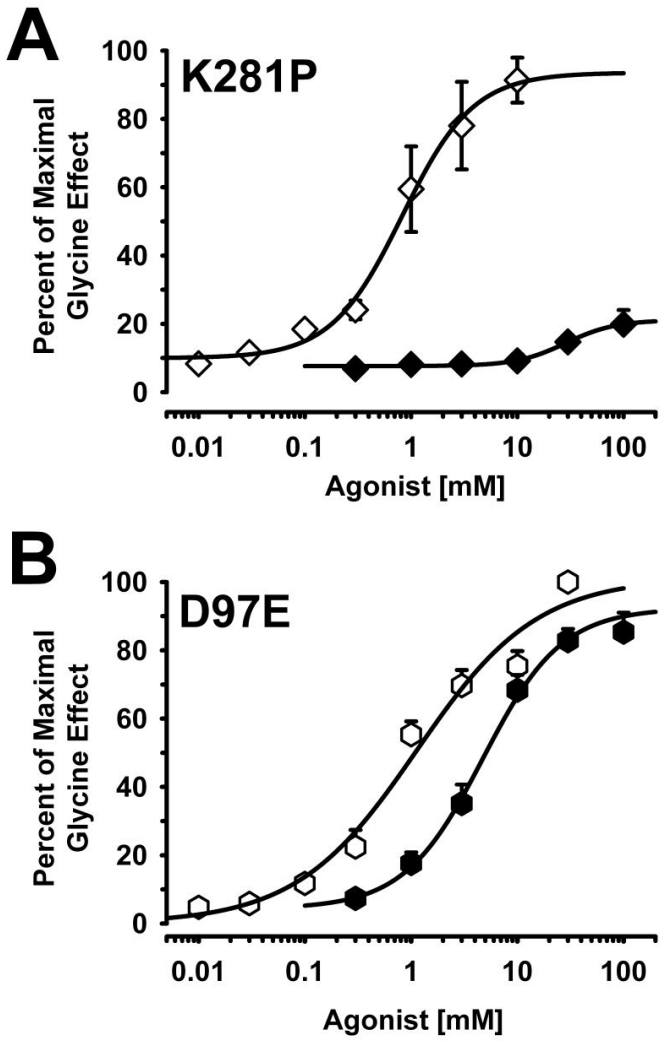

Figure 3.3 – Comparison of a conservative mutation at D97 with a mutation in the TM2-TM3 linker region for their effects on taurine efficacy

(A) Concentration-response curves for glycine (open symbols) and taurine (dark symbols) tested on K281P α1 GlyR. A concentration of 10 mM glycine elicited an average current of 1.27 ± 0.34 μA, considerably higher than the 0.25 ± 0.08 μA average current elicited by 100 mM taurine [$t(9) = 3.7$, $p<0.005$]. *(B)* Concentration-response curves for glycine (open symbols) and taurine (dark symbols) tested on D97E α1 GlyR. A concentration of 10 mM glycine elicited an average current of 11.9 ± 2.9 μA, which did not differ from the 11.4 ± 2.9 μA average current elicited by 100 mM taurine [$t(5) = 0.7$, $p>0.51$]. All current values in graphs are normalized to the maximal currents obtained with glycine (I/I_{max} glycine).

3.3.4 – MUTATIONS AT D97 INCREASE THE EFFICACY OF OTHER β-AMINO ACIDS

β-aminobutyric acid (β-ABA) and β-aminoisobutyric acid (β-AIBA) are also partial agonists of the WT GlyR and both have lower efficacies than taurine (Schmieden and Betz, 1995). We confirmed this in our studies demonstrating that β-ABA- and β-AIBA-induced maximal currents were 17.3 ± 9.2% and 15.3 ± 3.3% of those produced by a saturating concentration of glycine, respectively (**Table 3.1**). The D97R mutation increased the efficacy of both β-ABA and β-AIBA four- to five-fold, indicating that the effect of this mutation to increase the efficacy of a β-amino acid is not specific to taurine. In the case of β-ABA its efficacy increased to 89% that of glycine, while the efficacy of β-AIBA increased to 61% (**Table 3.1**). We also wanted to compare β-ABA and β-AIBA on D97E receptors. These receptors, like the D97R α1 GlyR are tonically active, displaying a holding current of 264 ± 49 nA, significantly higher than the 67 ± 12 nA holding currents that are seen in WT GlyR [$t(18)=3.2$, $p<0.01$]. We reasoned that the conservative D97E mutation might retain some electrostatic interaction with R119 on an adjacent subunit, unlike the D97R charge-reversal mutation, thus limiting the efficacies of β-ABA- and β-AIBA. Interestingly β-ABA and β-AIBA appeared to act on D97E GlyR in a manner that was intermediate between their actions on WT and D97R receptors, although only the D97E vs. WT responses were significantly different from one another (**Fig. 3.4**).

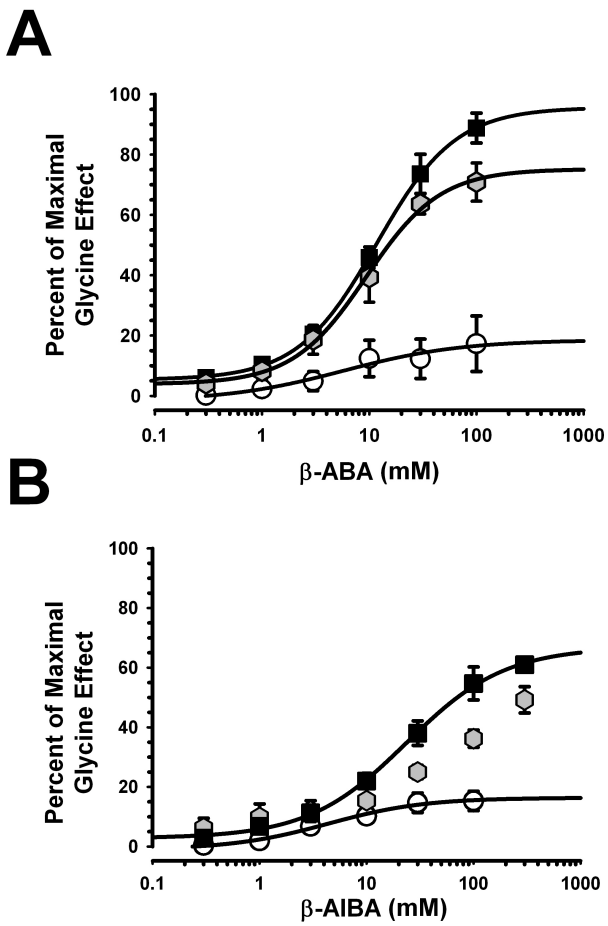

Figure 3.4 – Mutations at D97 increase the efficacy of weak partial agonists

(A) Concentration-response curves were generated for β-ABA on WT (open symbols), D97E (gray symbols), and D97R (closed symbols). One-way ANOVA (not repeated measures) showed significant differences in the responses of β-ABA on the three receptors [$F_{2,9} = 27.8$, $p<0.001$] and Tukey's post hoc comparisons showed significant differences between β-ABA effects on WT vs D97R and WT vs. D97E, but not D97R vs D97E, responses. *(B)* Concentration-response curves were generated for β-AIBA on WT (open symbols), D97E (gray symbols), and D97R (closed symbols). One-way ANOVA (not repeated measures) showed significant differences in the responses of β-AIBA on the three receptors [$F_{2,9} = 53.7$, $p<0.001$] and Tukey's post hoc comparisons showed significant differences between β-AIBA effects on WT vs D97R and WT vs. D97E, but not D97R vs D97E, responses. Current values are normalized to the maximal currents obtained with 10mM glycine (I/I_{max} glycine). Note: the D97E responses to β-AIBA could not be fit to equation 2.1 described in Methods chapter.

3.3.5 – THE CONVERSION OF AN ANTAGONIST TO A PARTIAL AGONIST

We next investigated the theory that partial agonism results from self-inhibition; i.e. that through the rotation around a C-C bond, taurine molecules can exist in either *cis*- (agonist) or *trans*- (antagonist) forms and that the net effect of taurine activation is a sum of these two actions (Schmieden and Betz, 1995). Since the piperidine-derived nipecotic acid mimics this trans- form of beta amino acids such as taurine, we investigated how the D97R mutation affects nipecotic acid pharmacology. As expected, 100 mM nipecotic acid acts as an antagonist on WT GlyRs when co-applied with 200 μM glycine, inhibiting 99.74 ± 0.03% of the current elicited by 200 μM glycine applied alone (**Fig. 3.5A**). In the presence of 200 μM glycine the half maximal inhibitory concentration (IC_{50}) of nipecotic acid was 806 μM with a Hill coefficient of 1.28 (**Fig. 3.5B**). Interestingly, nipecotic acid was clearly a partial agonist on the D97R mutant (**Fig. 3.5C**) and 100 mM nipecotic acid reliably produced inward currents with a magnitude of 460 ± 68 nA (n=5) (**Fig. 3.5D**). This is in contrast to the other spontaneously-active mutant, K281P, in which nipecotic acid stabilized the closed state by inhibiting both glycinergic currents (**Fig. 3.5B**) and its spontaneous activity (**Fig. 3.5D**).

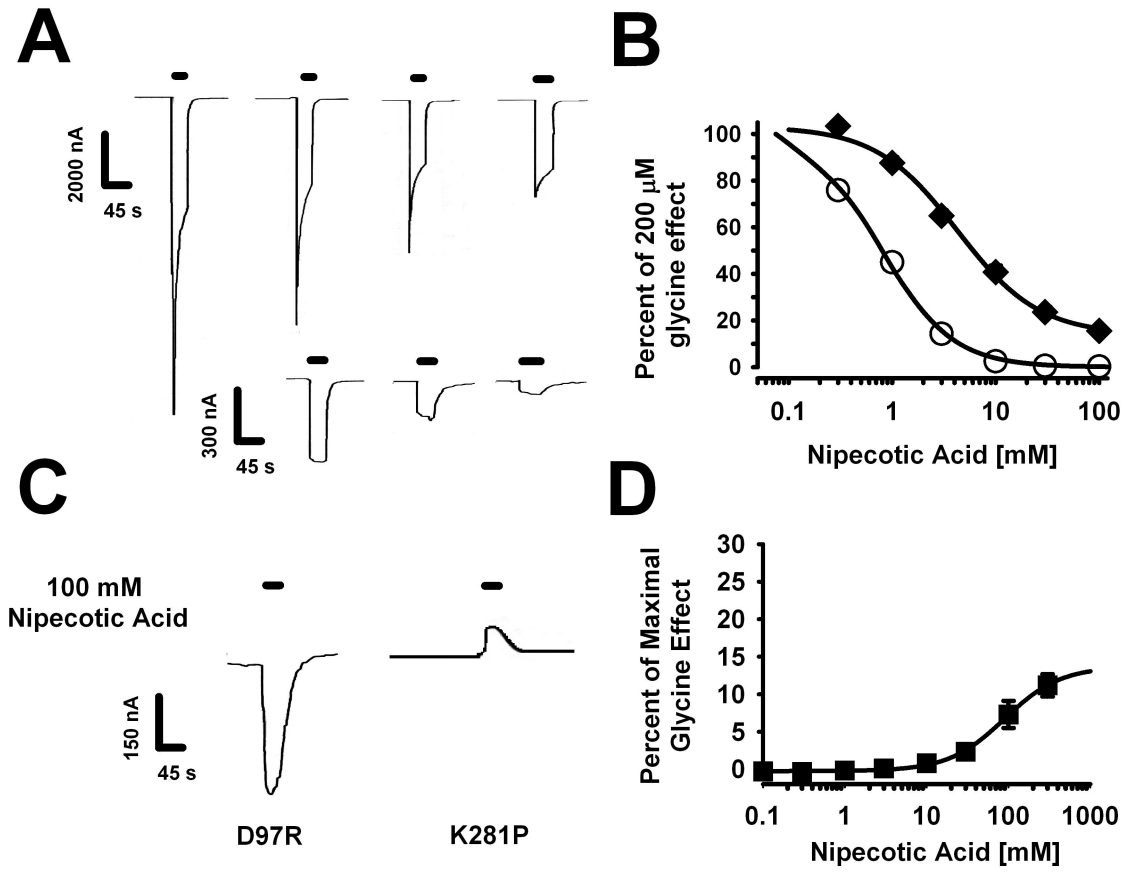

Figure 3.5 – The D97R mutation converts the GlyR antagonist nipecotic acid into a partial agonist

(A) Representative tracings from oocytes expressing WT GlyR demonstrating the inhibition of current responses elicited by 200 μM glycine by increasing concentrations of nipecotic acid. *(B)* Nipecotic acid inhibition of glycinergic currents elicited by 200 μM glycine applied to WT (open symbols) or K281P (closed symbols) α1 GlyR. *(C)* Concentration-response curve for nipecotic acid demonstrating the partial agonist effects of this compound in oocytes expressing D97R GlyR. Current values are normalized to the maximal current obtained with 10mM glycine (I/I_{max} glycine). *(D)* Left, nipecotic acid produces inward currents (activating receptors) when applied alone on D97R GlyR. Right, nipecotic acid produces outward currents (closing spontaneously-open channels) when applied to K281P GlyR.

3.3.6 – RECOVERY OF NIPECOTIC ACID ANTAGONISM WITH THE RESTORATION OF THE D97 ELECTROSTATIC INTERACTION

Mutations at the D97 position in the α1 GlyR disrupt a crucial salt-bridge leading to the spontaneous activity observed in D97R mutant, and this can be nearly eliminated by a second mutation at R119 (Todorovic et al., submitted). We speculated that the restoration of this electrostatic interaction would convert taurine back to a partial agonist so we investigated the double mutant D97R/R119E. This double mutant was extremely insensitive to glycine with an EC_{50} is greater than 300 mM (**Table 3.1**). True efficacy measurements could not be performed for this mutant due to an inability to observe a saturating glycine response. However, at its maximally-soluble concentration, 300 mM taurine produced only 2.9 ± 1.0% (n=7) of the maximal current elicited by 1 M glycine. Oocytes expressing D97R/R119E GlyR generated currents greater than 2 μA in response to 300 mM glycine. Co-application of 100 mM nipecotic acid with 300 mM glycine significantly reduced the current to 79.0 ± 2.2% of that of 300 mM glycine alone (**Fig. 3.6**).

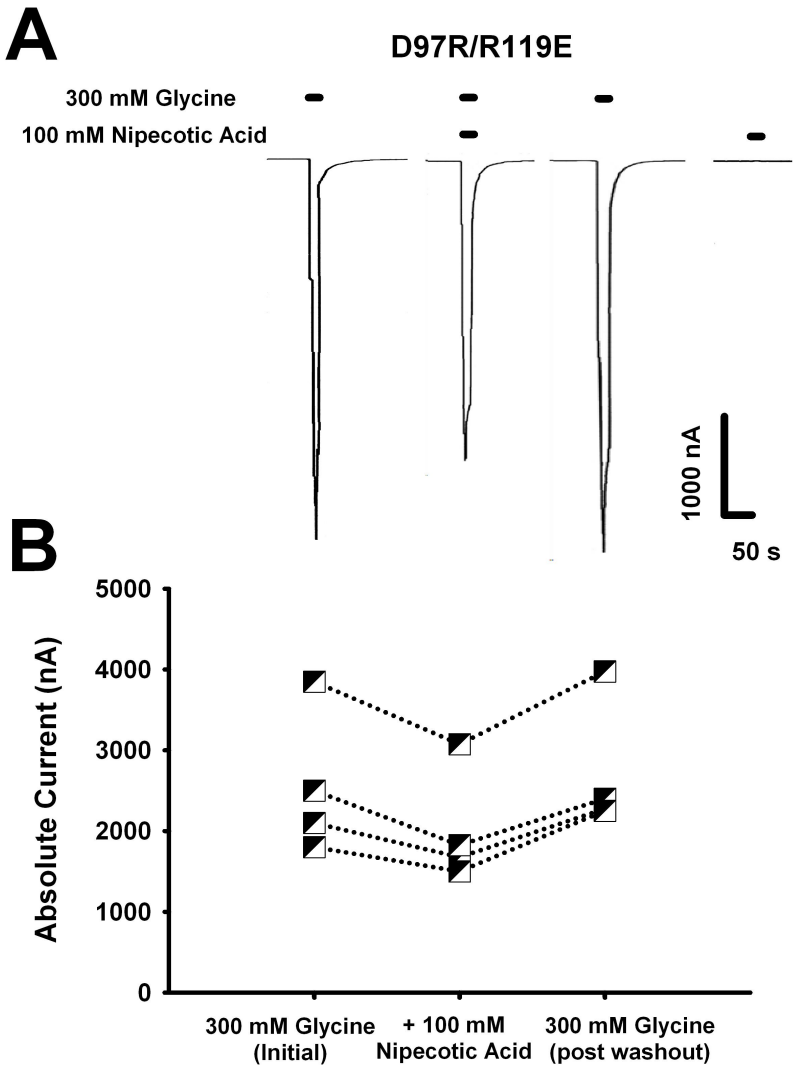

Figure 3.6 – Restoration of the D97-R119 electrostatic interaction restores the antagonist properties of nipecotic acid

(A) Current responses elicited by 300 mM glycine in D97R/R119E α1 GlyR can be inhibited by a co-application of 100 mM nipecotic acid. This concentration of nipecotic acid applied alone has no effect. *(B)* Nipecotic acid significantly inhibits currents evoked by 300 mM glycine and the effect can be reversed after washout as demonstrated by a repeated measures one-way ANOVA [$F(2,11) = 27$, $p<0.001$]. Responses of four oocytes to glycine before, during and after co-application of nipecotic acid are shown.

3.4 – Discussion

Partial agonism is defined as a saturating concentration of a drug not being able to produce a wholly maximal response relative to that produced by a full agonist. According to the two-state receptor theory, for many years it was thought that this diminished response arose from the inability of the partial agonist to effectively shift the receptor gating equilibrium from the closed state to the open state. In other words, efficacy was solely defined by the rates governing the transitions between closed and open states. However, our increased ability to measure fast transitions and the remarkable complexity of ligand-gated ion channel structures suggest that there are a multitude of stages that the protein must pass through following ligand binding, ultimately leading to channel opening. For the acetylcholine receptor, this process has been mapped and the gating of the receptor was described as a Brownian conformational wave of moving parts that begins in the extracellular portion of the receptor at the LBD (Auerbach, 2005; Grosman et al., 2000). Recently it was suggested that the efficacies of agonists and partial agonists in the nicotinic acetylcholine receptor superfamily are determined by transitions from a closed state to an intermediate closed state (flipped) that follows ligand binding but precedes channel opening (Lape et al., 2008). According to this model, efficacy is defined by the rates governing the transitions between closed and flipped states, as well as transitions between flipped and open. In order to explain partial agonism, Lape et al. (2008) postulated that a decreased rate of transitioning from a closed to a flipped state resulted in a lower P_{open} when a saturating concentration of a partial agonist such as taurine was applied, but that transition rates between flipped and open states were similar for partial and full agonists. One conclusion reached by the authors

was that the determination of whether a compound acts as a partial or full agonist occurs early in the process of receptor activation.

Here we focus on the D97 residue, which is well positioned in the LBD to play a role in receptor activation. This amino acid is invariably conserved across the entire nicotinic receptor subunit superfamily, residing at a subunit interface near residues previously implicated in ligand binding (Brejc, 2001). Our previous work demonstrated that D97 forms an inter-subunit electrostatic bond with R119 (Todorovic et. al., submitted), a residue that plays a role in determining glycine affinity (Grudzinska et al., 2005). We noticed that the spontaneous openings of the D97R α1 GlyR appeared to be quite similar to those elicited by a maximally-effective glycine concentration on wildtype GlyR; both generated similar closed and open dwell-time histograms, both exhibited openings grouped into clusters with P_{open} values greater than 0.9 and in both, clusters of channel-opening events appeared to conclude with desensitization (Todorovic et al., submitted). We reasoned that since the breakage of the D97-R119 electrostatic bond results in clusters of spontaneous activity with a very high P_{open}, this breakage represents an important initial step in determining an agonist's efficacy; i.e., our data are consistent with the hypothesis that the breakage of the D97-R119 bond may be a step leading to the GlyR adopting the flipped conformation.

Although the D97R α1 GlyR exhibits spontaneous channel opening, the receptor population also consists of GlyR that are in a closed and activatable state. Spontaneous channel opening results in whole-cell currents typically between 300-500 nA in magnitude, increasing to 3000-5000 nA in the presence of a saturating concentration of glycine. Since tonic activity exhibits a P_{open} of 0.92 it is inconceivable that the greatly increased currents observed after applying glycine are due to an increase in P_{open}; i.e., this must be due to the activation of channels that were previously closed. This suggests that

the breakage of the D97-R119 electrostatic bond is not the sole determinant of channel opening. In some D97R GlyR the channels may be closed until either glycine or taurine bind, whereupon they open with the same efficacy. This suggests that the ligand's ability to disrupt the D97-R119 bond may be crucial for determining its efficacy.

Of particular concern for this study was the possibility that zinc, a potential contaminant (Kay, 2004), might be activating the D97R mutant, resulting in spontaneous activity and possibly affecting the relative efficacies of agonists. Miller et al. (2008) investigated this aspartate residue for its possible role in zinc activation of the GlyR, suggesting that the carboxyl group of D97 may be involved in supporting the protein structure rather than directly binding zinc (Miller et al., 2008). In our single channel tracings of D97R receptors (**Fig. 3.2A**) there is robust spontaneous channel activity observed in presence of the zinc chelator tricine, eliminating the possibility that zinc is a required activator of this mutant channel. In addition, zinc influences the manner in which taurine gates the channel, producing a change in the efficacy of this partial agonist. One study suggests an allosteric role for zinc specifically in the potentiation of taurine-gated currents; i.e. zinc both decreases agonist dissociation and may ease the transition from the closed to open state (Lynch et al., 1998). A later single channel study of zinc GlyR modulation confirmed both of these mechanisms for taurine, with low concentrations of zinc (10 μM) greatly increasing the relative efficacy of this partial agonist (Laube et al., 2000). Here we present a zinc-independent mechanism that increases the relative efficacy of taurine and other partial agonists. The use of tricine in the experiments described above obviates any concerns regarding zinc contributions to the phenomena we observed.

The binding regions for taurine and glycine overlap in the α1 homomeric receptor (Schmieden et al., 1992) and in particular the I111 residue is involved in taurine

activation. Mutations of amino acids (104, 108, and 112) near I111 enhanced the efficacy of β-amino acids (Schmieden et al., 1999). Taurine, and to a lesser extent β-ABA, displayed significantly increased efficacies in these three mutants while efficacy for β-AIBA was not greatly enhanced. In our study the D97R mutation converts taurine and β-ABA into nearly full agonists while also significantly increasing the efficacy of β-AIBA (**Fig. 3.4**). In fact even the conservative D97E mutation results in a receptor in which taurine acts as a full agonist (**Fig. 3.3B**). This supports the idea that the efficacy of a ligand is exquisitely sensitive to this electrostatic interaction involving D97. β-ABA and β-AIBA are low-efficacy partial agonists on the WT α1 GlyR (**Fig. 3.4**) yet they have far greater efficacies on D97R receptors while the D97E mutant exhibits an intermediate phenotype. Ligands could thus be acting as partial agonists on wildtype GlyR because they are not as efficacious as glycine in breaking the D97-R119 bond. In mutants, this bond is weaker or absent, thereby eliminating a barrier to channel activation and increasing the relative efficacies of partial agonists.

The partial agonist properties of β-amino acids like taurine and β-ABA have also been suggested to arise from dual actions of the molecules, such that *trans*- isomers act as antagonists while *cis*- isomers act as agonists on the α1 GlyR (Schmieden and Betz, 1995). One possible explanation for this is that mutations at D97 alter the relative affinities of the *cis*- and *trans*- forms in favor of the former, thus increasing efficacy. To test this hypothesis nipecotic acid was used as a mimic of the *trans*- conformation of β-amino acids. Nipecotic acid acts as an antagonist in wild type receptors (**Fig. 3.5B**) and in previous studies retains its antagonist properties even in mutant receptors in which the efficacies of β-amino acids have been increased (Schmieden et al., 1999). However in the D97R mutant, nipecotic acid not only fails to inhibit the spontaneous activity that is present, it behaves as a partial agonist on these receptors (**Fig. 3.5C**). Furthermore, when

the D97-R119 electrostatic interaction is re-established, as in the D97R/R119E double mutant, nipecotic acid regains its antagonist properties and loses the ability to activate receptors (**Fig. 3.6A**). This suggests that mutations at D97 can convert *trans*- isomers from antagonists to agonists rather than just affecting the relative affinities of the *cis*- and *trans*- forms. In D97R α1 GlyR, the mutation allows *trans*- isomers to act as agonists as shown by the channel activating properties of nipecotic acid and this could also explain why taurine and β-ABA act as full agonists on that receptor.

Taurine did not behave as a full agonist on mutant GlyRs containing the K281P mutation despite this receptor also possessing a spontaneously-open phenotype, implying that the efficacy of a compound is determined before reaching the extracellular TM2-TM3 linker region of the protein. This is in agreement with Han et al. (2004) who studied movement in the residues within the extracellular TM2-TM3 linker region following glycine and taurine activation. They concluded that both taurine and glycine induce the same changes in this region and that the signal from agonist binding is integrated before reaching this domain. In fact, a recent study investigating conformational changes of the GlyR following partial agonist binding suggests that the closed-flip isomerization occurs in the microenvironment near alanine-52, directly above the TM2-TM3 linker (Pless and Lynch, 2009b). This is consistent with our hypothesis that disruption of the D97-R119 salt-bridge is an important step preceding the flipped state, since the A52 residue is located in Loop 2, downstream of the LBD in the proposed activation pathway of the GlyR (Bocquet et al., 2009).

Our data support the notion that ligand efficacy for the α1 GlyR is determined by conformational changes that occur within and near the LBD. We hypothesize that disruption of the D97-R119 interaction is a crucial element in receptor activation and that agonists must be able to efficiently disturb this interaction in order to destabilize the

initial closed state and encourage transitions towards the flipped state. However the role of D97 is not exclusive, i.e. there must be other interactions in the protein structure that allow for some of the receptors to remain closed and activatable state. In the wildtype receptor, full agonists like glycine are able to effectively disrupt these intersubunit interactions at every interface (at saturating glycine concentrations) and subsequently favor transitions towards flipped states while taurine, due to its structure, cannot effectively promote these disruptions. In conclusion our results suggest that the D97-R119 electrostatic interaction is an important element in the determination of whether a drug behaves as an agonist, a partial agonist, or an antagonist.

4.0 | ETHANOL ENHANCES TAURINE-ACTIVATED GLYCINE RECEPTOR FUNCTION

4.1 - Introduction

Many small amino acids such as glycine, taurine and β-alanine act as agonists at the glycine receptor (GlyR) and are found throughout the central nervous system (Shibanoki et al., 1993; Lynch, 2004; Albrecht and Schousboe, 2005). Although glycine is often assumed to be the endogenous ligand activating the GlyR, evidence exists for taurine also functioning as a neurotransmitter in many brain regions. For example, an amino acid uptake inhibitor for taurine increases the strychnine-sensitive current in CA3 pyramidal cells in hippocampal slice preparations (Mori et al., 2002), suggesting that taurine may regulate inhibitory tone by affecting tonic GlyR activity. Taurine has also been detected in the nucleus accumbens where it is hypothesized to act as the primary endogenous ligand for the GlyR (Ericson et al., 2006). In the rat hippocampus extracellular taurine is found at basal concentrations about the same as those of glycine, and NMDA receptor activation increases that 3-5 fold (Shibanoki et al., 1993) .

Unlike the full agonist glycine, taurine and β-alanine act as partial agonists at the GlyR. Taurine has approximately half the efficacy of glycine on homomeric α1 GlyR expressed in Xenopus oocytes and less than 10% of the efficacy of glycine on homomeric α2 GlyR (Schmeiden et al, 1992). A recent study of GlyR kinetics by Lape et al. (2008) showed that the intra-cluster open probability (P_{open}) of channels exposed to a saturating concentration of taurine was 54%, compared to 96% for glycine. By fitting single channel recordings obtained from α1β GlyRs in the presence of taurine or glycine the authors showed that the significant differences in P_{open} between the two were not due to differences in the rates of the final opening and closing transitions but rather in the rates

that governed transitions to and from a pre-open "flipped" state. Hence, the full agonist glycine appears to bind with much greater affinity to the flipped state compared to the resting state than does the partial agonist taurine.

Alcohols and volatile anesthetics act as allosteric modulators in enhancing glycine activation of the GlyR (Mascia et al., 1996a,b). They leftshift glycine concentration-response curves, but display no enhancing effects at saturating glycine concentrations. The mechanisms by which ethanol (EtOH) exerts these effects have recently been determined. Ethanol increases decay times of the glycinergic currents without affecting conductance (Eggers et al., 2004). Using a kinetic model to simulate GlyR whole-cell currents, Eggers et al. (2004) concluded that ethanol probably acts either to decrease the dissociation (k_{off}) or to increase the association (k_{on}) of glycine. In the present report we examined ethanol enhancement of GlyR function, comparing receptor activation by glycine with that produced by taurine. We also hypothesized that ethanol should not affect the magnitudes of currents elicited by maximally-effective taurine concentrations if the primary actions of ethanol are mediated through its effects on the agonist association and/or dissociation rates.

4.2 - Methods and Materials

Isolation, injection and two-electrode voltage clamp of *Xenopus* oocytes were conducted as described in Chapter 2. Specific methods pertaining to the experiments in this chapter are outlined below.

Two high-resistance (0.5-10 MΩ) glass electrodes filled with 3 M KCl were used to impale the animal poles of oocytes. Cells were voltage-clamped at –70mV using a Warner Instruments OC-725C oocyte-clamp (Hamden, CT) and MBS or MBS + 2.5 mM

tricine was perfused over them at a rate of 2 ml/min using a Masterflex USA peristaltic pump (Cole Parmer Instrument Co, Vernon Hills, IL) through 18-gauge polyethylene tubing. All drug solutions were prepared in either MBS or MBS + 2.5 mM tricine. Drug applications (5 - 90 sec) were followed by 6 - 15 minute washout periods as appropriate.

Experimental values are listed as the mean ± standard error. The equation (eq. 2.1): $y = min + (max - min)/(1+(x/EC_{50})^{-Hillslope})$ was used to fit concentration response curves in order to determine the half-maximal effective agonist concentrations (EC50) for each oocyte individually. In one oocyte in the taurine condition, a single datum was dropped as an outlier in order to achieve a proper fit for the concentration response curve.

Paired t-tests or one-way ANOVAs with Tukey's posthoc comparisons were performed using SigmaPlot ver. 11.0 (Systat Software, San Jose, CA).

4.3 - Results

4.3.1 - ETHANOL ENHANCES TAURINE-GATED CURRENTS IN A CONCENTRATION DEPENDENT MANNER

We compared the enhancing effects of ethanol on glycine- and taurine-induced currents elicited by wildtype (WT) α1 homomeric glycine receptors. In the first experiment, ethanol was co-applied, at concentrations of 25, 50, 75 or 100 mM, with a concentration of agonist producing between 5 and 10 percent of a maximally-effective agonist response (EC_5). For taurine the EC_5 concentration used was 5% of the effect of maximal taurine, while EC_5 glycine was calculated as that same fraction of the maximal effect of glycine. Sample tracings of currents elicited by EC_5 glycine or taurine in the absence and presence of 50 mM ethanol are shown in **Fig. 4.1A**. Ethanol was able to enhance both glycine- and taurine-mediated currents, in a concentration-dependent manner (**Fig. 4.1B**). Statistical analyses using a two-way ANOVA showed there was a

significant effect of ethanol concentration [$F(3,71) = 4.54$, $p < 0.006$), but no significant difference in the degree of ethanol enhancement of responses induced by glycine versus taurine [$F(1,71) = 0.09$, $p > 0.76$], and no interaction between the two factors [$F(3,71) = 0.8$, $p > 0.49$].

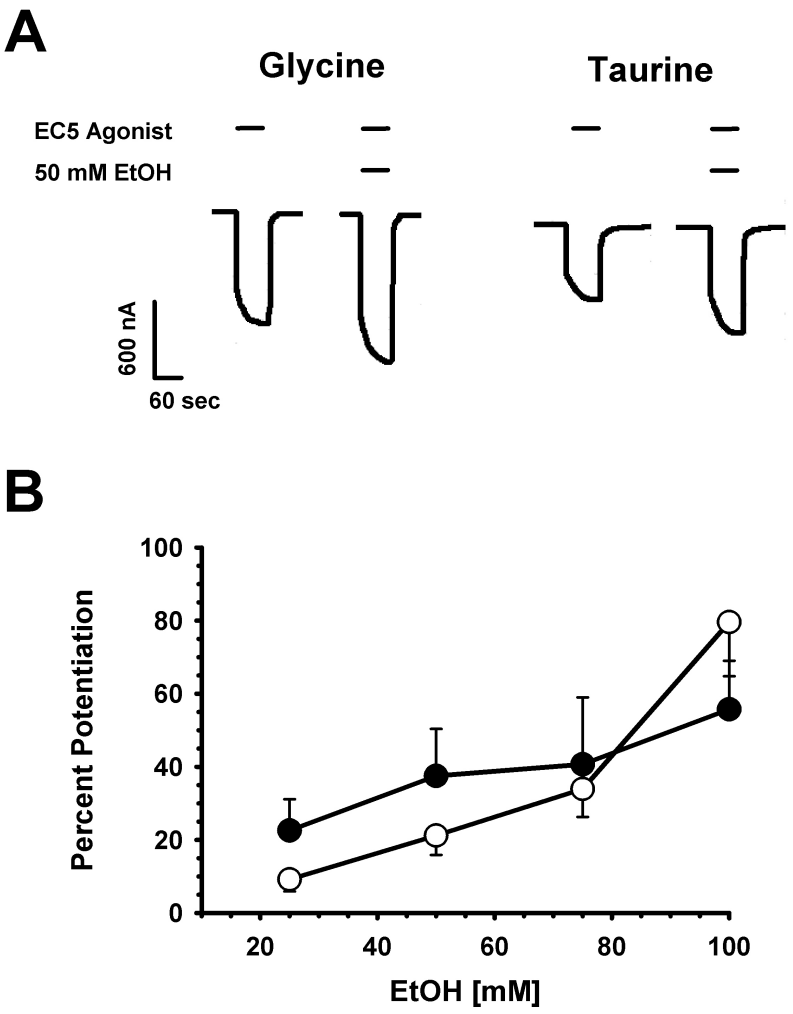

Figure 4.1 - Ethanol enhances glycine- and taurine-activated α1 GlyR in a concentration-dependent manner.

(A) Sample tracings of ethanol potentiation of glycine and taurine responses. Each pair of traces shows EC_5 agonist and EC_5 agonist co-applied with 50 mM EtOH applied for 60 sec. The left pair of tracings show glycine activation of GlyR while taurine responses are shown on the right. *(B)* Concentration-dependent potentiation of glycine and taurine responses by ethanol. The ordinate represents the percent potentiation of responses seen in the presence of EtOH compared to those produced by agonist applied alone. Open circles depict EtOH enhancement of glycine-activated α1 GlyR (n=6) and filled circles depict EtOH enhancement of EC_5 taurine responses (n = 12). Data are shown as mean + or - the standard error of the mean (S.E.M.).

4.3.2 - ETHANOL DOES NOT POTENTIATE CURRENT RESPONSES OF MAXIMALLY-EFFECTIVE CONCENTRATIONS OF GLYCINE AND TAURINE

Next we compared the effects of 200 mM ethanol on GlyR responses elicited by saturating concentrations of glycine and taurine. **Fig. 4.2A** shows that taurine produced smaller maximal currents than did glycine, in keeping with its classification as a partial agonist. EtOH (200 mM) did not affect currents produced by either 10 mM glycine or 100 mM taurine. Average responses are shown in **Fig. 4.2B** and the effect of 200 mM EtOH on maximally-effective agonist concentrations did not differ significantly between glycine and taurine [$t(10) = 0.63$, $p > 0.54$].

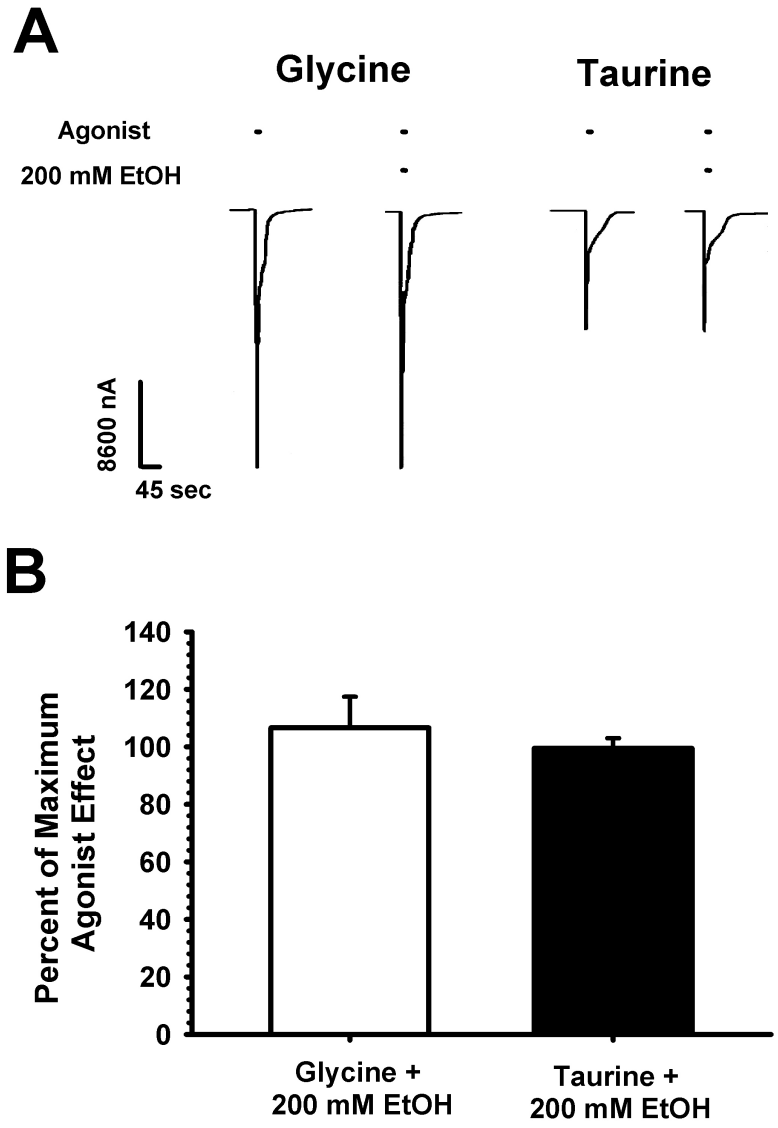

Figure 4.2 - Ethanol does not affect maximally-effective glycine and taurine responses.

(A) Sample tracings of saturating concentrations of glycine or taurine with and without 200 mM ethanol. The left pair of tracings show the effects of 10 mM glycine and 10 mM glycine + 200 mM EtOH with the right pair of traces show 100 mM taurine and 100 mM taurine + 200 mM EtOH effects. *(B)* Average effects of 200 mM EtOH on glycine and taurine responses. The ordinate depicts the percent current observed in the presence of 200 mM EtOH compared to that produced by glycine (open bar) and taurine (filled). Data are shown as mean + or - S.E.M. of six oocytes.

4.3.3 - ETHANOL DOES NOT POTENTIATE CURRENT RESPONSES OF MAXIMALLY-EFFECTIVE CONCENTRATIONS OF GLYCINE AND TAURINE

Previous studies demonstrated that ethanol acts as an allosteric modulator by leftshifting glycine concentration-response curves. We examined the effects of EtOH on currents observed in response to application of various concentrations of glycine and taurine, expressing all responses as a percentage of the current elicited by a saturating (10 mM) concentration of glycine (**Fig. 4.3**). Glycine activated the α1 GlyR in a concentration-dependent manner with EC_{50} of 0.31 ± 0.04 mM and a Hill coefficient, n_H of 1.47 ± 0.16. Addition of 100 mM ethanol leftshifted the glycine concentration-response curve, increasing potency ~1.6 fold but producing no change in efficacy (EC_{50} = 0.19 ± 0.01 mM, nH = 1.24 ± 0.14). Taurine applied alone (EC_{50} = 1.20 ± 0.07 mM, n_H = 1.40 ± 0.15) was about four-fold less potent than glycine and possessed 49% of its efficacy. Responses to taurine + 100 mM ethanol were leftshifted from the taurine alone curve, producing a ~2.3 fold increase in taurine potency (EC_{50} = 0.52 ± 0.04 mM, n_H = 1.35 ± 0.34). EtOH significantly decreased agonist EC_{50}s for both glycine [$t(6) = 3.28$, $p < 0.018$] and taurine [$t(6) = 8.39$, $p < 0.001$]. The percent decrease in agonist EC_{50} produced by ethanol was not significantly different when the receptor was activated by glycine compared to taurine [$t(6) = 1.85$, $p > 0.11$).

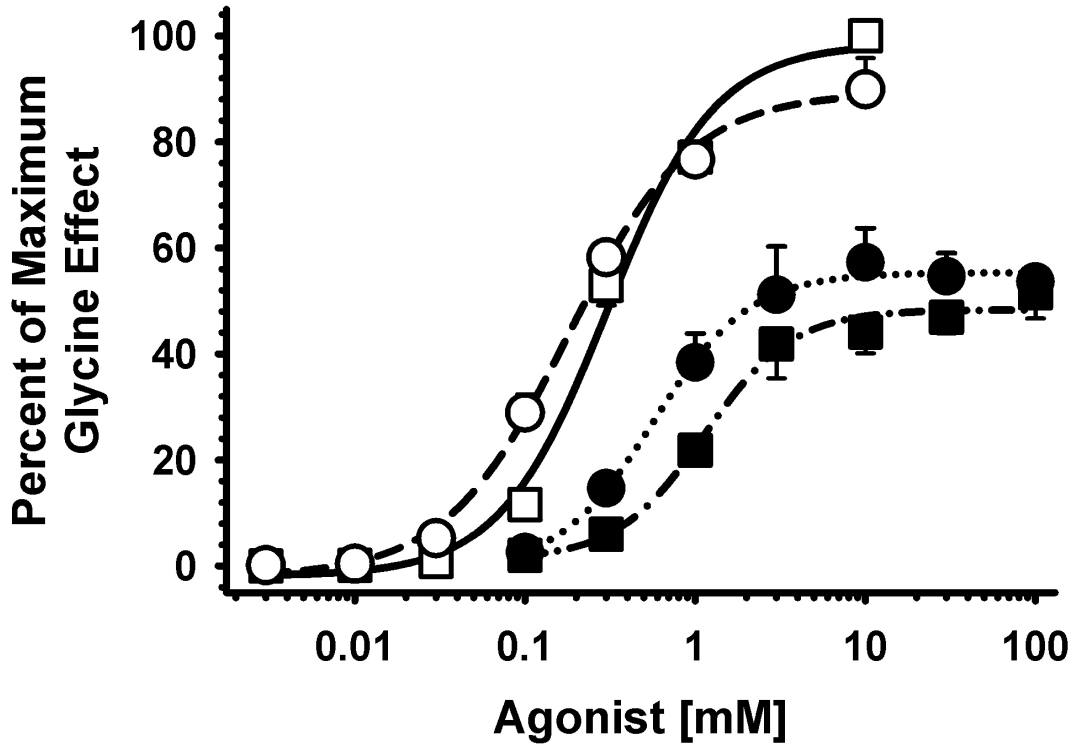

Figure 4.3 - Ethanol shifts glycine and taurine concentration-response curves to the left.

Open symbols represent glycine responses and filled symbols show taurine-mediated currents. Squares are responses elicited by agonist applied alone, and circles are agonist + 100 mM EtOH. Drug applications lasted 60 sec and all responses are expressed as percentages of the effects of 10 mM glycine. Lines are logistic fits to each set of data. Data are shown as mean +/- S.E.M. of four oocytes.

4.3.4 - REMOVAL OF ZINC DECREASES ALCOHOL POTENTIATION OF TAURINE-GATED CURRENTS

Recently we discovered that the zinc chelator tricine decreases the magnitude of EtOH potentiation of GlyR currents, suggesting that these two allosteric modulators interact in a synergistic fashion to enhance GlyR function (McCracken et al., in press). We tested if this synergism was also seen when EC_5 taurine activated the GlyR (**Fig. 4.4**). The filled circles in **Fig. 4.4** represent the same responses to EC_5 taurine plus four concentrations of ethanol as those shown in **Fig. 4.1**. The filled triangles show responses to the same concentrations of taurine + ethanol but in the presence of 2.5 mM tricine in the bath. Although the magnitude of EtOH enhancement was lower when tricine was present this did not reach the point of statistical significance [$F(1,60) = 1.50$, $p > 0.22$].

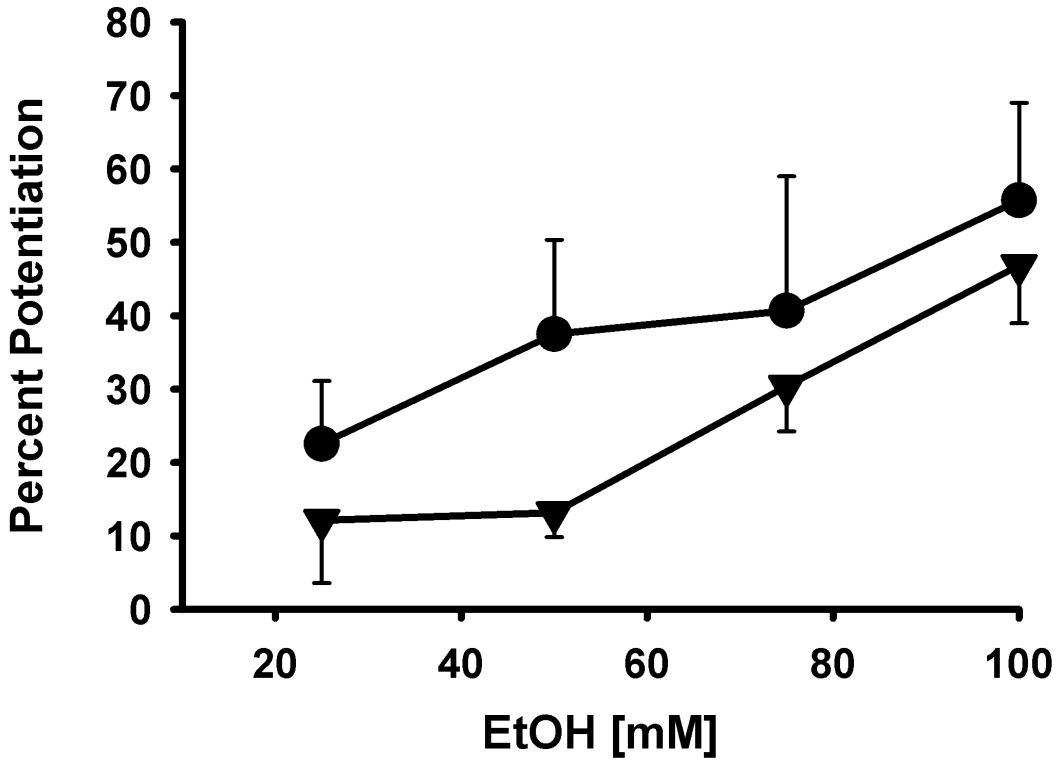

Figure 4.4 - The zinc chelator tricine decreases ethanol enhancement of taurine-mediated responses.

EC_5 taurine was applied with or without 25 – 100 mM EtOH for 60 sec in the absence or presence of 2.5 mM taurine. Ethanol concentration is plotted against percent potentiation compared to EC_5 taurine applied alone, with (filled triangles) or without tricine (filled circles). Data are shown as mean +/- S.E.M. of 5-12 oocytes.

4.3.5 - THE S267I MUTATION ELIMINATES THE ABILITY OF ETHANOL TO POTENTIATE TAURINE-ACTIVATED GLYCINE RECEPTORS

Lastly, we repeated previous experiments looking at ethanol effects on EC_5 taurine responses, but this time studying a mutant of the α1 homomeric GlyR in which residue serine-267 was mutated to isoleucine (S267I) (**Fig. 4.5**). Previous work showed that the S267I mutant was insensitive to the potentiating actions of EtOH, instead displaying a weak inhibitory effect on glycine-activated S267I α1 GlyR (Mihic et al., 1997). **Fig. 4.5A** shows sample traces resulting from EC_5 taurine applied alone and in the presence of 25, 50, 75, or 100 mM ethanol. Responses to application of taurine + ethanol on S267I α1 GlyR showed either slight inhibition or no effect compared to taurine applied alone.

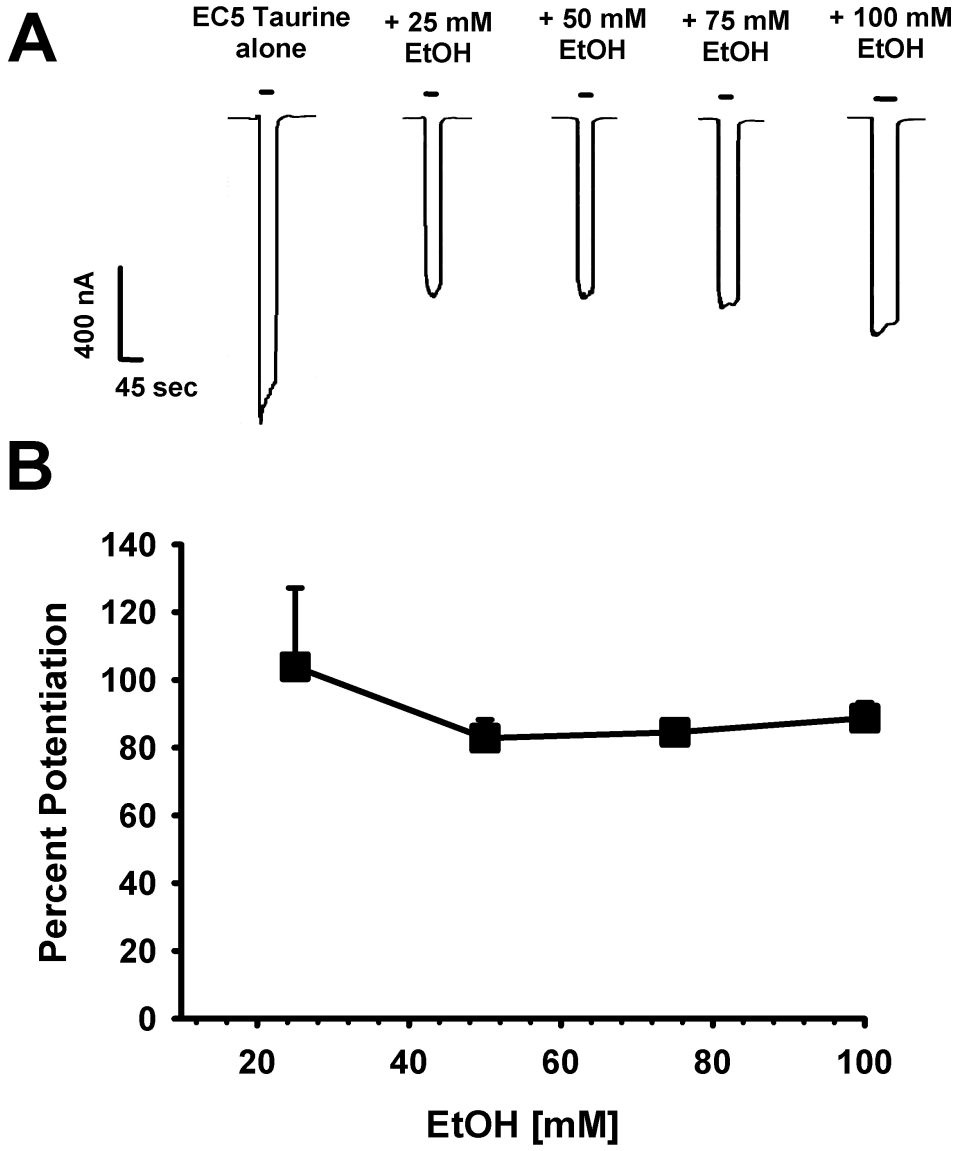

Figure 4.5 - Ethanol does not enhance taurine-mediated currents in the S267I mutant.

(A) Sample tracings of the effects of EC_5 taurine alone and taurine co-applied with 25, 50, 75 or 100 mM EtOH on current responses in S267I α1 GlyR. *(B)* Ethanol concentration is plotted against ethanol-induced percent potentiation of current compared to EC_5 taurine applied alone. Data are shown as mean +/- S.E.M. of four oocytes.

4.4 - Discussion

The mesolimbic dopamine pathway of the brain, which includes a dopaminergic projection from the ventral tegmental area to the nucleus accumbens, is thought to mediate the rewarding effects of many drugs of abuse including ethanol (Gonzales et al., 2004). At least some ethanol effects in this brain region appear to be due to its enhancement of GlyR function since microdialysis of glycine into the nucleus accumbens increases extracellular accumbal dopamine levels, resulting in a decrease in alcohol consumption by alcohol-preferring Wistar rats (Molander et al., 2005). Recently it was suggested that taurine rather than glycine may be the endogenous ligand acting on GlyR in the nucleus accumbens, as taurine perfusion into the accumbens leads to significant increases in dopamine release (Ericson et al., 2006). Since no studies had yet been performed on ethanol modulation of taurine-activated GlyRs, we compared the actions of ethanol on α1 homomeric GlyR activated by taurine with those activated by glycine.

Our study shows that ethanol enhances GlyR currents elicited by low concentrations of either glycine or taurine, with EtOH concentrations in the 25 – 100 mM range producing similar enhancement of the effects of each agonist. Previous work demonstrated that ethanol and octanol do not potentiate currents elicited by maximally-effective glycine concentrations (Mascia et al., 1996a,b), in agreement with our present findings. Because taurine possesses lower efficacy at the α1 GlyR, we determined whether ethanol-induced enhancement might also be observed at saturating concentrations of this partial agonist. Since the P_{open} of a saturating concentration of glycine is above 90% one could hypothesize that the lack of alcohol enhancement of maximally-effective glycine concentrations was due to a ceiling effect in P_{open}, assuming EtOH affected P_{open}, but no such ceiling effect would be expected with taurine which has

a P_{open} of about 50%. However, our data show that ethanol does not enhance GlyR function in the presence of saturating concentrations of taurine. These findings suggest that ethanol enhances taurine-gated GlyR currents by a mechanism similar to that by which it potentiates glycine-activated GlyRs.

In a recent paper, Lape et al. (2008) proposed that the efficacy disparity between glycine and taurine was the result of differences in the abilities of agonists to transition the receptor to an intermediate 'flipped' state before eventually opening the channel. Since EtOH does not increase the efficacy of saturating taurine or glycine concentrations, it suggests that alcohol doesn't promote the transition of the agonist-gated receptor from closed to flipped states. Interestingly, this may be somewhat different from the mechanisms of alcohol modulation of a partial agonist on the related 5-HT3 receptor. Using dopamine as the low-efficacy agonist, 100 mM ethanol was shown to significantly increase the response to a saturating concentration of dopamine by more than 50% (Lovinger et al., 2000). The authors concluded that ethanol potentiates 5-HT3 receptor function at least in part by increasing P_{open}; however they could not exclude the possibility that ethanol also had effects on agonist affinity that were not measurable using their experimental paradigm.

Zinc, another allosteric modulator of the GlyR, may be an important factor to consider when studying GlyR function. Zinc is found throughout the CNS, often co-localized with the GlyR and synaptically released in areas such as the hippocampus and spinal cord (Vogt et al., 2000; Schrøder et al., 2000). At low concentrations zinc enhances the effects of both glycine and taurine on the α1 GlyR (Miller et al. 2005; Miller et al. 2008). Detailed single channel studies of the mechanisms of zinc potentiation of the GlyR concluded that zinc's main effect was to produce a roughly four-fold increase in mean burst duration that kinetic modeling suggested was due to a

decrease in the unbinding rate of glycine (Laube et al., 2000). Of particular note however, is that zinc may potentiate taurine-activated GlyRs through a different mechanism than glycine-activated receptors because Zn^{2+} increases taurine, but not glycine, efficacy. It seems that, in addition to zinc decreasing taurine dissociation, as for glycine, it also increased transition rates from closed to open channel states, thereby promote gating (Laube et al., 2000). The investigators concluded that this constituted some evidence for a separate gating pathway for taurine.

In this study we used tricine to chelate zinc and show a decrease in the ability of ethanol to modulate the taurine-activated receptor. This indicates that there may be an interaction between the zinc signal and the ethanol signal during channel activation by taurine. This appears similar to the results obtained by McCracken et al. (in press) who showed that tricine significantly reduced the degree of ethanol potentiation observed. As originally proposed by the authors, it may be that ethanol and zinc act in concert to increase agonist affinity and that this conclusion holds true for taurine as well as glycine. In comparing alcohol effects on glycine- versus taurine-activated α1 GlyR we also investigated a single amino acid mutation that reduces ethanol potentiation of glycine-activated currents of the receptor to determine if similar effects were observed using a partial agonist. The S267 residue is proposed to play a role in the binding of alcohol and anesthetics, composing part of a binding pocket for these drugs (Mihic et al., 1997). The size of the residue at S267 has been shown to be inversely correlated with degree of ethanol potentiation, with the S267I mutation eliminating the enhancing effects of ethanol (Ye et al., 1998). When the S267I mutant was tested using EC_5 taurine as the agonist, slight inhibition of receptor function was observed in the presence of ethanol. This suggests that any differences that occur in the gating pathway between agonist binding and channel opening for glycine versus taurine converge by the time the gating signal

approaches the alcohol binding pocket between transmembrane segments two and three. This result is in agreement with a study showing that taurine and glycine produce similar conformational changes in this area (Han et al., 2004).

In conclusion, we compared ethanol enhancement of GlyR activated by the full agonist glycine with activation produced by the partial agonist taurine. In both cases EtOH shifted agonist concentration-response curves to the left and had no effects at saturating agonist concentrations. In addition, EtOH enhancement of taurine function was decreased in the presence of the zinc chelator tricine and absent in the S267I mutant, which we previously also reported for glycine. These data suggest that EtOH enhances the effects of taurine by mechanisms very similar to those of glycine. Our findings illustrate that taurine activation of the GlyR can be enhanced by pharmacologically-relevant EtOH concentrations and are timely given an increasing awareness of possible taurine effects on GlyR in vivo.

5.0 | SINGLE CHANNEL ANALYSIS OF ETHANOL ENHANCEMENT OF GLYCINE RECEPTOR FUNCTION

Portions of this chapter were published in an article in the *Journal of Pharmacology and Experimental Therapeutics* in July 2009 and are reprinted with permission of the American Society for Pharmacology and Experimental Therapeutics.

5.1 – Introduction

Glycine receptors (GlyR) constitute the major inhibitory neurotransmitter receptor system in the brainstem and spinal cord, but are also found in significant numbers in higher brain regions such as the olfactory bulb, midbrain, cerebellum and cerebral cortex (Betz, 1991). Along with the $GABA_A$, $GABA_C$, nicotinic acetylcholine and serotonin-3 receptors, the GlyR is a member of a large receptor superfamily of subunits, sharing a number of structural features: an extracellular N-terminal region that contains neurotransmitter-binding domains, four transmembrane (TM) domains, and a large intracellular loop between the third and fourth TM domains. Receptors in this superfamily contain an integral ion channel that selectively conducts anions in the case of GABA and glycine receptors, and each receptor is composed of five subunits. There are two classes of glycine receptor subunits: the α subunits, of which there are 4 subtypes, and one β subunit (Lynch et al., 2004). Most native GlyRs in adult animals consist of heteromeric $\alpha1\beta$ subunits, although homomeric $\alpha2$ subunits are the predominant form

found prenatally (Rajendra and Schofield, 1995). The glycine α, but not β, subunits can form homomeric receptors that express well in a variety of receptor expression systems.

Volatile anesthetics, propofol and alcohols enhance GlyR-mediated currents (Mascia et al., 1996a, 1996b). Electrophysiological studies show that ethanol (EtOH) enhances GlyR function in mouse and chick embryonic spinal neurons in a concentration-dependent manner (Celentano et al., 1988; Aguayo and Pancetti, 1994). The glycine EC_{50} is decreased by 100 mM EtOH, with no effect on the maximal glycinergic currents (Aguayo et al., 1996); i.e., EtOH left-shifts glycine concentration-response curves. Furthermore, concentrations of EtOH that enhance GlyR function in mouse spinal cord neurons (10-200 mM) have no effects on membrane lipid order (Tapia et al., 1998), suggesting a protein site of action. Studies using dissociated ventral tegmental area neurons also demonstrate EtOH enhancement of glycine receptor function (Ye et al., 2001). Finally, EtOH increases glycine-mediated chloride uptake into rat brain synaptoneurosomes (Engblom and Åkerman, 1991).

Structure-function studies involving amino acid mutations in GlyR subunits were conducted in an attempt to eliminate the actions of alcohols and thereby infer a site of ethanol action. Our initial studies (Mihic et al., 1997, Wick et al., 1998) suggested that amino acids in transmembrane (TM) regions two and three of these receptor subunits play a critical role in alcohol modulation of channel function, although TM1 and TM4 residues have also been implicated (Lobo et al., 2004, 2006, 2008). These data support the hypothesis that a water-filled cavity exists among the TM regions in which alcohols can act. Altering the sizes of amino acids lining this cavity also affected the size of alcohol that could fit and affect GlyR function (Wick et al., 1998). In addition, Crawford et al. (2007) implicated an amino acid in the extracellular N-terminal domain as also constituting part of this alcohol binding pocket, concluding that different amino acids

within the pocket are responsible for enhancing and inhibiting effects of ethanol on GlyR function. Application of alcohol-like thiol compounds such as propyl methanethiosulfonate to glycine receptors mutated to cysteine at critical residues identified which specific amino acids are important for this alcohol inhibition and potentiation (Mascia et al., 2000, Lobo et al., 2006, Crawford et al., 2007).

That EtOH potentiates glycinergic currents is well established, but the mechanisms by which this occurs remain poorly understood. We report on a series of studies we conducted on human α1 homomeric GlyR expressed in *Xenopus* oocytes, investigating a variety of single channel parameters for their sensitivities to modulation by intoxicating and anesthetizing concentrations of EtOH. We examined channel conductance, open and closed dwell times, as well as a variety of channel burst properties, determining that EtOH exerts its enhancing effects primarily by increasing burst durations. Kinetic modeling suggests that these increases in burst duration arise due to an EtOH-induced antagonism of glycine unbinding.

5.2 – Methods and Materials

Isolation, injection and two-electrode voltage clamp of *Xenopus* oocytes were conducted as described in Chapter 2. Specific methods pertaining to the experiments in this chapter are outlined below.

Ooctyes were surgically removed from *Xenopus laevis* housed at 19C on a 12hr light/dark cycle. Stage V and VI oocytes were manually isolated and placed in isolation media where the thecal and epithelial layers were manually removed using forceps. A 10-minute exposure to 0.5 mg/ml Sigma type 1A collagenase in buffer was used to remove the follicular layer of oocytes. A 30 nl sample of the glycine α1 receptor subunit

cDNA (1.5 ng/30 nl) in a modified pBK-CMV vector (Mihic et al., 1997) was injected into the animal poles of oocytes by the "blind" method of Colman (1984), using a digital microdispenser loaded with a micropipette with a 10 - 15 m tip size. Oocytes were stored in 96-well plates in the dark at 19°C in Modified Barth's Saline (MBS) sterilized by passage through a 0.22 micron filter. Oocytes expressed GlyR within 24 hours and all electrophysiological measurements were made within 5 days of cDNA injection. Before outside-out patches were pulled, the oocyte vitelline membrane was removed with forceps after placing the oocyte in a high-osmolarity stripping solution. The oocyte was then transferred to a bath containing MBS for patches to be pulled.

Outside-out patches were held at –80 mV and recordings were made according to standard methods (Hamill et al., 1981). Thick-walled borosilicate glass (World Precision Instruments, Sarasota, FL) was pulled to form patch pipettes, which were then coated with Sylgard 184 (Dow Corning, Midland, MI) and fire-polished to obtain tip resistances of 8-15 MΩ and filled with pipette internal solution. Glycine and EtOH were prepared in MBS before being perfused over outside-out patches using a Warner SF-77B Perfusion Fast Step apparatus.

Single channel data were acquired using an Axopatch 200B amplifier attached to a computer running pClamp ver. 9 software (Molecular Devices, Union City, CA). Data were digitized at 50 kHz, low-pass filtered at 7 kHz, and stored on a PC hard drive to be analyzed using the single channel analysis programs in QuB (Qin et al., 2000a,b); version 1.4.0.125 was used for preprocessing, open/closed dwell time analysis, burst duration analysis and kinetic modeling. Tracings were first baseline-corrected and bursts containing multiple openings (when present) were removed. The tracings were then idealized using the segmental-k-means algorithm (SKM) (Qin et al., 2000a,b). Data were initially idealized with a simple two-state C↔O model. This initial idealization was

then fit with multiple exponentials added sequentially to a star model (closed state as the center) using the maximum interval likelihood (MIL) method after imposing a deadtime resolution of 60 μS. Once the appropriate numbers of open and closed components (determined by log likelihood) were present, the data were re-idealized and used for dwell-time analyses. Dwell-time distributions were constructed and fit with a mixture of exponential components again using the MIL function, after the data had been binned using a log-time abscissa and a square-root count/total ordinate. Bursts of openings were defined as being separated by closed-time durations equal to or greater than a critical time (τ crit) that separated groups of openings. For each patch a τ crit was determined such that an equal number of short and long closed-time intervals were misclassified as falling inside and outside bursts (Magleby and Pallotta, 1983) according to equation 2.4.

Once data were chopped into bursts, a new file containing only the idealized burst lengths was created and used for subsequent burst analyses. Burst durations were plotted like the dwell-time histograms described above and fit with multiple exponential components using the MIL function. Statistical analyses were performed using SigmaStat (SPSS Inc., Chicago, IL), utilizing one-way and two-way ANOVAs as well as Students t-test, as indicated.

5.3 – Results

5.3.1 - SINGLE CHANNEL CONDUCTANCE AND MEAN OPEN TIME REMAIN UNCHANGED DURING ETHANOL EXPOSURE

We conducted a series of single-channel experiments on outside-out patches pulled from *Xenopus* oocytes expressing homomeric α1 GlyR. In these experiments intoxicating (50 mM) and anesthetic (200 mM) concentrations of EtOH were applied with 3 μM glycine and their effects on channel function compared to those produced by 3

μM glycine applied alone. This low concentration of glycine was chosen to minimize the likelihood that multiple channels would open concurrently. Glycine applied on its own, or co-applied with EtOH, produces clearly-defined channel opening events as shown in the sample tracings in **Fig. 5.1A**. The conductance observed in the presence of 3 μM glycine alone is 68 ± 4 pS (n = 5) and this is not affected by co-administration of EtOH [F2,13) = 0.13, p > 0.87] (**Fig. 5.1B**). A mean open time of 0.75 ± 0.11 (n = 5) ms is observed when 3 μM glycine is applied alone. Ethanol has no effects on the channel mean open time at a concentration of 50 mM and slightly, but not significantly, increases it at 200 mM [F(2, 13) = 1.03, p > 0.39] (**Fig. 5.1C**).

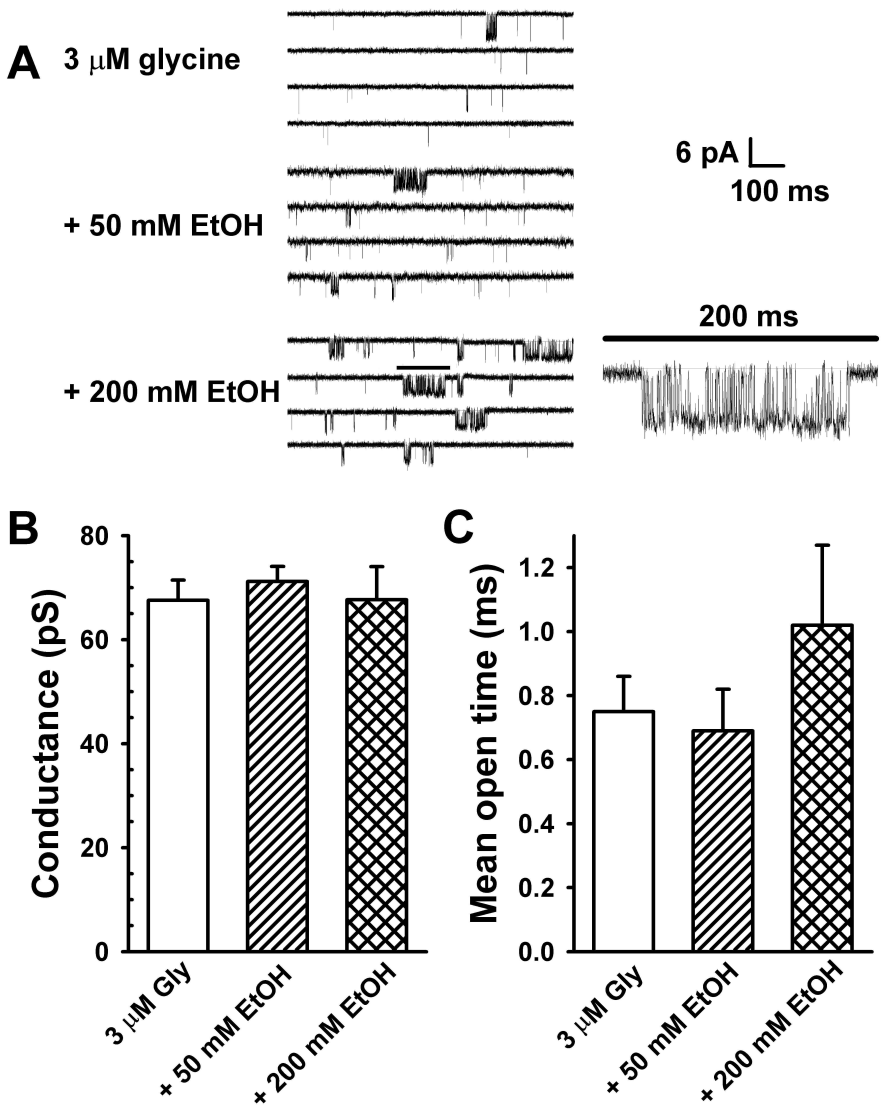

Figure 5.1 – Ethanol has no significant effect on GlyR channel conductance or mean open time

(A) Representative tracings of single channel homomeric a1 GlyR responses to 3 μM glycine (top), 3 μM glycine + 50 mM ethanol (middle), and 3 μM glycine + 200 mM ethanol (bottom). In the 200 mM ethanol tracing the burst directly underneath the horizontal line is magnified to the right. *(B)* Ethanol does not affect GlyR conductance, which was approximately 70 pS for full openings under all experimental conditions. *(C)* The addition of ethanol does not significantly affect mean channel open time.

5.3.2 - ETHANOL HAS NO EFFECT ON CHANNEL OPEN DWELL TIME COMPONENTS

Open dwell-time data are adequately described using four exponential components. Sample open dwell-time histograms obtained from single patches, under all three experimental conditions, show the four separate components (τ's, thin lines) and overall fit (thick line) of the data in **Figure 5.2A**. While there are clear and expected differences in mean channel open lifetimes (τs) among the four components [$F_{3,55} = 69$, $p < 0.001$], EtOH does not significantly affect the average durations of open dwell times [$F_{2,55} = 2.16$, $p > 0.12$] (**Fig. 5.2B**). Ethanol also does not significantly affect the likelihoods of openings to the four components [$F_{2,55} = 0.005$, $p > 0.99$] (**Fig. 5.2C**).

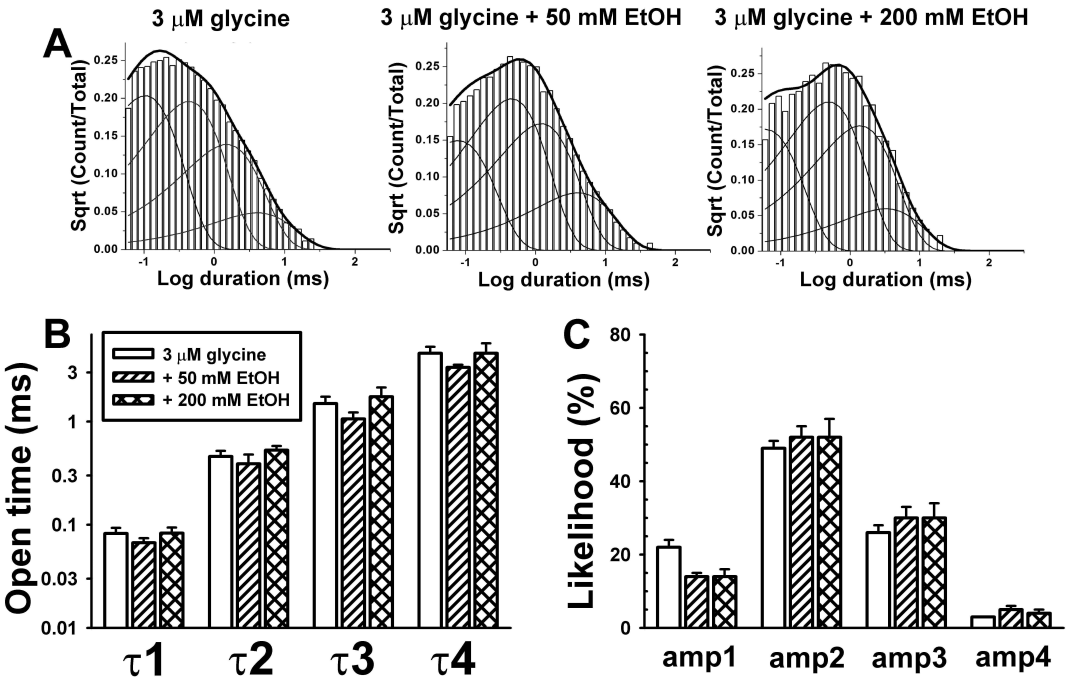

Figure 5.2 – Ethanol has no effect on the open dwell time components

(A) Representative histograms demonstrating the fits for the open-dwell times. Each condition was fit using four open time components (τs). The four thinner lines in each histogram describe the individual open dwell-time exponential functions while the thicker line is a fit of all the data. *(B)* The addition of ethanol has no effect on open dwell times. *(C)* Ethanol does not affect the likelihood of opening to any particular open time component.

5.3.3 - ETHANOL EXTENDS THE LIFETIME OF THE LONGEST-LIVED INTRABURST CLOSED TIME

A clear temporal separation between the first three (shorter) components and the fourth and fifth (longest) components (**Fig. 5.3A**) is seen in the closed dwell-time sample histograms. Ethanol significantly affects the three shortest closed-time durations [$F(2,41) = 3.81$, $p < 0.033$] (**Fig. 5.3B**) but does not affect the likelihoods of observing the three shortest closed dwell times [$F(2,41) = 0.52$, $p > 0.59$] (**Fig. 5.3C**). In addition, a two-way ANOVA indicates an interaction between τ and ethanol [$F(4,41) = 3.2$, $p < 0.025$], reflecting an ethanol-induced increase primarily in $\tau 3$. The longest closed dwell-time components ($\tau 4$ and $\tau 5$) vary considerably from patch to patch (e.g., for glycine alone $\tau 4 = 109 \pm 67$ ms and $\tau 5 = 642 \pm 404$ ms, $n = 5$), indicative of varying numbers of channels in each patch. Because of the greater inter-patch variability of $\tau 4$ and $\tau 5$ compared to $\tau 1$-3, we believe that the first three time constants represent closing events within bursts while $\tau 4$ and τ 5 describe inter-burst closing events.

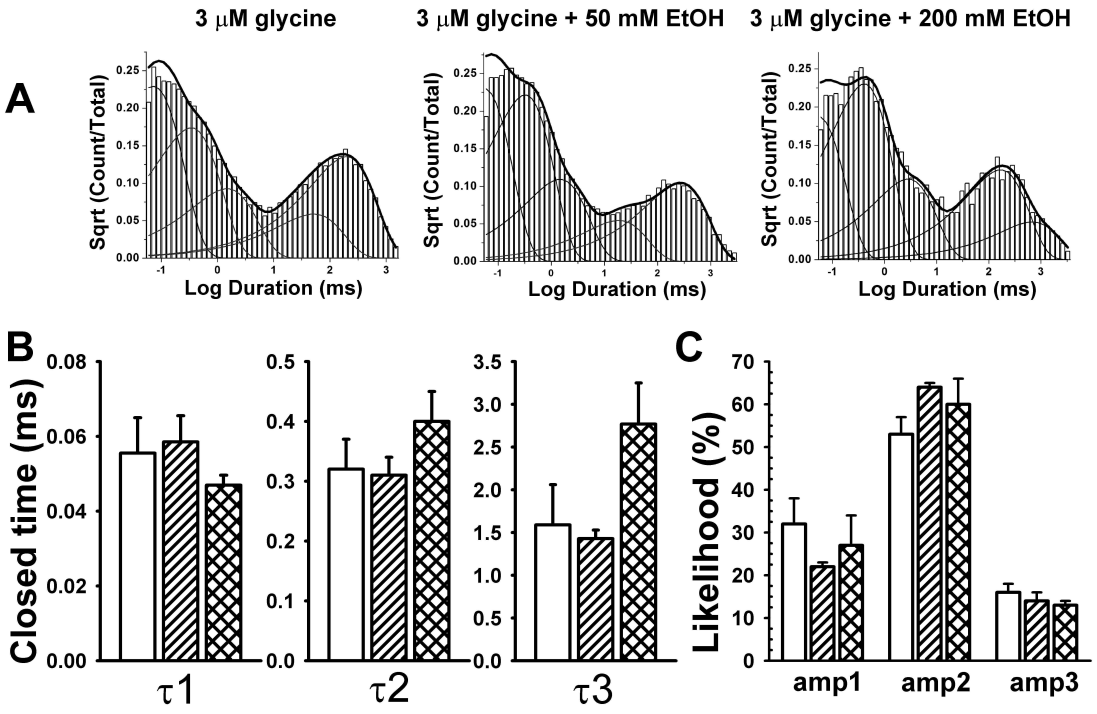

Figure 5.3 – Ethanol increases the longest intraburst closed time component

(A) Representative histograms demonstrating the fits for the closed dwell times. Each condition was fit using five closed time components (τs). τ_{crit} was chosen individually for each file to minimize the area between the tails of the overlapping components, corresponding closely to the valley between closed durations three and four. τ1, τ2, and τ3 are considered to represent intra-burst closed durations while τ4 and τ5 lie outside of bursts. *(B)* Closed time durations are increased by ethanol; the three intra-burst closed times are illustrated for the glycine alone condition (hollow bars), and in the presence of 50 mM EtOH (diagonal bars) or 200 mM EtOH (cross-hatched bars). There was also a statistically-significant interaction between τ and ethanol concentration. *(C)* The likelihoods of occurrence of each of the three shortest closed-time components are not affected by ethanol. The likelihoods are expressed as a percentage of closings of only the first three shut time components.

5.3.4 – BURST DURATIONS INCREASE IN THE PRESENCE OF ETHANOL

Closed dwell-time data were used in the selection of an appropriate τ_{crit}, to chop opening events into bursts. **Figure 5.4** shows the results of combining burst data obtained from all patches (using τ_{crit} values determined in each patch), and specifically that EtOH increases burst durations. On average the τ_{crit} values used were 4.6 ± 0.9 ms (n = 5) for the 3 μM glycine condition, 4.6 ± 0.3 ms (n = 5) for the 50 mM EtOH condition and 6.9 ± 1.3 ms (n = 4) for the 200 mM EtOH condition. Longer-lived bursts (>50 ms in duration) are rarely seen when 3 μM glycine is applied alone (1.5% of bursts), but become more prevalent in the presence of 50 mM (3.1%) and 200 mM EtOH (4.9%) (**Fig. 5.4**).

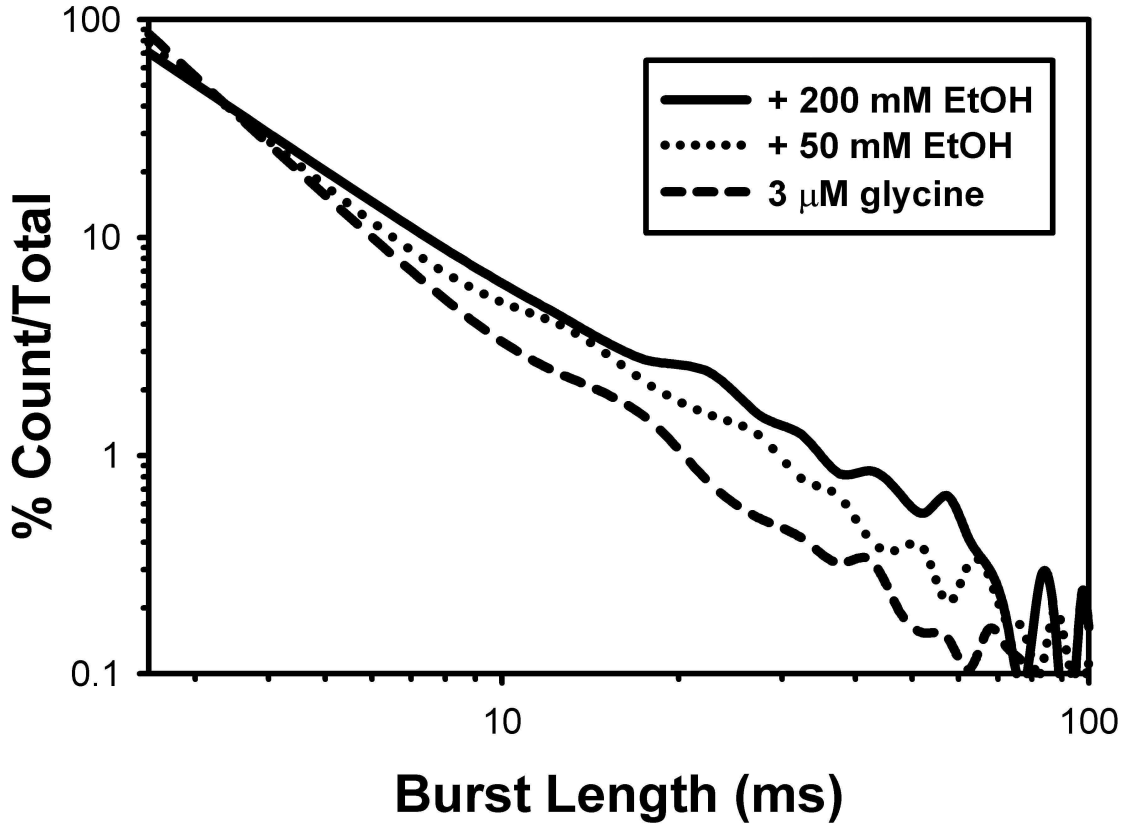

Figure 5.4 - Ethanol increases the durations of bursts

Bursts lengths were combined from all patches for each experimental condition, binned, counted and those counts normalized to generate the numbers on the ordinate. Burst lengths greater than 50 ms are more frequent in the presence of either 50 or 200 mM ethanol. The abscissa represents burst length while the ordinate represents the percentage of bursts seen at each duration. For example, 86% of bursts were between 0 and 5 ms in duration in the glycine alone condition.

5.3.5 – ETHANOL INCREASES MEAN BURST DURATION AND THE MEAN NUMBER OF OPENINGS PER BURST

Burst data are summarized in **Fig. 5.5A**, showing that 200 mM EtOH significantly increases burst durations [$t(7) = 2.7$, $p < 0.035$] (**Fig. 5.5B**). Ethanol increases the percentages of bursts containing two or more opening events [$F(2, 13) = 11.1$, $p < 0.002$], indicating that it favors the occurrence of opening events being grouped together rather than occurring singly (**Fig. 5.5B**).

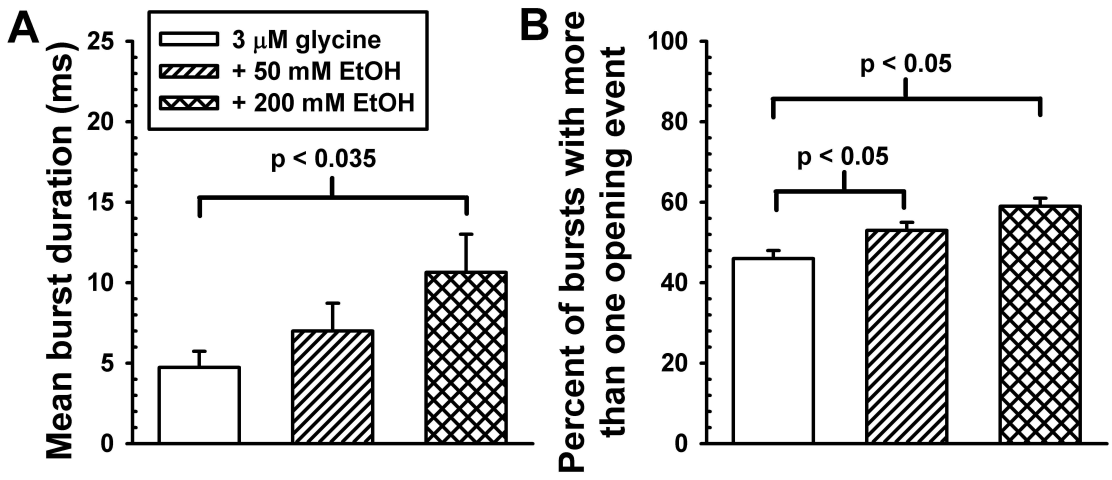

Figure 5.5 - Ethanol increases mean burst duration and the mean number of openings per burst

(A) Mean burst duration increases from 4.7 ms in the presence of 3 μM glycine applied alone, to 7.0 ms in the presence of glycine plus 50 mM ethanol and to 10.6 ms when 200 mM ethanol is co-applied. *(B)* Ethanol increases the percentage of bursts consisting of multiple opening events. In the presence of glycine alone, 54% of bursts consisted of single opening events while 46% consisted of multiple opening events. In the presence of ethanol, more than half of bursts displayed multiple openings.

5.3.6 – ETHANOL INDUCED INCREASED IN BURST DURATION IS DUE TO AN INCREASE IN THE BURST TIME CONSTANTS

The burst length distributions from every patch in each condition can be described by four exponential functions as summarized in **Fig. 5.6**. Ethanol has no enhancing effects on the shortest burst duration ($\tau 1$), which is not surprising since these largely consist of single opening events, which we earlier showed were insensitive to EtOH. Ethanol increases the durations of longer bursts [$F(2,54) = 8.51$, $p < 0.001$] (**Figs. 5.4 and 5.6A**) without affecting the likelihoods of entering any particular burst states [$F(2, 54) = 0.05$, $p > 0.95$] (**Fig. 5.6B**).

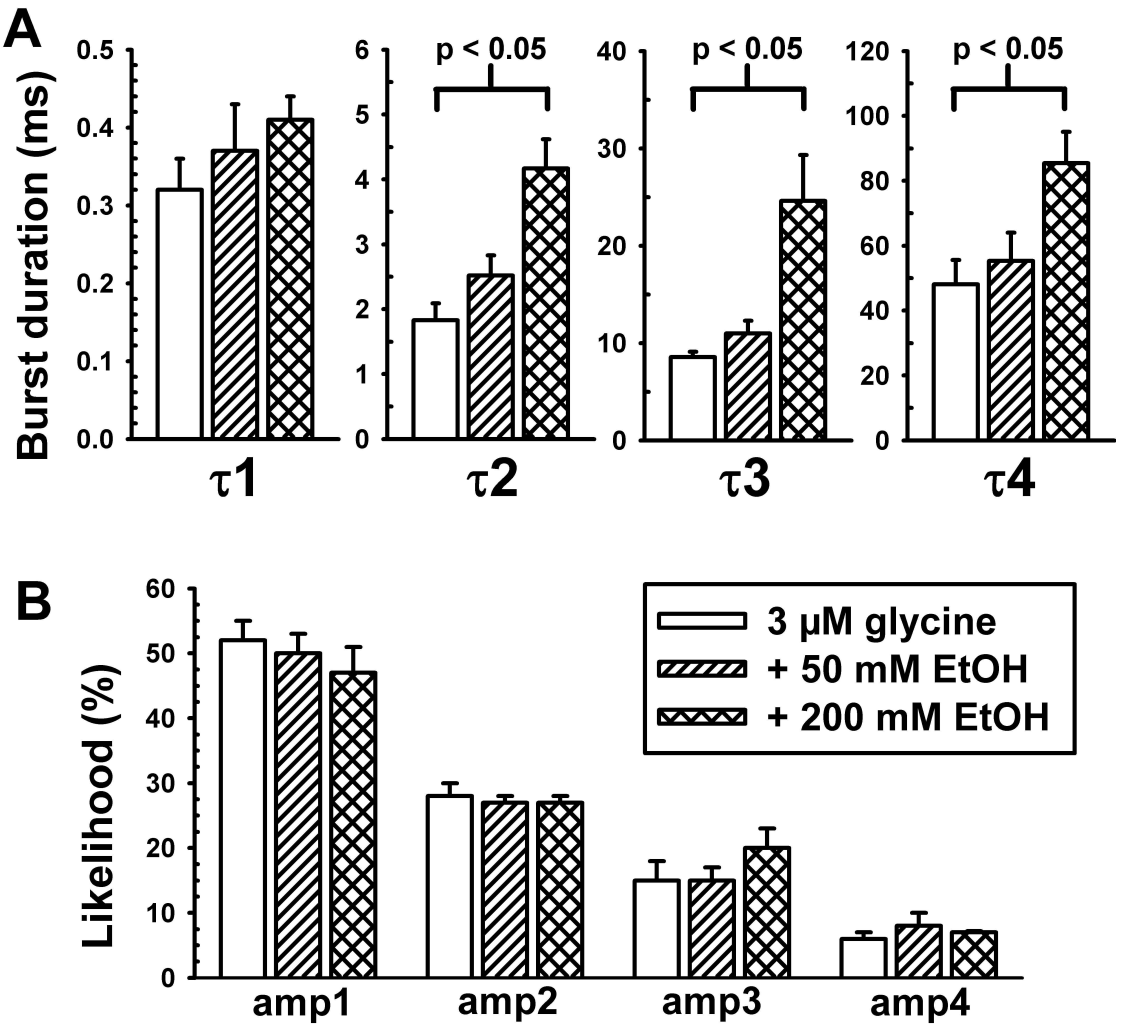

Figure 5.6 - Ethanol increases burst durations by increasing burst time constants

(A) Ethanol appears to act primarily by increasing the durations of the longer-lived burst states (τ2-τ4). *(B)* The percent likelihood of entering any particular burst state is unchanged by EtOH.

5.3.7 – ETHANOL INCREASES THE MEAN NUMBER OF OPENINGS PER BURST WITHOUT AFFECTING THE P_{OPEN} WITHIN THE BURST

This increase in burst duration is accompanied by an increased number of openings per burst in the presence of EtOH (**Fig. 5.7A**) [t((7) = 2.71, $p < 0.035$ comparing 0 and 200 mM EtOH]. However, the weighted probability of opening within bursts (P_{open}) is not significantly affected [$F(2, 13) = 0.4$, $p > 0.68$] by EtOH (**Fig. 5.7B**). The weighted P_{open} is determined by dividing total open time in a patch by the sum of burst lengths.

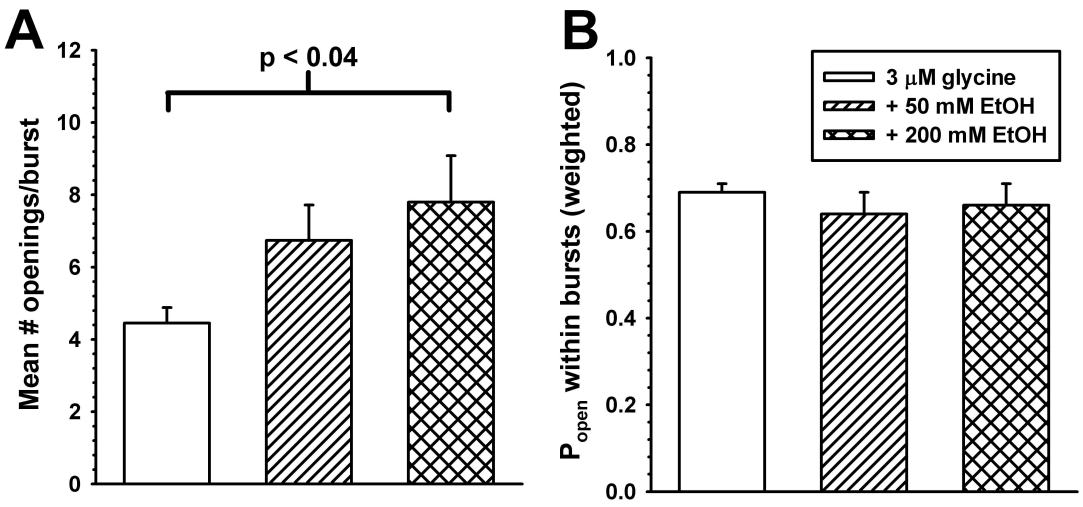

Figure 5.7 – Ethanol increases the mean number of openings per burst but has no effect on the P_{open} within bursts

(A) The mean number of opening events per burst was obtained for each patch by dividing the number of opening events by the number of bursts. EtOH at a concentration of 200 mM significantly increases the number of openings per burst. *(B)* Ethanol does not affect intra-burst P_{open}. The weighted average of the probability of the channel being found in the open state during a burst was determined by dividing the total open time by the total burst duration for each patch. That this parameter of channel function was not changed in the presence of ethanol suggests that ethanol does not markedly affect intra-burst properties as was expected due to the minor effects of ethanol on open- and closed-dwell times.

5.3.8 - MODELING AND SIMULATION OF ETHANOL ACTIONS ON THE GLYR

To provide a mechanistic understanding of our results, modeling was done using QuB with a kinetic scheme (**Fig. 5.8**) similar to that proposed in Beato et al. (2004).

In this model **R** represents the GlyR in the closed channel state with no glycine molecules bound. **AR** represents the GlyR with a single glycine molecule bound while $\mathbf{A_2R}$ represents the receptor after binding two glycine molecules. **AR*** and $\mathbf{A_2R^*}$ are open channel states while k, α, and β represent transition rates between states as indicated by arrows in the kinetic model shown above. The rates of entry into, and departure from, bursts are described by k_{+1} and k_{-1}, respectively. The other rates describe intra-burst transitions. Beato et al. (2002) showed that at low concentrations of glycine (~1 μM), the occupancy of a tri-liganded GlyR was less than 5% and in agreement with these findings, most of our patches could not be fit to a model containing a tri-liganded state. Once each patch was individually fit to the model shown above, all the rates were identified for each patch, and these are summarized in **Table 5.1**. One-way ANOVA was used to test for significant effects of alcohol on each rate and only in the case of k_{-1} was a significant effect found [$F(2,13) = 4.26$, $p < 0.045$]. The 200 mM ethanol condition k_{-1} rate was significantly lower than that of the glycine control. The 50 mM ethanol condition k_{-1} value, which fell between those of the other two conditions, did not differ significantly from either. The rates of the binding and unbinding of the second glycine molecule, as described by K_2 values, were not affected by ethanol [$F(2,13) = 1.22$, $p > 0.33$], nor were the two efficacies of opening [E1, $F(2,13) = 0.45$, $p > 0.6$; E2, $F(2,13) = 0.23$, $p > 0.79$].

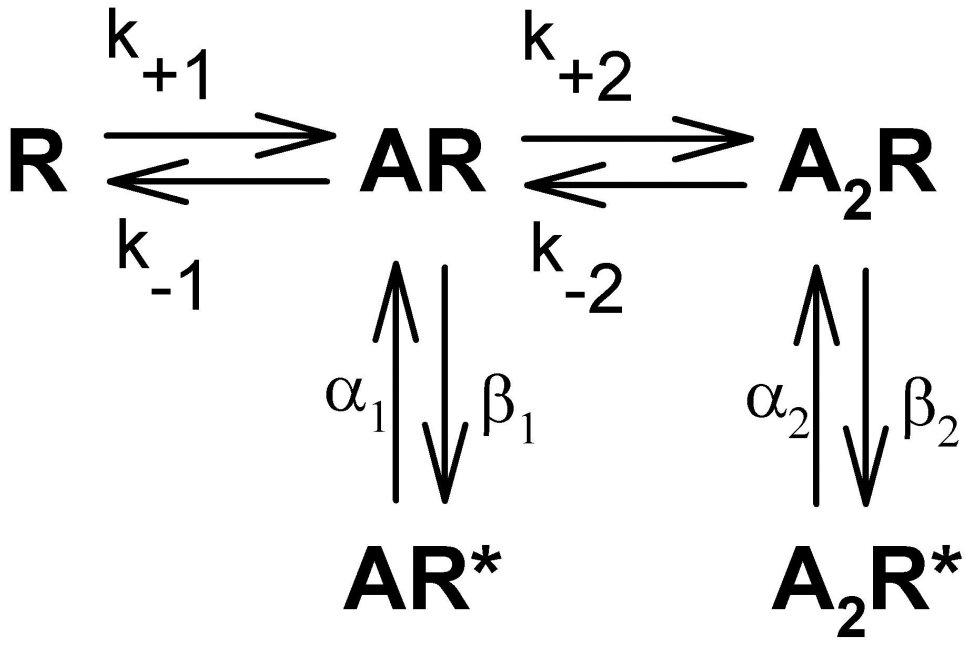

Figure 5.8 – GlyR kinetic scheme used for modeling and simulation

Kinetic scheme illustrating glycine receptor activation after the binding of one or two glycine molecules

Condition (n)	Rate	Mean ± S.E.M.	Coefficient of Variation	
3 μM glycine (n = 5)	k_{+1}	$6.5 \times 10^6 \pm 3.7 \times 10^6$	127	N.D.
	k_{-1}	767 ± 115	34	
	k_{+2}	$4.8 \times 10^7 \pm 8.4 \times 10^6$	39	$K_2 = 1.5 \times 10^{-5}$
	k_{-2}	752 ± 160	48	
	α_1	4691 ± 801	38	$E_1 = 0.28$
	β_1	1153 ± 322	62	
	α_2	1207 ± 190	35	$E_2 = 5.6$
	β_2	6034 ± 277	10	
3 μM glycine + 50 mM EtOH (n = 5)	k_{+1}	$2.7 \times 10^6 \pm 1.5 \times 10^6$	126	N.D.
	k_{-1}	540 ± 118	49	
	k_{+2}	$4.5 \times 10^7 \pm 6.9 \times 10^6$	34	$K_2 = 1.3 \times 10^{-5}$
	k_{-2}	562 ± 89	35	
	α_1	4650 ± 692	33	$E_1 = 0.31$
	β_1	1295 ± 85	15	
	α_2	1527 ± 204	30	$E_2 = 4.9$
	β_2	6721 ± 393	13	
3 μM glycine + 200 mM EtOH (n = 4)	k_{+1}	$2.5 \times 10^6 \pm 1.2 \times 10^6$	93	N.D.
	k_{-1}	329 ± 29	18	
	k_{+2}	$5.4 \times 10^7 \pm 1.5 \times 10^7$	57	$K_2 = 1.2 \times 10^{-5}$
	k_{-2}	620 ± 177	57	
	α_1	3258 ± 273	17	$E_1 = 0.22$
	β_1	740 ± 145	39	
	α_2	1058 ± 149	28	$E_2 = 6.4$
	β_2	5957 ± 54	54	

Table 5.1 – Fit of single-channel data to a mechanistic scheme

Table 5.1 (additional information). Rates were obtained for a reasonable kinetic model consisting of three closed states and two open states as described in *Results* and **Figure 5.8**. The k_{+1} and k_{+2} rate constants are described in units of M^{-1} s^{-1} while the k_{-1}, k_{-2} and α and β rates are expressed in units of s^{-1}. These rates were calculated separately for each patch and the mean ± S.E.M. of four to five patches is provided. The coefficient of variation was determined by dividing the S.D. for each experimental condition by the mean and expressing that value as a percentage. The K2 value was determined by averaging the k_{-2}/k_{+2} rates of individual patches. K1 was not determined (N.D.) because the k_{+1} values, which describe rates of departure from long-lived closed states into burst states, vary with the number of channels per patch (Beato et al., 2002). E1 and E2 are agonist efficacy values obtained from β/α.

We next conducted simulations to determine if changes in k_{-1} are sufficient to account for the altered GlyR responses in the presence of ethanol. As starting values this model used the average rates shown in **Table 5.1** for the 3 μM glycine alone condition. The resulting simulation quite accurately reproduced data matching the measured 3 μM glycine control condition in both mean open time (0.75 ms actual vs. 0.66 ms simulated) and mean burst duration (4.7 ms actual vs. 4.0 ms simulated). The simulation was then re-run with only the k_{-1} rate decreased 2.33 fold, from 770 s^{-1} in the 3 μM glycine simulation to 330 s^{-1} in the glycine + 200 mM EtOH simulation, in accordance with our observed data (**Table 5.1**). This change in k_{-1} did not affect mean open time (0.64 ms) yet markedly increased the mean burst duration (to 8.3 ms). The increase in simulated burst duration from 4.0 ms to 8.3 ms (a 108% increase) is almost identical to the increase we observed in the presence of 200 mM ethanol (4.7 ms to 10.6 ms, a 124% increase). Changing other rates, such as those governing the transitions between the mono-liganded and di-liganded closed states (k_{+2} and k_{-2}) or those between closed and open channel states either produced minimal effects on burst durations and/or markedly affected lifetimes or likelihoods of entering particular open states, which ethanol does not do to a significant extent.

5.4 – Discussion

Ethanol produces a variety of behavioral effects depending on the blood ethanol concentration (BEC). We defined 50 mM EtOH (235 mg/dl) as intoxicating and 200 mM EtOH as anesthetizing. C57BL/6J mice recover from the hypnotic effects of ethanol at a BEC of 370 mg/dl (Sharko and Hodge, 2008) and mice are able to remain on a rotorod at a BEC of 207 mg/dl (Deitrich et al., 2000). Further, binge-drinking college students

celebrating their 21st birthdays achieve BECs averaging 220 mg/dl (Wetherill and Fromme, 2009). The anesthetizing brain concentrations of ethanol in Sprague Dawley rats were assessed by failure to respond to a painful tail pinch and were found to be 151 mM in adults and 282 mM in 6-7 day-old animals (Fang et al., 1997).

Enhancement of GlyR function is consistent with the actions of EtOH observed in vivo. Ethanol-induced loss of righting reflex in mice is augmented by the intracerebroventricular administration of glycine (Williams et al., 1995). The hypnotic effects of EtOH are altered in spastic and spasmodic mice bearing dysfunctional GlyR (Quinlan et al., 2002). Furthermore, studies using knock-in mice bearing a point mutation at amino acid serine-267, rendering the receptors less sensitive to EtOH, support the hypothesis that GlyRs are important targets for the motor-incoordinating and anesthetic properties of EtOH (Findlay et al., 2002). Perhaps most interesting and relevant to alcoholism is the evidence that GlyR in the nucleus accumbens play a role in the voluntary drinking of EtOH. Microdialysis of glycine into the nucleus accumbens increases extracellular accumbal dopamine levels and is accompanied by a decrease in EtOH consumption by alcohol-preferring Wistar rats; in contrast strychnine has the opposite effects (Molander et al., 2005). Strychnine, applied via microdialysis, also prevents increases of accumbal dopamine levels after either local or systemic alcohol administration (Molander and Söderpalm, 2005). In line with these findings, the glycine reuptake inhibitor, Org 25935, decreases EtOH but not water intake, as well as EtOH preference (Molander et al., 2007).

Ethanol enhances GlyR function only at low glycine concentrations, decreasing the glycine EC_{50} with no effect on maximal glycinergic currents (Aguayo et al., 1996). Mascia et al. (1996a) demonstrated EtOH enhancement of the function of GlyR of defined composition expressed in Xenopus oocytes. Concentrations as low as 10 mM

EtOH were effective, especially when lower concentrations of glycine were tested. At the molecular level, investigations into ethanol's actions on native $\alpha 1\beta$ GlyRs in excised patches from rat hypoglossal motoneurons revealed that 100 mM EtOH increased the numbers of open channels without affecting channel conductance (Eggers and Berger, 2004). EtOH decreases the glycinergic response rise-time, as well as increasing the current decay time. Eggers and Berger (2004) concluded that EtOH acts to increase glycine affinity by enhancing glycine association with the GlyR (k_{on}) as well as antagonizing dissociation (k_{off}).

We compared our findings to those reported by Beato et al. (2002), who also performed outside-out patch single channel analysis of $\alpha 1$ homomeric GlyR, but expressed in HEK 293 cells instead of Xenopus oocytes. Like Beato et al. (2002) our data were free-fit with four open components and three intra-burst shut components, and the τ and likelihood values we report are similar to theirs. Also in common are the four burst components both studies found. In addition, our mean burst duration seen in the presence of 3 μM glycine (4.7 ms) was between the values reported by Beato et al. (2002) for 1 μM and 10 μM glycine (2.5 and 7.1 ms, respectively). They chopped their data into bursts using τ_{crit} values of 4.6 ms for 1 μM glycine and 5.8 ms for 10 μM glycine; in comparison the τ_{crit} value we used for chopping 3 μM glycine data averaged 4.6 ms.

In our studies we determined that the primary effect of EtOH on GlyR function appears to be its enhancement of burst durations. Longer bursts (τs) are seen in the presence of EtOH, thus resulting in an increased incidence of longer bursts (e.g., >50 ms). A reasonable kinetic scheme for the activation of GlyR such as that proposed by Beato et al. (2004), and shown in Results, can be useful to illustrate how we believe EtOH is acting to enhance GlyR function. In this scheme a total of eight rates (k, α, β)

are used to describe transitions between states. The results we obtained using this model are in agreement with those previously made by others as well as showing consistency with expectations. For example, the open lifetimes ($1/\alpha$) of receptors in the mono-liganded state are shorter than in the di-liganded state (213 μs vs. 829 μs in the 3 μM glycine condition) and quite similar to those shown by Beato et al. (2004), who found the two shortest channel open times to be 256 μs and 794 μs in duration using a model similar to ours. Secondly, efficacy (E1 vs. E2) increases with ligation, a feature common to ligand-gated ion channels. Both our results and those of Beato et al. (2004) find that the efficacy increase from mono-liganded to di-liganded receptors (E_2/E_1) is 20.

One can use a mechanistic model such as this to ask which rates might be changed by EtOH to explain our findings. Open dwell times are determined solely by α. Since we saw no significant effects of EtOH on open dwell times (**Fig. 5.2B**), it is not exerting its effects via α. Changing β could affect burst durations but would also be expected to affect open and closed state likelihoods, which we did not see (**Figs. 5.2C & 5.3C**). An ethanol-induced increase in k_{+2} or decrease in k_{-2} could increase the mean burst durations; however this would be accompanied by marked changes in the likelihoods of entering the open states, which EtOH does not produce. Our data suggest that EtOH enhances burst durations (**Figs. 5.4 and 5.5A**), by increasing the numbers of openings per burst (**Fig. 5.7A**) but without affecting P_{open} within bursts (**Fig. 5.7B**). Thus, bursts appear qualitatively unchanged in the presence of EtOH except that they are longer, and the increased number of openings per burst in the presence of EtOH reflects that. The k_{+1} and k_{-1} rate constants govern the rates of entering and leaving burst states, respectively. Increasing k_{+1} would be expected to have no effects on either mean open time or mean burst duration, although it would decrease extra-burst closed times; i.e., increasing k_{+1} would increase the number of bursts seen per unit time. However,

decreasing k_{-1} would increase burst durations by retarding the termination of bursts. In addition, changing k_{-1} would not affect open and closed lifetimes and durations, except perhaps increasing the lifetime of the **AR** closed state, assuming all other rates from **AR** remain unaffected. Interestingly, we observed that EtOH increased the longest-lived intra-burst closed time (**Fig. 5.3B**), consistent with this interpretation.

EtOH appears to slightly, but not significantly, increase mean open time at a concentration of 200 mM. Changes in the k_{-1} rate are unable to explain this minor effect of EtOH and fairly small changes of one or more of the other rates must be responsible for these effects. Our findings thus appear to be at odds with the molecular dynamics simulation performed by Cheng et al. (2008), who concluded that EtOH stabilizes open channel states of the GlyR. In contrast, our data suggest that EtOH, at intoxicating concentrations at least, does not stabilize the open state of the receptor at all. Furthermore, we saw minimal effects of either concentration of ethanol on efficacy (β/α) in our studies.

No single mechanism can explain how allosteric modulators affect channel function. For example, barbiturates and neurosteroids enhance $GABA_A$ receptor function primarily by increasing the mean channel open time and thus they act to stabilize an open state of the receptor (Steinbach and Akk, 2001; Akk et al., 2008). Zinc is a positive modulator of GlyR function at low micromolar concentrations. Single channel studies of zinc effects on the GlyR show many similarities to how EtOH acts: an enhancement of burst durations and individual burst τs and an increase in the numbers of opening events per burst, but no effects on mean channel open times and no effects on conductance (Laube et al., 2000). In addition it was concluded that zinc enhances GlyR function primarily by antagonizing glycine dissociation.

In summary we have determined that EtOH exerts its enhancing effects on GlyR function primarily by increasing burst durations. It does not appear to significantly stabilize open states, nor does it affect conductance. The primary mechanism of alcohol action seems to be its antagonism of glycine unbinding from the GlyR. This would have the effect of prolonging the duration of GlyR activation at the synapse and this is consistent with ethanol producing leftward shifts of glycine concentration-response curves. Ethanol's effect on select parameters of channel function is similar to the specificity exhibited by other modulators such as zinc (Laube et al., 2000) or neurosteroids (Akk et al., 2008) that interact with receptors at defined binding sites.

6.0 | CONCLUSIONS AND DISCUSSION

6.1 – Overview

As molecular techniques rapidly advance, the structure and function of ion channels are being related to each other in increasing detail. The research presented in this dissertation provides novel insights regarding both the activation and allosteric modulation mechanisms of the GlyR. The overall conclusions from these studies can be summarized in three main points. First, the disruption of a single electrostatic interaction near the ligand-binding region in the extracellular domain is sufficient to increase the efficacy of partial agonists, such as taurine. Second, on a whole-cell level, ethanol modulates taurine-activated GlyR currents in a similar manner as it does glycine-activated currents; i.e. ethanol potentiates the response to submaximal agonist or partial agonist concentrations without increasing the efficacy of a saturating concentration of either agonist. This suggests that the mechanism by which ethanol produces its allosteric effects occurs on channel-opening processes that are common to the partial agonist taurine and the full agonist glycine. Third, ethanol enhances GlyR function by decreasing the rate of glycine unbinding, measured as an increase in mean channel burst duration. Together these results increase our understanding of the relationship between GlyR activation and allosteric modulation of the receptor by ethanol.

6.2 – Partial Agonism in the GlyR

Recently there has been renewed interest in the study of partial agonism in ligand-gated ion channels, focusing on the activation mechanism and structural elements that explain the differences in agonist efficacies. The results, like the receptors being studied, are diverse. For example, partial agonists in the nAChR superfamily demonstrate a decreased ability to achieve a flipped state that precedes channel opening (Lape et al., 2008). This may be the result of structural changes that follow agonist binding such as in the AMPAR, in which partial agonists produce a smaller movement in the ligand binding region commensurate with the efficacy of the agonist (Armstrong and Gouaux, 2000). However, these mechanisms seem distinct from the more global effects on channel gating which were measured in the NMDAR (Kussius and Popescu, 2009). All of these studies underscore the different ways in which channel activation may be distinct depending on the ligand, and indicate that our understanding of partial agonism is more complicated than simply differences among agonists and their abilities to affect the rates of closed to open transitions. The data presented in this dissertation address partial agonism in the GlyR and identify a structural component of the receptor that is crucial for determining the efficacy of an agonist.

Our current view of ligand-gated ion channel activation is that the binding signal from an agonist produces a wave of conformational changes that progresses towards the gate, quickly resulting in pore-opening and the flow of ions. However, the fact that different agonists can open the gate yet produce lesser effects, suggests that these conformational changes are not equivalent for all ligands. A major question is, where in the process of activation is efficacy determined? Results from studies of the nAChR and the GlyR both suggest that the lower efficacy observed with partial agonists can be

pinpointed to structural changes that occur soon after the ligand binds (Grosman et al. 2000; Lape et al., 2008). The data in Chapter 3 of this thesis support this hypothesis and furthermore offer an element in the GlyR structure that may be important for determining agonist efficacy in these receptors. The demonstration that the α1 D97R GlyR mutation yields a receptor evincing a dramatic increase in the efficacy of partial agonists indicates that mutations near the agonist-binding region can affect efficacy. Specifically, by disrupting the D97-R119 interaction, the energetic barrier to activate the channel has been biased in favor of activation. This was first shown in Todorovic et al. (submitted) and confirmed to be zinc-independent as seen in **Fig 3.2**, since the homomeric α1 D97R GlyR exhibits a high probability of channel opening despite a lack of agonist. Because these residues reside at a subunit interface near the glycine-binding site and serve to stabilize a closed state, it is conceivable that their interaction may be affected during WT GlyR activation. In other words, as each glycine molecule binds at a subunit interface, it produces its own local disturbance of the bond. Differences in agonist efficacy could therefore be determined in part by the ligand's ability to disrupt the D97-R119 bond. Disruption of that bond would then presumably lead to adoption of what Lape et al. (2008) refer to as the flipped state, and the artificial elimination of this bond by the D97R mutation removes that structural and energetic barrier, thus converting taurine into a full agonist. In a mutant homomeric α1 D97R receptor, all five of the D97-R119 interactions are nullified and the receptor would be hypothesized to behave as if it were fully liganded. This is precisely the case as was demonstrated in Todorovic et al. (submitted). However, this implies that for antagonists to work on the D97R GlyR, they must stabilize a closed state that does not rely on the D97-R119 interaction.

The results from the rest of the experiments described in Chapter 3, using other β-amino acid partial agonists, highlight the importance of the ligand structure in ultimately

determining efficacy. Extensive research by Schmieden et al. (1995, 1999) demonstrated that the *trans*- form of β-amino acids has antagonist features, while the agonist properties of these partial agonists may result solely from the *cis*- conformation. That the D97R mutation could not convert the low efficacy partial agonist β-AIBA completely into a full agonist suggests that the understanding of partial agonist pharmacology may be more complicated than just the assertion that a bound ligand will display full efficacy once the D97-R119 interaction is abolished. Since solutions of β-amino acids may essentially be a mixture of antagonists and agonists, it is likely that the *trans*- isomer of β-AIBA is quite potent at antagonizing GlyR activity. Despite the spontaneously high P_{open} that is characteristic of D97R bursts and clusters, the *trans*- form of β-AIBA appears capable of antagonizing this opening. This particular point regarding *trans*- molecules is most relevant to the nipecotic acid results. Nipecotic acid, which exists only in a *trans*- configuration and acts as an antagonist on WT GlyR, instead has partial agonist properties on the D97R mutant. However, when the D97-R119 electrostatic interaction is re-established by means of a double mutation, as in the D97R/R119E GlyR, nipecotic acid regains its ability to inhibit glycinergic currents and loses the ability to activate the channel (See **Fig. 3.6**). This suggests that molecules in the *trans*- form are still binding to mutants containing the D97R mutation but that the D97-R119 electrostatic interaction is essential in determining the efficacy of the molecule.

6.3 – Ethanol Modulation of Partial Agonist Activation

Drug addiction, including alcoholism, is thought to a disorder of the brain in which the natural reward center is co-opted by the particular drug in question. The intricacies of the circuitry and details of cell signaling in this part of the brain are now

being investigated in-depth in order to better understand the disease. It is well established that the neurotransmitter dopamine is one of the key signals here, but the modulation of its release and action are not yet fully elucidated. For example, a recent study examining dopamine release in the nucleus accumbens has suggested that taurine, rather than glycine, is the endogenous neurotransmitter for the GlyRs that are expressed in this brain region (Ericson et al., 2006). This may mean that alcohol mediates some of its rewarding effects via taurine-activated GlyRs. It is surprising then that there is little available information regarding the modulation of taurine-activated GlyRs by ethanol. The data in this dissertation adds to our understanding of ethanol modulation of the GlyR when taurine is the agonist.

The major finding in Chapter 4 was that alcohol does not enhance the efficacy of a maximally-effective taurine concentration. As in Chapter 3, we again demonstrate that taurine is a partial agonist of the α1 GlyR, eliciting maximal currents that are less than half that of glycine, and this leaves open the potential for an increase in efficacy by a positive allosteric modulator such as ethanol. It was previously established that ethanol does not enhance the GlyR response to maximal glycine concentrations, but does robustly potentiate receptor function at lower agonist concentrations (Mascia et al., 1996a). We found that the same results hold true when taurine is the agonist indicating that ethanol is unable to increase taurine efficacy. This conclusion has implications for the channel activation mechanism that was proposed by Lape et al. (2008) to describe the taurine-activated GlyR. Lape et al. (2008) found that the major difference between the kinetic schemes used to describe GlyR activation for each agonist was that taurine had difficulty reaching the pre-open flipped state, implying that taurine had a lower affinity for this conformation, and that this was the cause for its reduced efficacy. Here we show that saturating taurine efficacy cannot be increased by ethanol, suggesting that ethanol does

not ease transitions from closed to flipped. If that were the mechanism by which ethanol enhanced channel function, then one would expect there to be an increase in taurine efficacy. This leaves open other possibilities for ethanol enhancement of GlyR function such as those that are addressed in Chapter 5.

Other research on the activation of the GlyR using taurine has suggested that taurine and glycine may have separate gating pathways, since zinc increases the effects of maximally-effective taurine concentrations but not those of maximally-effective glycine (Laube et al., 2000). As such, this effect of zinc on the GlyR to increase taurine efficacy appears to be different from the mechanism of enhancement by ethanol. Zinc is important to consider when studying the GlyR because of its presence throughout the nervous system where GlyRs are found (Vogt et al., 2000; Schrøder et al., 2000; Birinyi et al., 2001). Furthermore, McCracken et al. (in press) have shown synergism between alcohol and zinc in potentiating the glycine-activated GlyR. As expected then, we show that when tricine is used to remove zinc from our solutions, ethanol potentiation of taurine-gated currents is decreased. However, the fact that ethanol and zinc have synergistic effects yet zinc alone can increase taurine efficacy, suggests that the two modulators potentiate the receptor in different ways.

In terms of simply the ethanol modulation of GlyR activation, the gating pathways for taurine and glycine cannot be completely separate. Using the α1 S267I mutation which eliminates the ability of ethanol to enhance glycine-mediated GlyR currents (Ye et al., 1998), we demonstrate that the same is true for taurine-activated GlyRs; i.e. submaximal currents elicited by taurine on homomeric α1 S267I GlyRs show no ability to be enhanced by ethanol. This result, which is common to both agonists, indicates a convergence of the agonist signals by the time the activation wave reaches the

putative alcohol binding pocket between TM2 and TM3. The common mechanism by which ethanol potentiates channel function is therefore of great interest.

6.4 – Mechanisms of Ethanol Enhancement of the GlyR

Despite the fact that alcohol is one of the most used and abused drugs in society, the mechanisms by which it exerts its actions have only recently begun to be understood. Alcohol has many molecular targets throughout the body, many of which include ion channels such as BK channels, and a variety of ligand-gated ion channels such as those activated by NMDA, GABA or glycine. While it is now fairly well accepted that there is a site of action for ethanol on the GlyR, the mechanisms for its effects on channel function had not been thoroughly investigated. On one hand, there is abundant evidence that ethanol enhances GlyR function in whole cell studies. For instance, *in vitro* studies show that that ethanol enhances EC_2 glycinergic currents from α1 GlyR in oocytes by up to 120% at concentrations of 200 mM and is effective at concentrations as low as 5 mM (Mascia et al., 1996a). There is also growing evidence from Söderpalm's lab suggesting that GlyRs in the nucleus accumbens indeed play a role in alcohol consumption (Molander et al., 2005). However to date, only one study has proposed a mechanism by which ethanol enhances the function of native α1β GlyRs and this study based its conclusions on simulations from data recorded from macropatches. The data in this dissertation directly address the mechanism of alcohol's enhancement of the GlyR and deepen our understanding of an important molecular target for ethanol.

The parameters of GlyR function that remained unchanged in the presence of ethanol in the experiments in Chapter 5 are just as important for understanding ethanol actions as an allosteric modulator as those that were affected. First among them is

conductance, which remained unchanged at 70 pS for both ethanol concentrations. This was the main conductance state of the α1 GlyR in all the conditions, and conductance states greater than this were not observed. Although an increase in channel conductance could produce enhancement of receptor function and ethanol is proposed to bind quite close to the channel pore, there is no evidence that alcohol affects the open state in this manner. If it did increase conductance, one would expect ethanol to enhance the effects of maximally-effective concentrations of glycine, which is not seen. In addition, alcohol did not significantly affect channel open time at all, suggesting that ethanol does not stabilize the open state. Nor did the data require the addition of more open states to the GlyR model for an adequate fit, meaning that that ethanol did not appear to create novel open states. This may be somewhat unexpected given that with five potential glycine binding sites and at least five potential ethanol binding sites, there are a great many different possibilities for receptor modulation. Since we used a low concentration of glycine for the experiments, the receptor is rarely expected to be in a fully-liganded state. Thus, depending on where glycine was bound, ethanol could be found acting at that same subunit or it could be bound at another subunit that did not itself also bind glycine. It may be that the 50 mM and 200 mM ethanol concentrations used are high enough to saturate the alcohol binding sites and that subunits binding glycine are always also found in the ethanol-bound state.

The main effect of ethanol on GlyR receptor function was an increase in channel burst duration. In terms of the glycine kinetic mechanism, this was accounted for by a decrease in the unbinding rate of glycine. Of all eight parameters fit in the model, only the k_{-1} rate was significantly changed. It is interesting to note that ethanol did not have a more global effect on the rate constants and rather that its effect seems to be exerted upstream from where ethanol is suggested to bind. Ethanol must therefore send a

retrograde signal from the TM2/TM3 pocket back up along the protein to the glycine binding site in the LBD to antagonize unbinding of the agonist, emphasizing the concerted movement of the protein and the interconnectedness of the domains. As pointed out above in Chapter 5 and in the overview in Section 1.7.1, ethanol is similar to zinc with regards to its mechanism of potentiation of glycine-mediated currents. The location of the potentiating zinc binding site, like the ethanol binding site, has been debated. Interestingly, the residues that have been proposed to coordinate zinc binding and control zinc potentiation are not far from the TM2-TM3 linker region (Miller et al., 2005). It could be that some of the structural elements involved in Zn^{2+} potentiation are also involved in ethanol potentiation as the ethanol may produce a structural change that is similarly transduced through this region. However, the ability of zinc to increase taurine efficacy, which ethanol does not do (see Chapter 4) suggests differences between the mechanism of action of these two modulators.

With regards to ethanol's effects in the context of another kinetic scheme such as the flipped scheme of Lape et al. (2008) (**Fig. 1.5**), it is interesting and very important to consider that ethanol did not potentiate the effects of maximally-effective taurine concentrations as seen in Chapter 4. The flipped mechanism was enlightening for our understanding of partial agonist function because it proposes that taurine is a partial agonist due to its "reduced ability to flip" (Lape et al., 2008). In our fit of the data in Chapter 6, we do not include the flipped states in our model and these rates therefore have been collapsed into the closed to open state transition. However, if one supposes that ethanol was increasing transitions away from closed, towards open, through the flipped state then it would be expected that ethanol would increase the efficacy of taurine. Since this was not the case we can assume that ethanol does not increase these transitions for GlyR activation.

6.5 – Future Directions and Discussion

Scientific research should not only pointedly address the hypotheses that are initially set out but should also lead to interesting questions that arise due to the newly-acquired knowledge. While the work outlined here has added to our understanding of GlyR activation and how these signals are modulated by ethanol, there are many avenues left to pursue. Below, is a brief outline of possibilities for follow-up studies.

1. The single channel data for taurine on the D97R mutant GlyR are very crude. It would be helpful to pull enough single channel patches to fully examine how taurine, in addition to β-ABA, β-AIBA, and nipecotic acid affect the activation mechanism of this mutant. This could be complicated somewhat by an incomplete ability to fit the GlyR mechanism (see below) or by how the scheme relates to a spontaneously active mutant such as D97R, in which some of the openings of the channel are independent of agonist. Our assumption now is that taurine activates GlyR channels that have recovered from an auto-desensitized state and then that these receptors immediately transition to an open state with a high P_{open} once taurine binds. However, we know that this is not the case for all partial agonists of the GlyR since β-AIBA and nipecotic acid both clearly display reduced efficacies as partial agonists. Analysis of the data from detailed single channel experiments on D97R could help us understand which closed states the *trans*- forms of these partial agonists or antagonists stabilize and refine our understanding of partial agonism in the GlyR.

2. The research in Chapter 3 focused only on a handful of β-amino acid partial agonists, and there are other GlyR partial agonists that are α-amino acids that may not behave the same. Future studies could investigate the effect of the D97R mutation on other GlyR partial agonists or antagonists such as alanine and serine, both which also possess optical isomers but which do not have the *cis*- / *trans*- isomerism. By testing other drugs that act upon the GlyR on D97R mutants we can better understand the full extent to which the D97-R119 interaction affects agonist and antagonist function in this receptor.

3. Chapter 4 investigated the ethanol potentiation of taurine-activated currents in the GlyR; however other modulators may produce different results. For instance, there is evidence that volatile anesthetics increase the channel mean open time and intraburst P_{open} of the α1 GlyR (Roberts et al., unpublished observations). This suggests that these small molecules potentiate the receptor via, at least to some degree, a different mechanism than ethanol. If this were the case, one would expect that the whole-cell GlyR current response to a saturating taurine concentration could be increased with an anesthetic such as chloroform or isoflurane. Since taurine may be the endogenous neurotransmitter at various regions throughout the CNS, this information could provide a better understanding of how volatile anesthetics act to produce their effects *in vivo*.

4. The kinetic mechanism of GlyR enhancement by ethanol that is proposed in Chapter 5 may not wholly reflect ethanol effects on channel function. First, it would be useful to increase the glycine concentration range and simultaneously fit across that range so that one can study how ethanol affects the more fully liganded receptor. Our experiments used a very low concentration of glycine because the effects of ethanol are more apparent at these low concentrations, but this does not allow for much data collection at the right-

hand side of the mechanism in which the GlyR is expected to remain open longer. We know from whole-cell data that ethanol does not potentiate GlyR currents at saturating glycine concentrations (Mascia et al., 1996; Chapter 4) but a complete model should address all liganded states of the receptor. Secondly, the data could be re-fit using the expanded flipped mechanism. However, as argued above in Section 6.4, it seems unlikely that we would detect changes in rates leading from closed to flipped as a consequence of ethanol. Other changes such as the rate leading from flipped back towards closed could be affected though, and these would presumably be decreased. The data were not originally fit using this expanded mechanism because 1) they were fit adequately with the (simpler) mechanism proposed, which was also able to reproduce the data in simulations and 2) there are technical difficulties in getting the data to fit to a flipped scheme using QuB. Therefore to accomplish a fit to the flipped scheme it may be necessary to use David Colquhoun's HJCFIT and SCAN programs.

5. A frequent suggestion for the experiments in Chapter 5 was to use lower ethanol concentrations that might be more relevant to those achieved *in vivo* while consuming alcohol. The lowest ethanol concentration used in our study was 50 mM, which is almost 3x higher than the legal limit for driving, although concentrations in excess of this are routinely achieved by humans (Wetherill and Fromme, 2009). Additional data could be collected for 25 mM ethanol in order to address this point. However, there doesn't seem to be much reason to suspect that the mechanism of ethanol potentiation proposed would change at all at lower concentrations; rather it would be expected that the main conclusion of increased burst duration seen with ethanol would still be apparent (if measurable), albeit diminished. What may be of more interest though, rather than recordings of outside-out patches, would be to record the effects of ethanol on single

channel behavior in a cell-attached patch. This would allow for any intracellular processes that may contribute to ethanol potentiation of the GlyR, such as G-proteins that were suggested by Yevenes et al. (2006), to be measured. By comparing these results to the present data we may also be able to isolate which effects of ethanol are caused by the binding of ethanol in the binding pocket or to its effects on intracellular machinery.

6. In the context of better understanding ethanol modulation of the GlyR, it may also be interesting to investigate further the nature of changes made to the putative binding pocket, specifically to the S267 residue. Thus far no antagonist has been identified that specifically blocks the effects of ethanol on any ligand-gated ion channel. However, antagonists have been found for other alcohol targets. For example, octanol is an antagonist of ethanol effects on L1-mediated cell adhesion (Wilkemeyer et al., 2000). In addition small peptides also antagonize alcohol effects on L1 (Wilkemeyer et al., 2002; Wilkemeyer et al., 2003). We have previously determined that ethanol has no enhancing effects on the S267I mutant (Mihic et al., 1997; Ye et al., 1998) and ethanol even acts as a volatile anesthetic antagonist in this mutated GlyR (Beckstead et al., 2001). A single channel characterization of S267I with and without ethanol may help us understand why this mutant is insensitive to alcohol. Broadly speaking though, the volume of the residue at position S267 determines the receptor's response to ethanol. In particular, larger residues at the 267 position yield receptors that display an inhibitory response to ethanol (Ye et al., 1998). The precise nature of this inhibition is unknown. By studying receptors containing the S267F residue we have an opportunity to discover which aspects of channel function are inhibited by ethanol in these mutants in addition to the effect on channel function of a bulky amino acid at this important residue. The S267F mutant displays a significantly left-shifted glycine concentration-response curve, which is akin to

the left-shifting of the glycine concentration-response curve produced by ethanol and volatile anesthetics in WT GlyR. It may be expected then that the S267F mutant will display some of the same single channel properties as those produced by ethanol, specifically increased burst durations.

Bibliography

Aguayo LG and Pancetti FC (1994) Ethanol modulation of the γ-aminobutyric $acid_A$- and glycine- activated Cl^- current in cultured mouse neurons. *J Pharmacol Exp Ther* **270:** 61-69.

Aguayo LG, Tapia JC, Pancetti FC (1996) Potentiation of the glycine-activated Cl- current by ethanol in cultured mouse spinal neurons. *J Pharmacol Exp Ther* **279:** 1116-1122.

Ahmadi S, Lippross S, Neuhuber WL, Zeilhofer HU (2001) PGE_2 selectively blocks inhibitory glycinergic neurotransmission onto rat superficial dorsal horn neurons. *Nat Neurosci* **5:** 34-40.

Akk G, Li P, Bracamontes J, Reichert DE, Covey DF, Steinbach JH (2008) Mutations of the $GABA_A$ receptor alpha1 subunit M1 domain reveal unexpected complexity for modulation by neuroactive steroids. *Mol Pharmacol* **74:** 614-627.

Albrecht J and Schousboe A (2005) Taurine interaction with neurotransmitter receptors in the CNS: An update. *Neurochem Res* **30:** 1615-1621.

Armstrong N and Gouaux E (2000) Mechanisms for activation and antagonism of an AMPA-sensitive glutamate receptor: Crystal structures of the GluR2 ligand binding core. *Neuron* **28:** 165-181.

Assaf SY and Chung SH (1984) Release of endogenous Zn^{2+} from brain tissue during activity. *Nature* **308:** 734-736.

Auerbach A (2005) Gating of acetylcholine receptor channels: Brownian motion across a broad transition state. *Proc Natl Acad Sci USA* **102:** 1408-1412.

Auld DS (2001) Zinc coordination sphere in biochemical zinc sites. *Biometals* **14:** 271-313.

Beato M, Groot-Kormelink PJ, Colquhoun D, Sivilotti LG (2002) Openings of the rat recombinant α1 homomeric glycine receptor as a function of the number of agonist molecules bound. *J Gen Physiol* **119:** 443-466.

Beato M, Groot-Kormelink PJ, Colquhoun D, Sivilotti LG (2004) The activation mechanism of α1 homomeric glycine receptors. *J Neurosci* **24:** 895–906.

Beato M and Sivilotti LG (2007) Single-channel properties of glycine receptors of juvenile rat spinal motoneurons *in vitro*. *J Physiol* **580:** 497-506.

Becker K, Breitinger HG, Humeny A, Meink HM, Dietz B, Aksu F, Becker CM (2008) The novel hyperekplexia allele GLRA1(S267N) affects the ethanol site of the glycine receptor. *Eur J Hum Genet* **16:** 223-228.

Beckstead MJ, Phelan R, Mihic SJ (2001) Antagonism of inhalant and volatile anesthetic enhancement of glycine receptor function. *J Biol Chem* **276:** 24959-24964.

Beckstead MJ, Phelan R, Trudell JR, Bianchini MJ, and Mihic SJ (2002) Anesthetic and ethanol effects on spontaneously opening glycine receptor channels. *J Neurochem* **82**: 1343-1351.

Beckstead MJ, Weiner JL, Eger II EI, Gong DH, Mihic SJ (2000) Glycine and γ-Aminobutyric $Acid_A$ receptor function is enhanced by inhaled drugs of abuse. *Mol Pharm* **57:** 1199-1205.

Beckstein O, Biggin PC, Sansom MSP (2001) A hydrophobic gating mechanism for nanopores. *J Phys Chem B* **105:** 12902-12905.

Bertaccini EJ, Shapiro J, Brutlag DL, Trudell JR (2005) Homology modeling of a human glycine alpha 1 receptor reveals a plausible anesthetic binding site. *J Chem Inf Model* **45:** 128-135.

Bertrand J, Floyd RL, Weber MK (2005) Guidelines for identifying and referring persons with fetal alcohol syndrome. *Morb Mort Weekly Rep* **54:** RR11.

Betz H (1991) Glycine receptors: heterogeneous and widespread in the mammalian brain. *Trends Neurosci* **14:** 458-461.

Birinyi A, Parker D, Antal M, Shupliakov O (2001) Zinc co-localizes with GABA and glycine in synapses in the lamprey spinal cord. *J Comp Neurol* **433:** 208-221.

Bocquet N, Nury H, Baaden M, Le Poupon C, Changeux JP, Delarue M, Corringer PJ (2009). X-ray structure of a pentameric ligand-gated ion channel in an apparently open conformation. *Nature* **457:** 111-114.

Bormann J, Hamill OP, Sakmann B (1987) Mechanism of anion permeation through channels gated by glycine and γ-aminobutyric acid in mouse cultured spinal neurones. *J Physiol* **385:** 243-286.

Bormann J, Rundsröm N, Betz H, Langosch D (1993) Residues within transmembrane segment M2 determine chloride conductance of glycine receptor homo- and hetero-oligomers. *EMBO J* **12:** 3729-3737.

Bouzat C, Gumilar F, Spitzmaul G, Wang HL, Rayes D, Hansen SB, Taylor P, Sine SM (2004) Coupling of agonist binding to channel gating in an ACh-binding protein linked to an ion channel. *Nature* **430:** 896-890.

Brejc K, van Dijk WJ, Klaassen RV, Schuurmans M, van der Oost J, Smit AB, Sixma TK (2001) Crystal structure of an ACh-binding protein reveals the ligand-binding domain of nicotinic receptors. *Nature* **411**: 269-276.

Burzomato V, Beato M, Groo-Kormelink PJ, Colquhoun D, Sivilotti LG (2004) Single-channel behavior of hetermeric α1β glycine receptors: An attempt to detect a conformational change before the channel opens. *J Neurosci* **24:** 10924-10940.

Celentano JJ, Gibbs TT, Farb, DH (1988) Ethanol potentiates GABA and glycine induced currents in chick spinal cord neurons. *Brain Res* **455:** 377-380.

Celie PNH, van Rossum-Fikkert SE, van Dijk WJ, Brejc K, Smit AB, Sixma TK (2004) Nicotine and carbamylcholine binding to nicotinic acetylcholine receptors as studied in AChBP crystal structures. *Neuron* **41:** 907-914.

Cheng MH, Coalson RD, Cascio M (2008) Molecular dynamics simulations of ethanol binding to the transmembrane domain of the glycine receptor: Implications for the channel potentiation mechanism. *Proteins: Struct, Funct, Bioinf* **71:** 972-981.

Colman A (1984) Expression of exogenous DNA in Xenopus oocytes, in *Transcription and Translation: A Practical Approach* (Hames BD, Higgins SJ, eds), 49-69. Washington, DC: Oxford Press.

Colquhoun D and Hawkes AG (1977) Relaxation and fluctuations of membrane currents that flow through drug-operated channels. *Proc R Soc Lond B Biol Sci* **199:** 231-262.

Colquhoun D and Sakmann B (1985) Fast events in single-channel currents activated by acetylcholine and its analogues at the frog muscle end-plate. *J. Physiol.* **369:** 501-557.

Colquhoun D and Sivilotti LG (2004) Function and structure in glycine receptors and some of their relatives. *Trends Neurosci* **27:** 337-344.

Colquhoun D (2006) Agonist-activated ion channels. *Br J Pharmacol* **147:** S17-26.

Corry B (2006) An energy-efficient gating mechanism in the acetylcholine receptor channel suggested by molecular Brownian dynamics. *Biophys J* **90:** 799-810.

Crawford DK, Trudell JR, Bertaccini EJ, Li K, Davies DL, Alkana RL (2007) Evidence that ethanol acts on a target in Loop 2 of the extracellular domain of α1 glycine receptors. *J Neurochem* **102:** 2097-2109.

Cymes GD and Grosman C (2008) Pore-opening mechanism of the nicotinic acetylcholine receptor evinced by proton transfer. *Nat Nat Struct Mol Biol* **15:** 389-396.

Cymes GD, Ni Y, Grosman C (2005) Probing ion-channel pores one proton at a time. *Nature* **438:** 975-980.

Daly EC and Aprison MH (1974) Distribution of serine hydroxymethyltransferase and glycine transaminase in several areas of the central nervous system of the rat. *J Neurochem* **22:** 877-885.

Dupre ML, Broyles JM, Mihic SJ (2007) Effects of a mutation in the TM2-TM3 linker region of the glycine receptor alpha1 subunit on gating and allosteric modulation. *Brain Res* **1152**: 1-9.

Chakrapani S, Bailey TD, Auerbach A (2003) The role of Loop 5 in acetylcholine receptor channel gating. *J Gen Physiol* **122:** 521-539.

Cheng MH, Coalson RD, Cascio M. (2008) Molecular dynamics simulations of ethanol binding to the transmembrane domain of the glycine receptor: implications for the channel potentiation mechanism. *Proteins* **71:** 972-981.

Crawford DK, Trudell JR, Bertaccini EJ, Li K, Davies DL, Alkana RL (2007) Evidence that ethanol acts on a target in Loop 2 of the extracellular domain of α1 glycine receptors. *J Neurochem* **102:** 2097-2109.

Dahchour A, Quertemont E, De Witte P (1996) Taurine increases in the nucleus accumbens microdialysate after acute ethanol administration to naive and chronically alcoholised rats. *Brain Res* **735:** 9-19.

Davidoff RA, Shank RP, Graham LT Jr, Aprison MH, Werman R (1967) Is glycine a neurotransmitter? *Nature* **214:** 680-681.

Deitrich RA, Bludeau P, Erwin VG (2000) Phenotypic and genotypic relationships between ethanol tolerance and sensitivity in mice selectively bred for initial sensitivity to ethanol (SS and LS) or development of acute tolerance (HAFT and LAFT). *Alcohol Clin Exp Res* **32:** 67-76.

del Castillo J and Katz B (1957) Interaction at end-plate receptors between different choline derivatives. *Proc Royal Soc London* **89:** 1765-1769.

Dutton RC, Maurer AJ, Sonner JM, Fanselow MS, Laster MJ, Eger II EI (2001) The concentration of isoflurane required to suppress learning depends on the type of learning. *Anesthesiology* **94:** 514-519.

Eger II EI, Saidman LJ, Brandstate B (1965) Minimum alveolar anesthetic concentration: A standard of anesthetic potency. *Anesthesiology* **26:** 756-763.

Eggers ED and Berger AJ (2004) Mechanisms for the modulation of native glycine receptor channels by ethanol. *J Neurophysiol* **91:** 2685-2695.

Elmslie FV, Hutchings SM, Spencer V, Curtis A, Covanis T, Gardiner RM, Rees M (1996) Analysis of GLRA1 in hereditary and sporadic hyperekplexia: a novel mutation in a family cosegregating for hyperekplexia and spastic parapesis. *J Med Genet* **33:** 435-436.

Engblom AC and Åkerman KEO (1991) Effect of ethanol on γ-aminobutyric acid and glycine receptor-coupled fluxes in rat brain synaptoneurosomes. *J Neurochem* **57:** 384-390.

Ericson M, Molander A, Stomberg R, Soderpalm B (2006) Taurine elevates dopamine levels in the rat nucleus accumbens; antagonism by strychnine. *Eur J Pharmacol* **23**: 3225-3229.

Fang Z, Gong D, Ionescu P, Laster MJ, Eger II EI, Kendig JJ (1997) Maturation decreases ethanol minimum alveolar anesthetic concentration (MAC) more than desflurane MAC in rats. *Anesth Analg* **84:** 852-858.

Faroni JS and McCool BA (2004) Extrinsic factors regulate partial agonist efficacy of strychnine-sensitive glycine receptors. *BMC Pharmacol* **4:** 16.

Fatima-shad K and Barry PH (1993) Anion permeation in GABA- and glycine-gated channels of mammalian cultured hippocampal neurons. *Proc R Soc Lond B* **253:** 69-75.

Findlay GS, Wick MJ, Mascia MP, Wallace D, Miller GW, Harris RA, Blednov YA (2002) Transgenic expression of a mutant glycine receptor decreases alcohol sensitivity of mice. *J Pharmacol Exp Ther* **300:** 526-534.

Franks NP and Lieb WR (1982) Molecular mechanisms of general anaesthesia. *Nature* **300:** 487-493.

Franks NP and Lieb WR (1984) Do general anesthetics act by competitive binding to specific receptors? *Nature* **310:** 599-601.

Franks NP and Lieb WR (1994) Molecular and cellular mechanisms of general anesthesia. *Nature* **367:** 607-614.

Franks NP and Lieb WR (1997) Anesthetics set their sites on ion channels. *Nature* **389:** 334-335.

Fuchs CS, Stamper MJ, Colditz GA, Giovannucci EL, Manson JE, Kawachi I, Hunter DJ, Hankinson SE, Hennekens CH, Rosner B, Speizer FE, Willett WC (1995) Alcohol consumption and mortality among women. *N Engl J Med* **332:** 1245-1250.

Galzi JL, Devillers-Thiéry A, Hussy N, Bertand S, Changeux JP, Bertrand D (1992) Mutations in the channel domain of a neuronal nicotinic receptor convert ion selectivity from cationic to anionic. *Nature* **359:** 500-505.

Gao F, Bren N, Burghardt TP, Hansen S, Henchman RH, Taylor P, McCammon JA, Sine SM (2005) Agonist-mediated conformational changes in acetylcholine-binding protein revealed by simulation and intrinsic tryptophan fluorescence *J Biol Chem* **280:** 8443-8451.

Gonzales RA, Job MO, Doyon WM (2004) The role of mesolimbic dopamine in the development and maintenance of ethanol reinforcement. *Pharmacol Ther* **103:** 121-146.

Gotti C, Clementi F, Forani A, Gaimarri A, Guiducci S, Manfredi I, Moretti M, Pedrazzi P, Pucci L, Zoli M (2009) Structural and fucntional diversity of native brain and neuronal nicotinic receptors. *Biochem Pharmacol* **78**: 703-711.

Grenningloh G, Rienitz A, Schmitt B, Methfessel C, Zensen M, Beyreuther K, Gundelfinger ED, Betz H (1987) The strychnine-binding subunit of the glycine receptor shows homology with nicotinic acetylcholine receptors. *Nature* **328:** 215-220.

Grosman C, Zhou M, Auerbach A (2000) Mapping the conformational wave of acetylcholine receptor channel gating. *Nature* **403**: 773-776.

Grudzinska J, Schemm R, Haeger S, Nicke A, Schmalzing G, Betz H, Laube B (2005) The β subunit determines the ligand binding properties of synaptic glycine receptors. *Neuron* **45:** 727-739.

Grundwald E (1985) Structure-energy relations, reaction mechanism, and disparity of progress of concerted reaction events. *J Am Chem Soc* **107:** 125-133.

Gunthorpe MJ and Lummis CR (2001) Conversion of the ion selectivity of the 5-HT_3 receptor from cationic to anionic reveals a conserved feature of the ligand-gated ion channel superfamily. *J Biol Chem* **276:** 10977-10983.

Hamill OP, Marty A, Neher E, Sakmann B, Sigworth FJ (1981) Improved patch-clamp techniques for high-resolution current recording from cells and cell-free membrane patches. *Pflugers Arch* **391:** 85-100.

Hamill OP, Bormann J, Sakmann B (1983) Activation of multiple-conductance state chloride channels in spinal neurons by glycine and GABA. *Nature* **305:** 805-808.

Han NR, Haddrill JL, Lynch JW (2001) Characterization of a glycine receptor domain that controls the binding and gating mechanisms of the β-amino acid agonist, taurine. *J Neurochem* **79:** 636-647.

Han NR, Clements JD, Lynch JW (2004) Comparison of Taurine- and Glycine-induced conformational changes in the M2-M3 domain of the glycine receptor. *J Biol Chem* **279:** 19559-19565.

Harvey RJ, Thomas P, James CH, Wilderspin A, Smart TG (1999) Identification of an inhibitory Zn^{2+} binding site on the human glycine receptor α1 subunit. *J Physiol* **520:** 53-64.

Hatton CJ, Shelley C, Brydson M, Beeson D, Colquhoun D (2003) Properties of the human muscle nicotinic receptor, and of the slow-channel myasthenic syndrome mutant εL221F, inferred from maximum likelihood fits. *J Physiol* **547:** 729-760.

Hilf RJC and Dutzler R (2008) X-ray structure of a prokaryotic pentameric ligand-gated ion channel. *Nature* **452:** 375-380.

Hogg RC, Buisson B, Bertrand D (2005) Allosteric modulation of ligand-gated ion channels. *Biochem Pharmacol* **70:** 1267-1276.

Hsiao B, Mihalak KB, Magleby KL, Luetje CW (2008) Zinc potentiates neuronal nicotinic receptors by increasing burst duration. *J Neurophysiol* **99:** 999-1007.

Huxtable, RJ (1992) Physiological Actions of Taurine. *Physiol Rev* **72:** 101-163.

Inanobe A, Furukawa H, Gouaux E (2005) Mechanism of partial agonist action at the NR1 subunit of NMDA receptors. *Neuron* **47:** 71-84.

Jackson MB (1986) Kinetics of unliganded acetylcholine receptor channel gating. *Biophys J* **49:** 663-672.

Jha A, Cadugan DJ, Purohit P, Auerbach A (2007) Acetylcholine receptor gating at extracellular transmembrane domain interface: the Cys-loop and M2-M3 linker. *J Gen Physiol* **130:** 547-558.

Jin R, Banke TG, MAyer ML, Traynelis SF, Gouaux E (2003) Structural basis for partial agonist action at ionotropic glutamate receptors. *Nat Neurosci* **6:** 803-810.

Jones MV and Westbrook GL (1995) Desensitized states prolong $GABA_A$ channel responses to brief agonist pulses. *Neuron* **15:** 181-191.

Jonsson S, Kerekes N, Hyytiä P, Ericson M, Söderpalm B (2009) Glycine receptor expression in the forebrain of male AA/ANA rats. *Brain Res* Epub ahead of print.

Karlin A (2002) Emerging structure of the nicotinic accetylcholine receptors. *Nat Rev Neurosci* **3**: 102-114.

Kash TL, Jenkins A, Kelley JC, Trudell JR, Harrison NL (2003) Coupling of agonist binding to channel gating in the $GABA_A$ receptor. *Nature* **421:** 272-275.

Kay AR (2004) Detecting and minimizing zinc contamination in physiological solutions. *BMC Physiol* **4**: 4.

Kelley SP, Dunlop JI, Kirkness EF, Lambert JJ, Peters JA (2003) A cytoplasmic region determines the single-channel conductance in 5-HT_3 receptors. *Nature* **424:** 321-324.

Kim MS, Repp A, Smith DP (1998) LUSH Odorant-binding protein mediates chemosensory responses to alcohols in *Drosophila melanogaster*. *Genetics* **150:** 711-721.

Kruse SW, Zhao R, Smith DP, Jones DNM (2003) Structure of a specific alcohol-binding site defined by the odorant binding protein LUSH from *Drosophila melanogaster*. *Nat Struct Biol* **10:** 694-700.

Kuhse J, Betz H, Kirsch J (1995) The inhibitory glycine receptor: architecture, synaptic localization and molecular pathology of a postsynaptic ion-channel complex. *Curr Opin Neurobiol* **5:** 318-323.

Kussius CL and Popescu GK (2009) Kinetic basis of partial agonism at NMDA receptors. *Nat Neurosci* **12:** 1114-1120.

Langosch D, Thomas L, Betz H (1988) Conserved quaternary structure of ligand-gated ion channels: The postsynaptic glycine receptor is a pentamer. *Proc Natl Acad Sci USA* **85:** 7394-7398.

Langosch D, Laube B, Rundsröm N, Schmieden V, Bormann J, Betz H (1994) Decreased agonist affinity and chloride conductance of mutant glycine receptors associated with human hereditary hyperekplexia. *EMBO J* **13:** 4223-4228.

Lape R, Colquhoun D, Sivilotti LG (2008) On the nature of partial agonism in the nicotinic receptor superfamily. *Nature* **454:** 722-728.

Larson AA and Kitto KF (1997) Manipulations of zinc in the spinal cord, by intrathecal injection of zinc chloride, disodium-calcium-EDTA, or dipicolinic acid, alter nociceptive activity in mice. *J Pharmacol Exp Ther* **282:** 1319-1325.

Laube B, Kuhse J, Betz H (2000) Kinetic and mutational analysis of Zn^{2+} modulation of recombinant human inhibitory glycine receptors. *J Physiol* **522:** 215-230.

Laube B, Kuhse J, Rundström N, Kirsch J, Schmieden V, Betz H (1995) Modulation by zinc ions of native rat and recombinant human inhibitory glycine receptors. *J Physiol* **483:** 613-619.

Laube B, Makasay G, Schemm R, Betz H (2002) Modulation of glycine receptor function: a novel approach for therapeutic intervention at inhibitory synapses? *Trends Pharmacol Sci* **23:** 519-527.

Lee WY and Sine SM (2005) Principal pathway coupling agonist binding to channel gating in nicotinic receptors. *Nature* **438:** 243-247.

Legendre P (2001) The glycinergic inhibitory synapse. *Cell Mol Life Sci* **58:** 760-793.

Lewis CA, Aiimed Z, Faber DS (1991) A characterization of glycinergic receptors present in cultured rat medullary neurons. *J Neurophys* **66:** 1291-1303.

Lewis TM, Schofield PR, McClellan AML (2003) Kinetic determinants of agonist action at the recombinant human glycine receptor. *J Physiol* **549:** 361-374.

Lewis TM, Sivilotti LG, Colquhoun D, Gardiner RM, Schoepfer R, Rees M (1998) Properties of human glycine receptors containing the hyperekplexia mutation α1(K276E), expressed in *Xenopus* oocytes. *J Physiol* **507:** 25-40.

Lobo IA, Mascia MP, Trudell JR, Harris RA (2004) Channel gating of the glycine receptor changes accessibility to residues implicated in receptor potentiation by alcohols and anesthetics. *J Biol Chem* **279:** 33919-33927.

Lobo IA, Mascia MP, Trudell JR, Harris RA (2006) Accessibility to residues in transmembrane segment four of the glycine receptor. *Neuropharmacology* **50:** 174-181.

Lobo IA, Harris RA, Trudell JR (2008) Cross-linking of sites involved with alcohol action between transmembrane segments 1 and 3 of the glycine receptor following activation. *J Neurochem* **104:** 1649-1662.

Lovinger DM (1999) 5-HT_3 receptors and the neural actions of alcohols: An increasingly exciting topic. *Neurochem Int* **35:** 125-130.

Lovinger DM, Sung KW, Zhou Q (2000) Ethanol and trichloroethanol alter gating of 5-HT3 receptor-channels in NCB-20 neuroblastoma cells. *Neuropharmacology* **39:** 561-570.

Lummis SCR, Beene DL, Lee LW, Lester HA, Broadhurst RW, Dougherty DA (2005) *Cis-trans* isomerization at a proline opens the pore of a neurotransmitter-gated ion channel. *Nature* **438:** 248-252.

Lüscher B and Keller CA (2004) Regulation of $GABA_A$ receptor trafficking , channel activity, and functional plasticity of inhibitory synapses. *Pharmacol Ther* **102:** 195-221.

Lynch JW, Jacques P, Pierce KD, Schofield PR (1998) Zinc potentiation of the glycine receptor chloride channel is mediated by allosteric pathways. *J Neurochem* **71:** 2159-2168.

Lynch JW (2004) Molecular structure and function of the glycine receptor chloride channel. *Physiol Rev* **84:** 1051-1095.

Magleby KL and Pallotta BS (1983) Burst kinetics of single calcium-activated potassium channels in cultured rat muscle. *J Physiol* **344:** 605-623.

Malosio ML, Marquèze-Poey B, Khuse J, Betz H (1991) Widespread expression of glycine receptor subunit mRNAs in the adult and developing rat brain. *EMBO J* **10**: 2401-2409.

Mascia MP, Mihic SJ, Valenzuela CF, Schofield PR, Harris RA (1996a) A single amino acid determines differences in ethanol actions on strychnine-sensitive glycine receptors. *Mol Pharmacol* **50:** 402-406.

Mascia MP, Machu TK, Harris RA (1996b) Enhancement of homomeric glycine receptor function by long-chain alcohols and anaesthetics. *Br J Pharmacol* **119:** 1331-1336.

Mascia MP, Trudell JR, Harris RA (2000) Specific binding sites for alcohols and anesthetics on ligand-gated ion channels. *Proc Natl Acad Sci USA* **97:** 9305-9310.

Mascia MP, Wick MJ, Martinez LD, Harris RA (1998) Enhancement of glycine receptor function by ethanol: role of phosphorylation. *Br J Pharmacol* **125:** 263-270.

McCool BA and Botting SK (2000) Characterization of strychnine-sensitive glycine receptors in acutely isolated adult rat basolateral amygdala neurons. *Brain Res* **859:** 341-351.

McCracken LM, Trudell JR, Goldstein BE, Harris RA, Mihic SJ (in press) Zinc enhances ethanol modulation of the alpha1 glycine receptor. *Neuropharmacology*.

McGovern PE, Zhang J, Tang J, Zhang Z, Hall GR, Moreau RA, Nunez A, Butrym ED, Ricards MP, Wang CS, Cheng G, Zhao Z, Wang C (2004) Fermented beverages of pre- and proto-historic China. *Proc Natl Acad Sci USA* **101:** 17593-17598.

Meyer G, Kirsch J, Betz H, Langosch D (1995) Identification of a gephyrin binding motif on the glycine receptor β subunit. *Neuron* **15:** 563-572.

Mihic SJ, Ye Q, Wick MJ, Koltchine VV, Krasowski MD, Finn SE, Mascia MP, Valenzuela CF, Hanson KK, Greenblatt EP, Harris RA, Harrison NL (1997) Sites of alcohol and volatile anaesthetic action on GABAA and glycine receptors. *Nature* **389**: 385-389.

Mihic SJ (1999) Acute effects of ethanol on $GABA_A$ and glycine receptor function. *Neurochem Int* **35:** 115-123.

Miller PS, Da Silva HMA, Smart TG (2005) Molecular basis for zinc potentiation at strychnine-sensitive glycine receptors. *J Biol Chem* **280:** 37877-37884.

Miller PS, Topf M, Smart TG (2008) Mapping a molecular link between allosteric inhibition and activation of the glycine receptor. *Nat Struct Mol Biol* **15**: 1084-1093.

Mishina M, Takai T, Imoto K, Noda M, Takahashi T, Numa S (1986) Molecular distinction between fetal and adult forms of muscle acetylcholine receptor. *Nature* **321**: 406-411.

Mitra A, Bailey TD, Auerbach AL (2004) Structural dynamics of the M4 transmembrane segment during acetylcholine receptor gating. *Structure* **12:** 1909-1918.

Miyazawa A, Fujiyoshi Y, Stowell M, Unwin M (1999) Nicotinic acetylcholine receptor at 4.6 resolution: Transverse tunnels in the channel wall. *J Mol Biol* **288:** 765-786.

Miyazawa A, Fujiyoshi Y, Unwin N (2003) Structure and gating mechanism of the acetylcholine receptor pore. *Nature* **423:** 949-955.

Molander A and Söderpalm B (2005) Accumbal strychnine-sensitive glycine receptors: an access point for ethanol to the brain reward system. *Alcohol Clin Exp Res* **29:** 27-37.

Molander A, Löf E, Stomberg R, Ericson M, Söderpalm B (2005) Involvement of accumbal glycine receptors in the regulation of voluntary ethanol intake in the rat. *Alcohol Clin Exp Res* **29:** 38-45.

Molander A, Lidö HH, Löf E, Ericson M, Söderpalm B (2007) The glycine reuptake inhibitor Org 25935 decreases ethanol intake and preference in male Wistar rats. *Alcohol Alcohol.* **42:** 11-18.

Monod J, Wyman J, Changeux JP (1965) On the nature of allosteric transition: A plausible model. *J Mol Biol* **12:** 88-118.

Moorehouse AJ, Jacques P, Barry PH, Schofield PR (1999) The startle disease mutation Q266H, in the second transmembrane domain of the human glycine receptor, impairs channel gating. *Mol Pharm* **55:** 386-395.

Mori M, Gahwiler BH, Gerber U (2002) β-alanine and taurine as endogenous agonists at glycine receptors in the rat hippocampus *in vitro*. *J Physiol* **539:** 191-200.

Mukhtasimova N, Lee WY, Wang HL, Sine SM (2009) Detection and trapping of intermediate states priming nicotinic receptor channel opening. *Nature* **459:** 451-454.

Narahashi T, Aistrup GL, Marszalec W, Nagata K (1999) Neuronal nicotinic acetylcholine receptors: A new target site of ethanol. *Neurochem Int* **35:** 131-141.

Nevin ST, Cromer BA, Haddrill JL, Morton CJ, Parker MW, Lynch JW (2003) Insights into the structural basis for zinc inhibition of the glycine receptor. *J Biol Chem* **278:** 28985-28992.

O'mara M, Barry PH, Chung SH (2003) A model of the glycine receptor deduced from Brownian dynamics studies. *Proc Natl Acad Sci USA* **100:** 4310-4315.

O'mara M, Comer B, Parker M, Chung SH (2005) Homology model of the $GABA_A$ receptor examined using Brownian dynamics. *Biophys J* **88:** 3286-3299.

Oswald RE, Changeux JP (1982) Crosslinking of α-Bungarotoxin to the acetylcholine receptor from *Torpedo Marmorata* by ultraviolet light irradiation. *FEBS Lett* **139**: 225-229.

Pallotta BS (1991) Single ion channel's view of classical receptor theory. *FASEB J* **5:** 2035-2043.

Pfeiffer F, Graham D, Betz H (1982) Purification by affinity chromatography of the glycine receptor rat spinal cord. *J Biol Chem* **257:** 9389-9393.

Pless SA, Dibas MI, Lester HA, Lynch JW (2007) Conformational variability of the glycine receptor M2 domain in response to activation by different agonists. *J Biol Chem* **282:** 36057-36067.

Pless SA and Lynch JW (2009a) Ligand specific conformational changes in the α1 glycine receptor ligand-binding domain. *J Biol Chem* **284:** 15847-15856.

Pless SA and Lynch JW (2009b) Magnitude of a conformational change in the glycine receptor β1-β2 loop is correlated with agonist efficacy. *J Biol Chem* **284:** 27370-27376.

Plested AJR, Groot-Komelink PJ, Colquhoun D, Sivilotti LG (2007) Single-channel study of the spasmodic mutation α1A52S in recombinant rat glycine receptors. *J Physiol* **581:** 51-73.

Price TJ, Cervero F, Gold MS, Hammond DL, Prescott SA (2009) Chloride regulation in the pain pathway. *Brain Res Rev* **60:** 149-170.

Pringle MJ, Brown KB, Miller KW (1981) Can the lipid theories of anesthesia account for the cutoff in anesthetic potency in homologous series of alcohols? *Mol Pharm* **19:** 49-55.

Purohit P, Mitra A, Auerbach A (2007) A stepwise mechanism for acetylcholine receptor channel gating. *Nature* **446:** 930-933.

Qin F, Auerbach A, Sachs F (2000a) A direct optimization approach to hidden Markov modeling for single channel kinetics. *Biophys J* **79:**1915-1927.

Qin F, Auerbach A, Sachs F (2000b) Hidden Markov modeling for single channel kinetics with filtering and correlated noise. *Biophys J* **79:**1928-1944.

Quinlan JJ, Ferguson C, Jester K, Firestone LL, Homanics GE (2002) Mice with glycine receptor subunit mutations are both sensitive and resistant to volatile anesthetics**.** *Anesth Analg* **95:** 578-582.

Rajendra S and Schofield PR (1995) Molecular mechanism of inherited startle disorders. *Trends Neurosci* **18:** 80-82.

Rajendra S, Vandenberg RJ, Pierce KD, Cunningham AM, French PW, Barry PH, Schofield PR (1995) The unique extracellular disulfide loop of the glycine receptor is a principal ligand binding element. *EMBO J* **14:** 2987-2998.

Rajendra S, Lynch JW, Schofield PR (1997) The glycine receptor. *Pharmacol Ther* **73**: 121-146.

Rice DP (1999) Economic costs of substance abuse, 1995. *Proc Assoc Am Physicians* **111**: 119-125.

Rudolph U and Antkowiak B (2004) Molecular and neuronal substrates for general anaesthetics. *Nat Rev Neurosci* **5:** 709-720.

Rundsröm N, Schmieden V, Betz H, Bormann J, Langosch D (1994) Cyanotriphenylborate: Subtype-specific blocker of glycine receptor chloride channels. *Proc Natl Acad Sci USA* **91:** 8950-8954.

Ryan SG, Dixon MJ, Nigro MA, Kelts A, Markland ON, Terry JC, Shiang R, Wasmuth JJ, O'Connell P (1992) Genetic and radiation hybrid mapping of the hyperekplexia region on chromosome 5q. *Am J Hum Genet* **51:** 1334-1343.

Salimäki J, Scriba G, Piepponen TP, Rautolahti N, Ahtee L (2003) The effects of systemically administered taurine and N-pivaloytaurine on striatal extracellular dopamine and taurine in freely moving rats. *Naunyn-Schmiedeberg's Arch Pharmacol* **368:** 134-141.

Schmieden V, Grenningloh G, Schofield PR, Betz H (1989) Functional expression in *Xenopus* oocytes of the strychnine binding 48kd subunit of the glycine receptor. *EMBO J* **8:** 695-700.

Schmieden V, Kuhse J, Betz H (1992) Agonist pharmacology of neonatal and adult glycine receptor α subunits: Identification of amino acid residues involved in taurine activation. *EMBO J* **11**: 2025-2032.

Schmieden V, Kuhse J, Betz H (1993) Mutation of glycine receptor subunit creates β-alanine receptor responsive to GABA. *Science* **262:** 256-258.

Schmieden V and Betz H (1995) Pharmacology of the inhibitory glycine receptor: Agonist and antagonist actions of the amino acids and piperidine carboxylic acid compounds. *Mol Pharmacol* **48**: 919-927.

Schmieden V, Kuhse J, Betz H (1999) A Novel Domain of the Inhibitory Glycine Receptor Determining Antagonist Efficacies: Further Evidence for Partial Agonism Resulting From Self-Inhibition. *Mol Pharm* **56**: 464-472.

Schofield CM, Jenkins A, Harrison NL (2003) A highly conserved aspartic acid residue in the signature disulfide loop of the α1 subunit is a determinant of gating in the glycine receptor. *J Biol Chem* **36:** 34079-34083.

Schrøder HD, Danscher G, Jo SM, Su H (2000) Zinc-enriched boutons in rat spinal cord. *Brain Res* **868:** 119-122.

Sharko AC and Hodge CW (2008) Differential modulation of ethanol-induced sedation and hypnosis by metabotropic glutamate receptor antagonists in C57BL/6J mice. *Alcohol Clin Exp Res* **32:** 67-76.

Shibinoki S, Kogure M, Sugahara M, Ishikawa K (1993) Effect of systemic administration of N-methyl-D-Aspartic acid on extracellular taurine level measured by microdialysis in the hippocampal CA1 field and striatum of rats. *J Neurochem* **61:** 1698-1704.

Sigworth FJ and Sine SM (1987) Data transformations for improved display and fitting of single-channel dwell time histograms. *Biophys J* **52:** 1047-1054.

Sine SM (2002) The nicotinic receptor ligand binding domain. *J Neurobiol* **53**: 431-446.

Sine SM and Engel AG (2006) Recent advances in Cys-loop receptor structure and function. *Nature* **440:** 448-455.

Sonner JM, Antognini JF, Dutton RC, Flood P, Gray AT, Harris RA, Homanics GE, Kendig J, Orser B, Raines DE, Trudell J, Vissel B, Eger II EI (2003) Inhaled anesthetics and immobility: Mechanisms, mysteries, and minimum alveolar anesthetic concentration. *Anesth Analg* **97:** 718-740.

Suwa H, Saint-Amant L, Triller A, Drapeau P, Legendre P (2000) High-affinity zinc potentiation of inhibitory postsynaptic glycinergic currents in zebrafish hindbrain. *J Neurophysiol* **85:** 912-925.

Steinbach JH and Akk G (2001) Modulation of $GABA_A$ receptor channel gating by pentobarbital. *J Physiol* **537:** 715-733.

Tapia JC, Aguilar LF, Sotomayor CP, Aguayo LG (1998) Ethanol affects the function of a neurotransmitter receptor protein without altering the membrane lipid phase. *Eur J Pharmacol* **354:** 239-244.

Thun MJ, Peto R, Lopez AD, Monaco JH, Henley SJ, Heath Jr. CW, Doll R (1997) Alcohol consumption and mortality among middle-aged and elderly U.S. adults. *N Engl J Med* **337:** 1705-1714.

Todorovic J, Welsh BT, Bertaccini E, Trudell J, Mihic SJ (2009) Disruption of an inter-subunit electrostatic bond constitutes an initial step in glycine receptor activation. submitted.

Twyman RE and Macdonald RL (1991) Kinetic properties of the glycine receptor main- and subconductance states of mouse spinal cord neurones in culture. *J Physiol* **435:** 303-331.

Unwin N (1993) Nicotinic acetylcholine receptor at 9 ´ resolution. *J Mol Biol* **229:** 1101-1124.

Unwin N (1995) Acetylcholine receptor channel imaged in the open state. *Nature* **373:** 37-43.

Unwin N (2003) Structure and action of the nicotinic acetylcholine receptor explored by electron microscopy. *FEBS Lett* **555:** 91-95.

Vafa B, Lewis TM, Cunningham AM, Jacques P, Lynch JW, Schofield PR (1999) Identification of a new ligand binding domain in the α1 subunit of the inhibitory glycine receptor. *J Neurochem* **73:** 2158-2166.

van den Pol AN and Gorcs T (1988) Glycine and glycine receptor immunoreactivity in brain and spinal cord. *J Neurosci* **8:** 472-492.

Vandenberg RJ, French CR, Barry PH, Shine J, Schofield PR (1992) Antagonism of ligand-gated ion channel receptors: Two domains of the glycine receptor α subunit form the strychnine-binding site. *Proc Natl Acad Sci USA* **89:** 1765-1769.

Vogt K, Mellor J, Tong G, Nicoll R (2000) The actions of synaptically released zinc at hippocampal mossy fiber synapses. *Neuron* **26:** 187-196.

Welsh BT, Goldstein BE, Mihic SJ. (2009) Single channel analysis of ethanol enhancement of glycine receptor function. J Pharmacol Exp Ther **330:** 198-205.

Werman R, Davidoff RA, Aprison MH (1967) Inhibition of motoneurones by iontophoresis of glycine. *Nature* **214:** 681-683.

Wetherill RR and Fromme K (2009) Subjective Responses to Alcohol Prime Event-Specific Alcohol Consumption and Predict Blackouts and Hangover. *J Stud Alcohol Drugs* **70:** 593-600.

Wick MJ, Mihic SJ, Ueno S, Mascia MP, Trudell JR, Brozowski SJ, Ye Q, Harrison NL, Harris RA (1998) Mutations of gamma-aminobutyric acid and glycine receptors change alcohol cutoff: evidence for an alcohol receptor? *Proc Natl Acad Sci USA* **95:** 6504-6509.

Wilkemeyer MF, Sebastian AB, Smith SA, Charness ME (2000) Antagonists of alcohol inhibition of cell adhesion. *Proc Natl Acad Sci USA* **97:** 3690-3695.

Wilkemeyer MF, Menkari CE, Spong CY, Charness ME (2002) Peptide antagonists of ethanol inhibition of l1-mediated cell-cell adhesion. *J Pharmacol Exp Ther* **303:** 110-116.

Wilkemeyer MF, Chen SY, Menkari CE, Brenneman DE, Sulik KK, Charness ME (2003) Differential effects of ethanol antagonism and neuroprotection in peptide fragment NAPVSIPQ prevention of ethanol-induced developmental toxicity. *Proc Natl Acad Sci USA* **100:** 8543-8548.

Williams KL, Ferko AP, Barbieri EJ and Di Gregorio GJ (1995) Glycine enhances the central depressant properties of ethanol in mice. *Pharmacol Biochem Behav* **50:** 199-205.

Wilson GG and Karlin A (1998) The location of the gate in the acetylcholine receptor channel. *Neuron* **20:** 1269-1281.

Ye JH, Tao L, Ren J, Schaefer R, Krnjevic K, Liu PL, Schiller DA, McArdle JJ (2001) Ethanol potentiation of glycine-induced responses in dissociated neurons of rat ventral tegmental area. *J Pharmacol Exp Ther* **296:** 77-83.

Ye Q, Koltchine VV, Mihic SJ, Mascia MP, Wick MJ, Finn SE, Harrison NL, Harris RA (1998) Enhancement of glycine receptor function by ethanol is inversely correlated with molecular volume at postion α267. *J Biol Chem* **273:** 3314-3319.

Yevenes GE, Maraga-Cid G, Guzmán L, Haeger S, Oliveira L, Olate J, Schmalzing G, Aguayo LG (2006) Molecular determinants for G protein βγ modulation of ionotropic glycine receptors. *J Biol Chem* **281:** 39300-39307.

Yevenes GE, Maraga-Cid G, Peoples RW, Schmalzing G, Aguayo LG (2008) A selective Gβγ-linked intracellular mechanism for modulation of ligand-gated ion channels by ethanol. *Proc Natl Acad Sci USA* **105:** 20523-20528.

Zarbin MA, Wamsley JK, Kuhar MJ (1981) Glycine receptor: Light microscopic autoradiographic localization with [^{3}H]Strychnine. *J Neurosci* **1:** 532-547.

Zeilhoffer HU (2005) The glycinergic control of spinal pain processing. *Cell Mol Life Sci* **62:** 2027-2035.

Zhong W, Gallivan JP, Zhang Y, Li L, Lester HA, Dougherty DA (1998) From *ab initio* quantum mechanics to molecular neurobiology: A cation-π binding site in the nicotinic receptor. *Proc Natl Acad Sci USA* **95:** 12088-12093.

Zhu L and Ye JH (2005) The role of G proteins in the activity and ethanol modulation of glycine-induced currents in rat neurons freshly isolated from the ventral tegmental area. *Brain Res* **1033:** 102-108.

Vita

Brian Thomas Welsh was born in Baltimore, Maryland on September 8th, 1978 to Mark and Susan Welsh and has two younger sisters, Erin Boehm and Alexandra Welsh. He attended the University of Maryland, College Park from 1996 to 2000 where he graduated with honors receiving a Bachelor of Science degree in Neurobiology & Physiology. In the Spring of 2000 he began working for Baxter Pharmaceuticals, developing vaccines using protein purification. He left Baxter to work for the American Red Cross in September of 2003 and there he researched blood plasma purification processes. In August 2004 he moved to Austin, TX to become a graduate student in the Institute for Neuroscience.

Permanent address : 2000 Cullen Ave #26, Austin, TX 78757

briantw42@gmail.com

This dissertation was typed by the author.